

Instituto Tecnológico y de Estudios Superiores de Monterrey

Campus Estado de México

School of Engineering and Sciences



Causal order assistance for the quantum teleportation algorithm

A thesis presented by

Carlos Cardoso Isidoro

Submitted to the
School of Engineering and Sciences
in partial fulfillment of the requirements for the degree of

Master of Science

in

Nanotechnology

Atizapán, Estado de México, December, 2020

Dedication

I want to dedicate this work mainly to my parents, Virginia and Florencio, who have been the motor and main motivation for pushing through this work. They have been with me in every important moment of my life giving me support and being the best example of values and enthusiasm for doing the things. They have taught me that I can achieve everything I set my mind to.

To my niece, Sofía, just because my sister told me to dedicate it to her, but also, because she has come bringing us joy and as a blessing to our lives.

To all my friends and people in general who, in some or another way, have supported me in my way to finish this work. Thanks for all your unconditional confidence, support, patience, and encouragement.

Acknowledgements

To God, Who gives me every day a new opportunity to continue pursuing my goals.

I would like to express my deepest gratitude to my advisor, Dr. Francisco Javier Delgado Cepeda, who has been my biggest support with his orientation with the topics that I did not know before and has been with me all along the process to finish the work, always orienting me and driving me to continue working.

I would like to thank my parents Virginia and Florencio for their invaluable support with my plans and the enthusiasm shown every time I talked to them about my project, although they did not understand me. Also for believing in me.

I would like to thank my sister Sandra, for her confidence shown in every moment during the development of this project.

I would like to thank my friend Karime, who told me about the opportunity of studying at Tecnológico de Monterrey, for her support during the process of finishing this work and for her priceless friendship.

Special thanks are given to Tecnológico de Monterrey in gratitude for their support on tuition and CONACyT with the support for living.

Causal order assistance for the quantum teleportation algorithm

by

Carlos Cardoso Isidoro

Abstract

With the introduction of indefinite causal order, quantum communication have presented notorious advances regarding the quality of information transmitted. For the specific case of the quantum teleportation process, indefinite causal order scheme has shown notorious advances in the last decade by using additionally an appropriate measurement on the control state ruling the causal order, being even successfully deployed in the experimental field since a while. Recently, regarding the application of indefinite causal order along with measurement on the teleportation process, it has been demonstrated a valuable enhancement of teleportation to avoid channel imperfections. In this work, teleportation is tackled when it is assisted by indefinite causal order to correct the use of an imperfect entangled resource in the traditional process. First, a model of a generic quantum channel for single qubits in terms of Kraus operators in the form of Pauli operators is presented in order to understand the behavior of a general quantum channel, that is also applicable for the teleportation channel, where it is stated that the output state going through the channel can be obtained analytically and then analysis of the quality by means of the quantum fidelity can be developed.

By primarily analysing sequential teleportation under definite causal order (redundant application of teleportation channels), a comparison basis is performed for the notable outcomes obtained derived from the application of indefinite causal order. For the strategy being developed, indefinite causal order introduces the use of a control state in order to address the order of the channels to be applied, then, by the use of measurement, post-selection complements the teleportation improvement. It can be obtained analytically the fidelity for the entire process under an arbitrary initialization of such control state and performing an optimal measurement on it, thus obtaining a perfect teleportation. Also, an analysis for other values characterizing the imperfect entangled state has been made, where a perfect teleportation process with $\mathcal{F} = 1$ can not be reached. It has also been found, notably, that the best fidelity does not depend on the preparation of the control state ruling the order of the channels applied but instead on the imperfect initial entangled resource assessing the teleportation. The analysis is followed with the use of an increasing number of teleportation channels applied in superposition of causal order, thus suggesting additional alternatives in order to exploit the more valuable outcomes by using a strategy based on weak measurement as a complementary resource.

Additionally, the affordability of an experimental implementation with the current technologies for experimental developments on light and matter is studied. A scheme with the process needed is presented. Finally, the conclusions and future work to be developed in order to continue the project are presented.

List of Figures

1.1	Quantum Teleportation Circuit. Where $ \psi\rangle = \alpha 0\rangle + \beta 1\rangle$ and, for the simplest case, $ \chi\rangle$ is the Bell state where $ \chi\rangle = \beta_{00}\rangle = \frac{1}{\sqrt{2}}(00\rangle + 11\rangle)$. The CNOT and Hadamard gates are explicitly represented, the arrows represent the measurements and the X and Z represent the Pauli matrices [1]	2
1.2	Representation of one depolarizing communication gate. $ \psi\rangle$ represents the quantum state of the system in which the information is encoded and $ \psi'\rangle$ is the information once the gate is applied.	4
1.3	Representation of two quantum communication gates in superposition of causal order. a) depicts the order where G_1 goes first and the G_2 , b) is the contrary order in b) and c) is the superposition of the previous orders.	5
1.4	Distribution of the contents by chapters.	9
2.1	Channel characterization in the space $(\alpha_1, \alpha_2, \alpha_3)$ marking some emblematic channels.	14
3.1	Fidelity given by the number of teleportation channels when applied sequentially for the first five sequentially applied channels.	19
3.2	Teleportation circuit represented as a teleportation channel.	19
3.3	Two causal order combinations depending on the control state depicted in: a) when the control state is in $ 0\rangle\langle 0 $, b) when it is in $ 1\rangle\langle 1 $ and c) when the control state is a superposition of the previous states.	20
3.4	Fidelity given for the case of two channels as function of p . The blue dashed upper line corresponds to $ \psi_m\rangle = +\rangle$ and $q_0 = \frac{1}{2}$ reaching $\mathcal{F} = 1$ in $p = \frac{1}{3}$. The orange dashed line represents the case when the protocol fails with $ \psi_m\rangle = -\rangle$ and $q_0 = \frac{1}{2}$ and there is no advantage on the application of two channels in superposition of causal order	22
3.5	Best fidelity \mathcal{F}_2 for the two channels case as function of p_1, p_2, p_3 . Each point inside the polyhedron corresponds to their acceptable values and it is coloured in agreement with its fidelity value (see the color-scale besides); the cut of polyhedron region exhibits the inner structure.	23
4.1	Diagram summarizing the research lines to follow in order to improve the teleportation process when it is assisted by indefinite causal order. Each branch represents each one of the main contents in this research report which will be addressed in the next chapters.	27

5.1	In the contour plots a) - e) for \mathcal{F}_2 , it is indicated the values for θ and ϕ such that $\mathcal{F}_2 = 1$ is reached ($q_0 = 0.1, 0.3, 0.5, 0.7, 0.9$ and $\mathcal{P} = 0.12, 0.28, 0.33, 0.28, 0.12$ respectively). Color bar shows the values of fidelity. Plot f) exhibits the relation between θ and q_0 under the election of the best control measurement ($\phi = 0$ always).	31
5.2	Outcomes for the fidelity \mathcal{F} for other values of p different from $\frac{1}{3}$. a) Shows the contour plot for \mathcal{F} for $p = \frac{1}{6}$ and $q_0 = \frac{1}{4}$; b)-c) depicts the dependence of \mathcal{F} and θ from p and q_0 .	32
5.3	Condensed outcomes for the case $N = 2$. The respective probability \mathcal{P}_m of measurements are included as function of q_0 and θ in $ \psi_m\rangle = \cos\frac{\theta}{2} 0\rangle + \sin\frac{\theta}{2}e^{i\phi} 1\rangle$ ($\phi = 0$ in the optimal measurement). Fidelity depends entirely from p and \mathcal{P}_m goes down while $p \rightarrow \frac{1}{3}$.	33
5.4	a) Best fidelity \mathcal{F}_2 for the two channels case as function of p_1, p_2, p_3 . Each point inside the polyhedron corresponds to their acceptable values and it is coloured in agreement with its fidelity value (see the color-scale besides); the cut of polyhedron region exhibits the inner structure; b) The corresponding values for measurement probabilities \mathcal{P}_m denoting disperse values around 0.5. The upper inset confirms the statistical distribution $\rho_{\mathcal{P}_m}$ exhibiting symmetry around $\mathcal{P}_m = 0.5$.	34
5.5	Best fidelity \mathcal{F}_2 for the two channels case as function of p_1, p_2, p_3 in the frontal face.	34
6.1	$N!$ causal order combinations for N identical teleportation channels $T_i, i = 1, 2, \dots, N$ conforming finally a superposition of those causal orders. Each one is ruled by the control state above.	38
6.2	Probability \mathcal{P}_m to obtain different values of fidelity \mathcal{F}_N when the measurement states $ \varphi_+\rangle$ or $ \varphi_-\rangle$ are applied for cases a) $N = 2$, b) $N = 3$ and c) $N = 4$. Color-scale bar depicts the respective value for p for $N = 2, 3, 4$.	39
6.3	Comparison of Fidelity obtained when the channels are applied sequentially and with causal order depending on the measurement state.	40
6.4	Bloch sphere showing under the assumption $p_j \ll 1, j = 1, 2, 3$ for each state: a) $\Delta_{\theta, \phi}^{\alpha_1, \alpha_2, \alpha_3}$ in color obtained for each syndrome in (6.12), $\sigma_1 \rho \sigma_1, \sigma_2 \rho \sigma_2, \sigma_3 \rho \sigma_3$ respectively, and b) the standard deviation $\sigma_{\Delta_{\theta, \phi}^{\alpha_1, \alpha_2, \alpha_3}}$ in (6.18). Red is the best fidelity in a) and the lower dispersion in b).	42
6.5	Optimal fidelity using two teleportation channels in indefinite causal order followed by an appropriate measurement $ \varphi_m\rangle$. a) The best fidelity obtained for certain teleported state if optimal control measurement is obtained, b) the probability \mathcal{P}_m of success for the last process, and c) the statistical distribution for \mathcal{F}_2 and \mathcal{P}_m .	43
6.6	Distribution of \mathcal{P}_m on the frontal face.	45
7.1	Schematic teleportation process assisted by weak measurement.	48
7.2	Distribution of \mathcal{P}_{Tot} : a) as function of (p_1, p_2, p_3) , and b) as statistical distribution by itself obtained numerically from the data of a).	48

7.3	Schematic teleportation process assisted by indefinite causal order using N -teleportation channels and weak measurement.	49
7.4	a) to c) values of \mathcal{P}_{Tot} as function of (p_1, p_2, p_3) , for N_2, N_3 and N_4 respectively. d) statistical distribution numerically obtained for $\mathcal{P}_{\text{Tot}2}, \mathcal{P}_{\text{Tot}3}$ and $\mathcal{P}_{\text{Tot}4}$	50
8.1	a) Quantum circuit generating the weak measurement on $ \chi\rangle$, and b) contour plots for the map on the region (p_1, p_2, p_3) between those probabilities and p_1^* (red), p_2^* (green) and p_3^* (blue).	53
8.2	Diagram for an implementation of teleportation with causal ordering as it is discussed in the text. Photons are splitted on two different set of paths to superpose the two causal orders of two sequential teleportation process. In this diagram, photon 1 works as the target qubit while photons a and b works as the target qubits. SWAP gates are used to move information from one red path to another one letting to meet the information on the corresponding green path (on the same system) at the end of the circuit upon the recombination.	55
8.3	Teleportation processes are assumed to perform measurements on the Bell states basis.	56
B.1	\mathcal{P}_m on the $\alpha_0 = 0$ face together with the fidelity on the Bloch ball for the input ρ for three specific channels P_a, P_b, P_c with $N = 2$ using a) $ \psi_m^{N=2,-}\rangle$, and b) $ \psi_m^{N=2,+}\rangle$ for the control measurement. Both, \mathcal{P}_m and $\Lambda^{2,\pm}[\rho]$ are reported in color in the scale 0(red)-1(blue).	63

List of Tables

- 1.1 Table listing the published articles for the work developed. 7
- 1.2 Table listing the conferences where the work done was presented. 8

Contents

Abstract	v
List of Figures	viii
List of Tables	ix
1 Introduction	1
1.1 Introduction to teleportation	1
1.2 Experimental approaches to teleportation	2
1.3 Introduction to Causal Order	3
1.3.1 Quantum switch	4
1.3.2 Causal Order in Communication	4
1.3.3 Causal order in Teleportation	6
1.4 Papers and presentations regarding this thesis	7
1.5 General scheme for this document	7
2 The Quantum Channel	11
2.1 Introduction	11
2.2 Noisy channels for a single qubit in terms of Pauli operators	12
3 Teleportation Assisted by Indefinite Causal Order	16
3.1 Preliminaries for the Teleportation assisted by Indefinite Causal Order	16
3.2 Redundant case for teleportation with N -channels	17
3.3 Scheme for teleportation with indefinite causal order	18
3.4 Teleportation with $N = 2$ teleportation channels in indefinite causal order	20
3.4.1 Two teleportation channels under indefinite causal order considering $p_1, p_2, p_3 \in [0, 1]$	22
4 Research Questions and Objectives	24
4.1 Research Questions	24
4.1.1 Improvement of the teleportation process with arbitrary control states and measurement basis	24
4.1.2 Enhancements in teleportation when more than two teleportation chan- nels in indefinite causal order are introduced	25
4.2 Research objectives	25

4.2.1	To explore other control states and measurement control basis to improve \mathcal{F}	25
4.2.2	To explore the application of a larger number of teleportation channels in indefinite causal order to improve \mathcal{F} in the teleportation process	26
4.2.3	To establish a procedure in order to use indefinite causal order with improved outcomes for \mathcal{F} and \mathcal{P}_m	26
4.2.4	To present an insight for an experimental approach for the constructed procedure	26
4.3	General diagram for teleportation enhancement	27
5	Two channels in Indefinite Causal Order	29
5.1	Formalism to set quantum teleportation under an indefinite causal order scheme with two channels	29
5.2	Quantum teleportation ruled by an arbitrary control state for two channels under indefinite causal order	30
5.3	Two quantum channels in indefinite causal order with an entangled state with $p \in [0, \frac{1}{3}]$	32
5.4	Two quantum channels in indefinite causal order with an entangled state with $p_1, p_2, p_3 \in [0, 1]$	33
6	N-channels in Indefinite Causal Order	36
6.1	Preliminaries to the analysis of the teleportation process with N -channels under indefinite causal order	36
6.2	Analysis of quantum teleportation when increasing the number of channels applied	38
6.2.1	Case $p_1 = p_2 = p_3 \equiv p$	38
6.2.2	Case $p_j \ll 1, j = 1, 2, 3$	40
6.2.3	Notable behavior on the frontal face of the parametric region: case $p_0 = 0$	42
7	Teleportation assisted by weak measurement	47
7.1	General case for $N = 2$ assisted by a weak measurement	47
7.2	General case for $N \geq 2$ assisted by a weak measurement	49
8	Experimental Implementation	52
8.1	Weak measurement to project $ \chi\rangle$	52
8.2	An insight about teleportation implementing indefinite causal orders experimentally with light	53
9	Conclusions and future work	58
9.1	Conclusions	58
9.2	Future work	60
A	Formulas \mathcal{F}_N and \mathcal{P}_N for $N = 2, 3, 4$	61
B	Channel characterization for mixed states	62

C	Formulas of output for mixed states under indefinite causal order	65
D	Probabilities of successful measurement \mathcal{P}_m	66
E	Formulas for $\mathcal{P}_{m,N}^{\text{ff},\{p_i\}}$ and \mathcal{F}	67
	Bibliography	73

Chapter 1

Introduction

In this chapter, the necessary elements for the teleportation process are presented as well as some experimental approaches and some attempts to enhance the process by different techniques. Thus, section 1.1 presents the basis for teleportation and section 1.3 makes an introductory for causal order as a technique used for improvement of quantum communication as well as teleportation. Finally, section 1.5 presents a general view of this document described by chapters.

1.1 Introduction to teleportation

Transmission of information is the base for the communication protocols and, in this sense, some enhancements have been sought and new technologies have emerged. Such is the case of the quantum protocols for communication and transmission of information as well as teleportation protocols. For this purpose it is necessary the use of the so called quantum channels. A quantum channel is a communication channel that makes possible the transmission of quantum information (not necessarily moved) and can be used in quantum communication as well as in teleportation processes for that specific purposes. For the specific case of teleportation, the quantum teleportation channel is the main element that allows the teleportation process to be done and has specific elements to be called teleportation channel, each one of them are configured thus being able to obtain a perfect teleportation process.

Teleportation has been studied since a while and, despite the fact that instantaneous information transfer is no possible, it has been shown that by establishing EPR correlations it is possible to teleport an unknown quantum state [1]. Nevertheless, in order to make the teleportation possible, it is necessary to make use of classical means along the process by sending a message about the original state and, this way, make the necessary operations to make the output state be the same as the originally sent.

The teleportation process has been described as a traditional algorithm represented in Figure 1.1, where the implementation of a generic teleportation circuit (the quantum teleportation channel) is shown. The main components of the teleportation circuit are a CNOT gate between a qubit of the entangled state that asses the teleportation ($|\chi\rangle = |\beta_{00}\rangle = \frac{1}{\sqrt{2}}(|00\rangle + |11\rangle)$ one of the Bell states) and the unknown state wanted to be teleported ($|\psi\rangle = \alpha|0\rangle + \beta|1\rangle$) in addition to a Hadamard gate. These elements allow the quantum entanglement between the

unknown state wanted to be teleported $|\psi\rangle$ and the entangled state that assees the teleportation $|\chi\rangle$. Later on, some measurements are taken in order to know the necessary operations required to copy exactly the state at the entrance in the other qubit of the entangled resource $|\chi\rangle$, which is going to be the output of the channel. These measurements taken are transmitted by classical means and the necessary operations are done in relation of the requirements for the output state to be equal to the entrance according to the measurements, then the superscripts i and j shown in Figure 1.1 indicate whether the X or Z (according to the Pauli matrices) or both operations ($-iY$) are applied. It is in this sense that information can not be transmitted faster than the speed light because it depends on the knowledge of the measurements that are transmitted by classical communication.

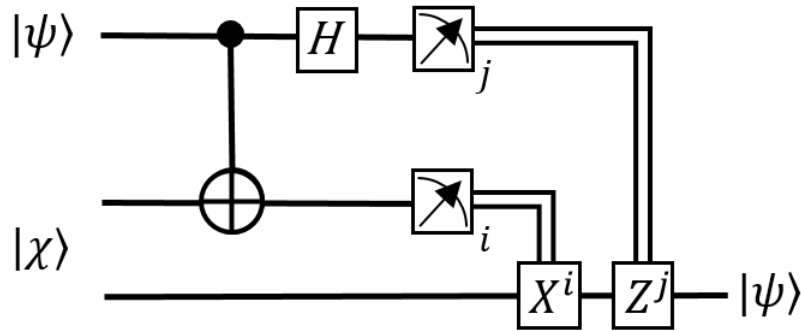


Figure 1.1: Quantum Teleportation Circuit. Where $|\psi\rangle = \alpha|0\rangle + \beta|1\rangle$ and, for the simplest case, $|\chi\rangle$ is the Bell state where $|\chi\rangle = |\beta_{00}\rangle = \frac{1}{\sqrt{2}}(|00\rangle + |11\rangle)$. The CNOT and Hadamard gates are explicitly represented, the arrows represent the measurements and the X and Z represent the Pauli matrices [1]

1.2 Experimental approaches to teleportation

In order to test the feasibility of the teleportation algorithm, some strategies have been developed and it has been found since a while that, somehow, quantum teleportation exists when the teleportation algorithm is carried out experimentally through photonic entanglement [2, 3]. Some other authors suggest a way to experimentally determine a successful teleportation by preparing an initial photon which carries a certain polarization that will be transferred (teleported) and then, a pair of entangled photons are subjected to a measurement such that the second photon of the entangled resource acquires the polarization of the initial photon, therefore, if both polarizations coincide, then it means that teleportation is successfully achieved [2, 4, 5]. Since then, other approaches have come out showing the possibility of teleportation as it is shown in [6] with a semiconductor single photon source, using a target and an ancilla qubits, each defined by a single photon occupying two optical modes. In that case, they were able to obtain a measure of the fidelity of the teleportation process observing a fidelity of 80%, in agreement with the residual distinguishability between consecutive photons from the source [7].

Some other approaches for long distance quantum teleportation include those with the use of a fiber-delayed Bell state measurement (BSM) [8] and also some using optical fiber in

order to avoid using large-aperture optics and other complex techniques [9, 10].

Unfortunately, the process depicted is not always the best situation because of the resources needed to fit the best teleportation process and then, some issues are presented when trying to develop an experimental realisation. One of the elements that results affected on an experimental approach is the entangled resource necessary for the teleportation process, which, in practice, is not exactly the state required in order to reach a perfect teleportation (remarking that the perfect teleportation is achieved with the Bell state $|\beta_{00}\rangle$ on the entangled state) due to some interactions like the Ising interactions described in [11] that can produce distortion in entangled pairs. In a practical model, such entangled resource depicted in Figure 1.1 as $|\chi\rangle$, usually varies slightly from the desire state (being able to reach a total distortion). This variation does not allow the process to be done perfectly, therefore, some attempts in order to enhance the fidelity of the process have been studied considering these variations [12].

1.3 Introduction to Causal Order

The way quantum communication is developed has been looking for improvements. It is in this sense where new approaches have come out. It has been shown, for instance, that the communication in quantum channels can be improved through the superposition principle of such quantum channels. Communication enhancement has been first shown in depolarizing channels, where the combination of quantum channels in a superposition of different orders can result in the transparency of the quantum channel [13] and thenceforth, superpositions of causal orders have been widely studied and several experimental implementations have been developed in order to see their advantages [14, 15, 16]. In this sense, the application of causal structure in superposition has been studied for the specific case of quantum channel discrimination, showing an advantage over causally ordered quantum circuits [17, 18].

Enhancements in communications have had approaches both theoretically and experimentally [19, 20]. In the case for two quantum channels, it has been shown that even though no information can be transmitted through depolarizing channels by classical means due to the noise, it could be possible to transmit information by combining two depolarizing channels in a superposition of causal order [13, 21]. As an example, in a quantum teleportation model with very noisy singlets, it has been shown the possibility of transmitting perfectly the state to be send when apply causal order in superposition of two quantum channels [22].

Recently it has been researched about the possibility of extrapolate superposition of causal order to more than two channels. To get started, it has been shown the enhancement of transmission of information for the three channel scenario [23] and it has been settled down the increasing of classical information transmitted as the number of causal orders increases [23, 24].

Some important approaches regarding causal order have been taken in account since a while, such those considering quantum correlations [25], quantum metrology [26] and communication [27]. In communication, it has been shown the capability of transmitting information in a more efficient way when a superposition of different causal orders is applied. That is why the importance of the study of some features found regarding causal order. It can be highlighted this importance though the study of two different fields: communication and

teleportation.

1.3.1 Quantum switch

The standard model of information theory established by Shannon [28], usually assumes that the communication channels along the process are used in a perfectly defined configuration. However, it is also known that quantum mechanics is able to allow scenarios where the configuration for the quantum communication channels is not longer defined, but it can be in a quantum superposition [17]. This scenario can be described by the quantum switch, where the quantum superposition can also involve the order of the channels applied in time [29]. In the quantum switch, the order of application of two quantum channels becomes indefinite, due to the superposition of definite orders, thus obtaining a feature called causal non-separability [25, 30]. Therefore, we can explain the quantum switch as an example of quantum control where this switch can make a system go through two operators (A and B as example for the case of two quantum operations) following one definite causal order (first A and then B) or in the other way around (first B and then A), or even, a superposition of the two trajectories described, thus obtaining an indefinite causal order for the two operators. Recently, it has been studied the possibility of describing the quantum switch for the case of more than two quantum operators [31, 30].

Also, regarding the experimental realizations, the quantum switch have been recently proposed for a practical model by the use of photons [14, 32, 33]. Another experimental approaches suggest other means of the realisations, like those suggesting the involvement of quantum superpositions of spacetimes [31], whereas another approaches have been made with closed timelike curves [21].

1.3.2 Causal Order in Communication

In communication it is very important to have a certain security on what is being transmitted. It can be measured by a function called Holevo information that depicts how exact the information has been transmitted. When the channel used for such transmission is a very noisy channel, so called depolarizing quantum channel, it has been noticed that no information can pass. Figure 1.2 shows the application of such depolarizing channel.

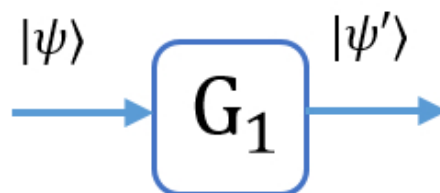


Figure 1.2: Representation of one depolarizing communication gate. $|\psi\rangle$ represents the quantum state of the system in which the information is encoded and $|\psi'\rangle$ is the information once the gate is applied.

It can be followed that if we continue applying depolarizing quantum channels subsequently, the information is going to continue being zero (no information transmitted). Nevertheless, it has been shown that when two completely depolarizing channels are applied in addition with indefinite causal order, we can actually transmit information and, surprisingly, the quantity of information transmitted becomes higher once indefinite causal order is applied. Figure 1.3 depicts the way of applying two channels in superposition of definite causal orders, since this superposition is indefinite, in the literature is more common the term indefinite causal order, which will be used from now on. More specifically, for the case of two quantum channels, some developed researches have been working with depolarizing channels and have shown that, when such two completely depolarizing channels are combined in an indefinite causal order, it could be possible to transmit information instead to destroy it [13, 21]. As this example, some other approaches, both theoretical [23] and experimental [20], have been studied. It is in this same sense that, recently, it has been experimentally verified the success of the indefinite causal order superposition applied to two channels for transmitting information [20, 15, 16].

Following such trend in communication, recently it has been researched about the possibility of extrapolate superposition of causal order to more than two channels by developing a combinatorics approach to the problem. As a matter of fact, it has been shown that the amount of information transmitted, in comparison with the two channel scenario, increases for the three channel scenario [23] and, therefore, it has been settled down that the amount of classical information transmitted becomes higher as the number of causal orders increases [23, 24].

All in all, in communication, it has been shown the capability of transmitting information in a more efficient way when a superposition of causal order is applied. That is why the importance of the study of some features found regarding causal order. It can be highlighted this importance through the study of implications of indefinite causal order applied not only in communication, but also in teleportation.

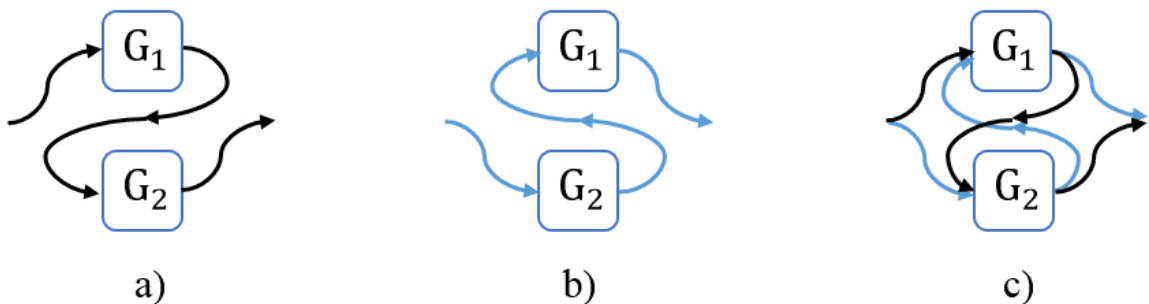


Figure 1.3: Representation of two quantum communication gates in superposition of causal order. a) depicts the order where G_1 goes first and the G_2 , b) is the contrary order in b) and c) is the superposition of the previous orders.

1.3.3 Causal order in Teleportation

Information can be transmitted from one party to another one as a quantum state by preparing it as an Einstein-Podolsky-Rosen state [1], such quantum process is called teleportation and plays an important role for processes related with quantum computation and quantum communication. Teleportation algorithm for one single qubit has been described using an entangled Bell state and a channel for classical communication in order to achieve teleporation [34], nevertheless, such algorithm has been shown to be useful to teleport larger system states as a composite of two-level systems [35]. Up to date the standard quantum teleportation algorithm have been widely studied and new approaches have come up as well as variants on the algorithm in order to make it either more efficient in terms of the quantum resources used for the teleportation process [36] or more adaptive to some specific quantum systems [37, 38, 39]. Following these studies, recently, a new approach has shown the impact of assistance of indefinite causal order in the teleportation process to improve its performance when using two completely noisy channels for the teleportation [22]. Additionally, several tests have been made experimentally in a successful way in order to prove the feasibility of teleportation when the distance increases [2, 9, 40] and also tests with larger multidimensional states rather than qubits have been performed successfully [41].

Regarding to indefinite causal order, some recent works have introduced it to the traditional quantum teleportation algorithm. For instance, a comparison on the effect of employing a quantum switch for the entanglement distribution process within the quantum teleportation process has been developed in [12], making an analysis to quantify the performance gain that can be achieved by employing such quantum switch with respect to the case of the absence of quantum switch. In a proper manner, teleportation assisted by indefinite causal order has been introduced in [22] by pointing out that teleportation is a quantum channel itself. In [22], a quantum teleportation model with very noisy singlets is proposed and it has been shown that, despite those very noisy singlets make impossible the teleportation, there is still the possibility of transmitting perfectly the state to be send when applying causal order in superposition of two quantum channels. Such teleportation process has been conducted considering two identical teleportation channels with the same imperfect entangled resources but in indefinite causal order through an evenly quantum control system. Finally, the outcome is measured on a specific basis in order to improve in the best possible way the fidelity of the teleportation.

Following this study and considering the same two imperfect channels but with an arbitrary initialized quantum control system, it has been investigated the possibility to get again the highest possible fidelity with alternative scenarios [42]: a proper selection of the post measurement state on the control system, thus generalizing the results obtained in [22]. In addition, it has be shown that for the no-noisiest cases of teleportation, the effect is still limited as in [22].

It is also important in teleportation to know how successful the teleportation has been. It can be established by simply calculating the fidelity as a measure of how equal is the state obtained at the output in relation with the state to be teleported (input). In order to carry out such teleportation, it is necessary to make use of an entangled resource $|\chi\rangle$ as Figure 1.1 shows. Is in this sense when teleportation can turn difficult. It is possible to reach a perfect teleportation when this entangled state is a singlet equal to $|\beta_{00}\rangle$, but for the worst case (the most imperfect entangled state with a mixture of all possibilities in the Bell basis) the fidelity

goes down to zero.

It is in this sense where we can make use of causal order to aid in the improvement of the teleportation process. It has been shown that it is possible to correct this lack of fidelity when working with the worst entangled state by applying indefinite causal order and, in some cases with the correct chose of some specific features, it is possible to reach a perfect teleportation.

1.4 Papers and presentations regarding this thesis

It is important to mention that all the results obtained from this thesis project are not only on this document, but the results have been published in four articles along all the process for the development of the project. The mentioned articles are listed in the Table 1.1 below for the reader to have another references for the work developed here.

Title	Journal	Year	DOI
Featuring Causal Order in Teleportation With Two Quantum Teleportation Channels	Journal of Physics: Conference Series	2020	doi:10.1088/1742-6596/1540/1/012024
Performance of two redundant quantum channels for single qubits under indefinite causal order	Journal of Physics	2020	In press
Characterization of N quantum channels assisted by indefinite causal order and measurement	Quantum Information & Computation	2020	doi.org/10.26421/QIC20.15-16
Teleportation assisted by N -channels in an indefinite causal order and measurement	Symmetry	2020	doi.org/10.3390/sym12111904

Table 1.1: Table listing the published articles for the work developed.

Additionally, much of these works have been presented in the conferences shown in Table 1.2.

1.5 General scheme for this document

Before the statement of the proper questions and objectives of research, Chapter 2 and 3 present general theory and results about quantum channels and the teleportation process using indefinite causal order. Since this work is aimed to describe the quantum teleportation process assisted by indefinite causal order, with the purpose of describing the quantum teleportation channel, Chapter 2 starts developing an analysis on the quantum channel. In this chapter, the quantum channel is modeled in terms of the Pauli operators and the expressions for a very noisy channel for single qubits are developed.

Name of the Conference	Title of the work	Date	Country
International Conference on Quantum Phenomena, Quantum Control and Quantum Optics	Featuring causal order in teleportation of two quantum teleportation channels	October 28- November 1, 2019	Mexico
50 Congreso de Investigación y Desarrollo	Teleportation with two quantum channels in superposition of causal order	February 25-28, 2020	Mexico
9th International Conference on Mathematical Modeling in Physical Sciences	Performance of two redundant quantum channels for single qubits under indefinite causal order	September 7-10, 2020	Greece
NQN Quantum Programming in Theory, Experiment and In the Classroom (QPTEC)	Indefinite causal order enhances quantum teleportation	September 16-18, 2020	United States of America
Quantum 2020	Improving imperfect quantum teleportation with indefinite causal order assisted by post-measurement and weak measurement	October 19-22, 2020	United States of America

Table 1.2: Table listing the conferences where the work done was presented.

Later on, Chapter 3 presents a studied case found in literature for the teleportation process assisted by indefinite causal order with the specific case with two channels. In this chapter, outcomes for the teleportation process when applied sequentially are reported in section 3.2 in order to have a comparison with the case assisted by indefinite causal order, presented in 3.4 for two channels. Enhancements are reported here and a comparison between two channels applied sequentially and under an indefinite causal order scheme is presented.

From now on, it is necessary to define the objectives for this work and, from then, determine the steps to follow in order to reach them. In this sense, Chapter 4 presents the research questions for the improvement of the teleportation algorithm and the objectives to follow in order to achieve those improvements. Section 4.3 presents a diagram for the general general view for teleportation enhancement.

For the analysis regarding the use of an indefinite causal order scheme, Chapter 5 presents a more detailed analysis for the case with two channels in superposition of causal order. This chapter begins to consider an arbitrary control state for those two channels in superposition of causal order as presented in section 5.2. When considering a practical model, slightly variations on the entangled state needed for the teleportation are presented and, therefore, in sections 5.3 and 5.4 this variations are presented. Improvements on the fidelity given and the probability to obtain that fidelity are presented.

Continuing with the analysis of indefinite causal order when increasing the number of channels applied, Chapter 6 sets the use of more than two channels in superposition of causal order, The formalism to set quantum teleportation under an indefinite causal order with N –channels is presented in section 6.1 together with the analysis when increasing the number

of channels applied in superposition of causal order. Different cases presented when introducing a model with different effects are presented. Sections 6.2.1 to 6.2.3 focus on these cases and the outcomes as well as improvements regarding the fidelity and probability of measurement are presented here.

It is important to consider different techniques that can help with the enhancement of the teleportation process. It is in this sense that Chapter 7 presents another approach for teleportation improvement complemented with weak measurements. The analysis is made at the beginning for the case widely studied with $N = 2$ and then, the analysis goes to an increasing number of N . There, the enhancements regarding fidelity and probability of measurements is made.

All in all, it is important to confirm theory with practice, that is why Chapter 8 presents a proposal for an experimental implementation starting with the case with two channels under an indefinite causal order scheme. For facility, it is intended to be developed with photons as the unknown quantum state to be teleported. Therefore, this chapter presents the main scheme to be physically implemented as well as the materials and equipment needed to develop the experiment.

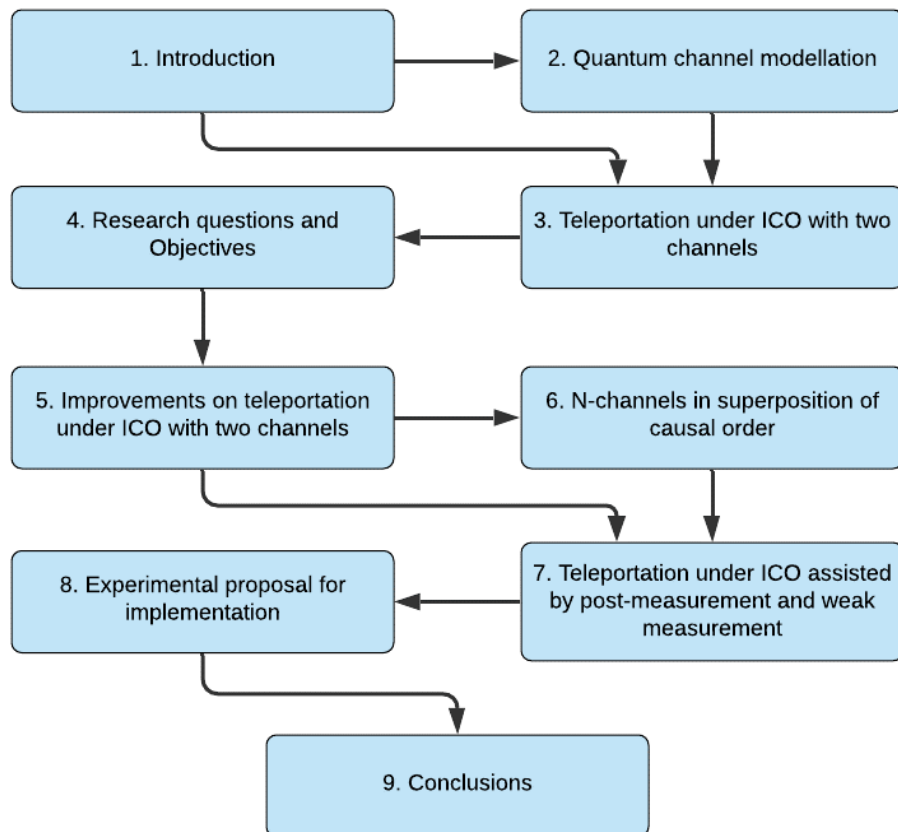


Figure 1.4: Distribution of the contents by chapters.

Finally, Chapter 9 presents the final conclusions regarding the work done so far as well as some recommendations for the data and procedure here. Possible future works to be done in order to continue with the quantum teleportation process enhancement are presented too. Figure 1.4 shows the organisation of the content of this document in a general view.

Chapter 2

The Quantum Channel

Before establishing the research questions and objectives, the general concepts will be presented. As a preliminary to understand the teleportation channel and its behavior under an indefinite causal order scheme, in this chapter, it is studied a parametric quantum channel in general terms. They are considered single qubits for the modeling of such quantum channel through Kraus operators, which are expressed in terms of the Pauli operators. Furthermore, an analysis to obtain the formulas for the output state of the channel when it goes through a certain imperfect quantum communication channel is presented. Then, the fidelity of the output is also analysed in order to determine the performance of such quantum channel in terms of its parameters.

2.1 Introduction

Quantum channels are the main component in quantum communication in order to maintain or transport quantum states being used in quantum processing. Nevertheless, when such channels become imperfect or noisy, the information transmission process is not optimal. If the process continue being applied recursively through similar imperfect channels the quality of the information transmitted worsens.

It has been remarked in section 1.3.2 that with the introduction of the concept of indefinite causal order, which is a quantum treat to superpose two or more orders in which quantum information goes through the quantum channels, it can be shown important improvements for certain channels as the depolarizing [13], the teleportation [22] and the dephasing noise ones [43]. With this process, whether directly or under additional procedures, It is possible to actually still transmit information with quality. It can be also compared with the redundant definite causal order case actually obtaining advantages [23, 14].

The process under indefinite causal order requires a second quantum system, a control state managing the superposition of causal orders. Such control state normally becomes entangled with the output state being transmitted. Then, the analysis of the quality of information being transmitted has been quantified through the tracing control system [13] or stochastically by measuring the control state in certain basis [22], more information about this process will be given in Chapter 3. In the first case the Holevo bound for the transmission rate is estimated, while in the second one the improved transmission is reached only with certain probability and

otherwise dropped.

Following that trend in communication, the aim of this chapter is to analyse an arbitrary noisy channel modelled through Kraus operators and expressed in terms of Pauli operators for a single qubit when the indefinite causal order is involved on N channels in superposition of causal order. It will also be presented some outcomes and notation for such depicted noisy channel in the previous terms.

2.2 Noisy channels for a single qubit in terms of Pauli operators

A quantum channel is considered in quantum information, as a medium through a quantum systems is transmitted until it is used. Such system or its quantum state (then, more precisely, a quantum channel transmits quantum information) is transferred (which not necessarily implies its movement) or inclusively teleported to meet certain quantum processing in combination with other systems. Along the process, the transmission could imply the change of the quantum state due to several factors [44] such as noise, decoherence, environment, etc.

Therefore, each channel is susceptible to modify the quantum information of the original state planned to be transmitted. Thus, in quantum information theory, a quantum channel [45] is considered a completely positive trace-preserving map (CPTP) [46] between two spaces of operators (in spite that quantum information could be moved from one system to another in the channel). This CPTP map could represent not only a quantum operation obtained from the quantum dynamics, instead, a circuit moving quantum information from one point or instant to another. The reason because such map is positive and trace-preserving is due to maintaining of the properties of the density matrix representing the quantum information involved. In the last terms, a state, a quantum evolution and a traced state can be considered as quantum channels [38].

Particularly in this chapter, but in general in all the work developed in this document, we are solely interested in the analysis of quantum channels for single qubits (dimension 2). As it is well known, the general form for the density matrix representing such quantum state ensemble is [45]:

$$\rho = \frac{1}{2}(\sigma_0 + \vec{n} \cdot \vec{\sigma}) \quad (2.1)$$

represented in terms of the Pauli operators σ_0 , where $\vec{\sigma} = (\sigma_1, \sigma_2, \sigma_3)$. There, $\vec{n} = (n_1, n_2, n_3)$ is a three-dimensional vector that fulfills the condition $|\vec{n}| \leq 1$. For the specific case where $|\vec{n}| = 1$, we have a pure state $\rho = |\psi\rangle\langle\psi|$ but otherwise a mixed state. In such terms, it can be introduced the form of the output state of a CPTP map through its Kraus operators [47]:

$$\Lambda[\rho] = \sum_{i=0}^3 K_i \rho K_i^\dagger = \sum_{i=0}^3 \text{Tr}(K_i \rho K_i^\dagger) \frac{K_i \rho K_i^\dagger}{\text{Tr}(K_i \rho K_i^\dagger)} = \sum_{i=0}^3 P_i \rho_i \quad (2.2)$$

with : $P_i = \text{Tr}(K_i \rho K_i^\dagger), \quad \rho_i = \frac{K_i \rho K_i^\dagger}{\text{Tr}(K_i \rho K_i^\dagger)}$

being ρ_i and P_i the populations and their associated probabilities. The set of four operators $K_i, i = 0, 1, 2, 3$ fulfills $\sum_{i=0}^3 K_i^\dagger K_i = \mathbf{1}$ (σ_0 for the case of qubits) in order to preserve the unitary trace of $\Lambda[\rho]$. Note in (2.2), it could be understood as the mixture of possible outcomes when a measurement is performed on ρ . The form of Kraus operators depends on the way the system being transmitted relates with the environment and then additionally of the base being used to express ρ . If channel involves only N -local operations on the system being transmitted and possibly classical communication (LOCC), it could be expressed easier in terms of unitary operators U_i fulfilling $K_i = \sqrt{\alpha_i} U_i$ with $\sum_{i=0}^3 \alpha_i = 1$ and $1 \leq M \leq N^2$.

Depending on the base used, ρ could be expressed in alternative ways through a unitary base transformation T as $\rho = T\tilde{\rho}T^\dagger$. Such transformation could be used to transform the Kraus operators. Then, for a LOCC on qudits, one possible representation is the $su(d)$ -representation [48] with the Kraus operators being proportional to the generators $\{\lambda_i | i = 1, 2, \dots, N^2 - 1\}$ of the $su(d)$ algebra, together with the identity, λ_0 : $K_i = \sqrt{\alpha_i} \lambda_i$. It is not difficult to solve the linear system $TU_iT^\dagger = \lambda_i, i = 0, 1, 2, \dots, d^2 - 1$. Such representation is very useful to manage because its algebraic properties. In this work, we will restrict the analysis to single qubit channels ($N = 2$) thus the generators being used will be the Pauli operators $\{\sigma_i | i = 1, 2, 3\}$ and the identity, σ_0 :

$$\Lambda[\rho] = \sum_{i=0}^3 \alpha_i \sigma_i \rho \sigma_i^\dagger \quad (2.3)$$

which corresponds to a particular case of more general maps for qubits, which are called *Pauli maps* or *Pauli channels* and describe more extensive operations in quantum information than LOCC [49]. They includes noise sources which are present in many computing architectures, while, at the same time, they establish a single practical model for the analysis of error correction and fault tolerance [50]. This kind of quantum channels exhibits important features due to their relative easier treatment. In addition, (2.3) could be understood as a combination of several syndromes generated on the state ρ [38]. Due to the Pauli operators properties, by noting that: $\sum_{i=0}^3 \alpha_i \sigma_i \sigma_0 \sigma_i^\dagger = \sigma_0$, $\sum_{i=1}^3 \alpha_i \sigma_i \vec{n} \cdot \vec{\sigma} \sigma_i^\dagger = \sum_{i,j=1}^3 2n_i \alpha_j \sigma_i (2\delta_{ij} - 1)$, and then applying (2.1) on (2.3):

$$\Lambda[\rho] = \frac{1}{2}(\sigma_0 + \sum_{i=0}^3 n_i (2(\alpha_0 + \alpha_i) - 1) \sigma_i) \quad \rightarrow \quad n'_i = n_i (2(\alpha_0 + \alpha_i) - 1) \quad (2.4)$$

being $\vec{n}' = (n'_1, n'_2, n'_3)$ the corresponding vector for $\Lambda[\rho]$ in agreement with (2.1). Note that restriction $\sum_{i=0}^3 \alpha_i = 1$ automatically fulfills the Fujiwara-Algoet conditions in order to have a completely positive map [51]. Last formulas exhibit the behavior of the channel: if $\alpha_0 = 1, \alpha_i = 0, i = 1, 2, 3$ we get a transparent channel, while if $\alpha_i = \frac{1}{4}, i = 0, 1, 2, 3$ the channel is the depolarizing one. Other syndromes as bit-flipping and dephasing noise (or a combination of both) arise when we set only one of $\alpha_i \neq 0, i = 1, 2, 3$. Figure 2.1 shows schematically the characterization of the channel (2.3) on the $(\alpha_1, \alpha_2, \alpha_3)$ space, remarking the three regions mainly dominated by the syndromes: dephasing, bit-flipping and both combined. Transparent and depolarizing channels are remarked there. If additionally $\alpha_0 \neq 0$, we get the last channels stochastically combined with the transparent channel.

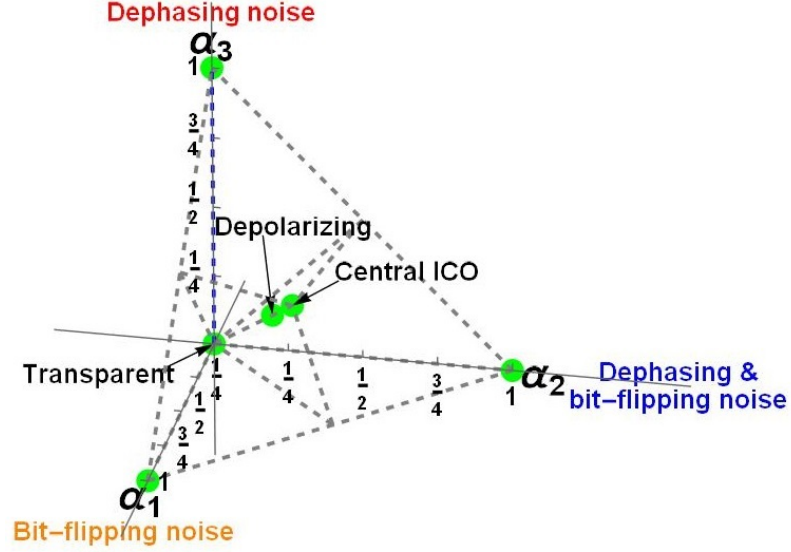


Figure 2.1: Channel characterization in the space $(\alpha_1, \alpha_2, \alpha_3)$ marking some emblematic channels.

In the previous sense, sometimes a channel could be modeled as a stochastic one. It means that channel can work perfectly as a transparent one $\Lambda_T[\rho] = \rho$ or as noisy one, $\Lambda_N[\rho]$ with certain probabilities q_0 and $1 - q_0$ respectively. Then, the resulting channel becomes:

$$\Lambda[\rho] = q_0\rho + (1 - q_0)\Lambda_N[\rho] = \sum_{i=0}^3 \beta_i \sigma_i \rho \sigma_i^\dagger \quad (2.5)$$

it is direct that if $\Lambda_N[\rho]$ have the form (2.3), then $\beta_0 = q_0 + (1 - q_0)\alpha_0$ and $\beta_i = (1 - q_0)\alpha_i$ for $i = 1, 2, 3$. In this chapter we will not put emphasis in this kind of channels but the generalization of the results including the parameter q_0 is immediate due to those last formulas.

As a measure for the performance of the quantum channel, we will use the fidelity defined as [52]:

$$\mathcal{F}(\rho, \Lambda[\rho]) = \left[\text{Tr} \left(\sqrt{\sqrt{\rho} \Lambda[\rho] \sqrt{\rho}} \right) \right]^2 \quad (2.6)$$

which, when ρ is a pure state, is reduced because $\rho = |\psi\rangle\langle\psi|$ then $\rho = \sqrt{\rho}$, thus for (2.3):

$$\begin{aligned} \mathcal{F}(\rho, \Lambda[\rho]) &= \text{Tr}^2(\sqrt{|\psi\rangle\langle\psi| \Lambda[\rho] |\psi\rangle\langle\psi|}) \\ &= \sum_{i=0}^3 \alpha_i \langle\psi| \sigma_i \rho \sigma_i^\dagger |\psi\rangle \text{Tr}^2(|\psi\rangle\langle\psi|) = \sum_{i=0}^3 \alpha_i \text{Tr}(\sigma_i \rho \sigma_i^\dagger) \end{aligned} \quad (2.7)$$

nevertheless, for mixed states ρ , the use of (2.3) is necessary. In such case, for single qubits due to (2.1), then we can find $\sqrt{\rho} = \sum_{i=0}^3 s_i \sigma_i$ by substituting it in $\rho = \sqrt{\rho} \sqrt{\rho}$ and then solving for s_i . It conducts to the system $\sum_{i=0}^3 s_i^2 = \frac{1}{2}$ and $2s_0 s_i = \frac{n_i}{2}, i = 1, 2, 3$. Finally, we get ($n = |\vec{n}|$):

$$s_0 = \frac{1}{2} \sqrt{1 \pm \sqrt{1 - n^2}} \quad (2.8)$$

$$s_i = \frac{n_i}{2n} \sqrt{1 \mp \sqrt{1 - n^2}}, \quad i = 1, 2, 3 \quad (2.9)$$

those results, together with the fact that for $\rho = \sum_{i=0}^3 s_i \sigma_i$ arbitrary then $2s_k = \text{Tr}(\rho \sigma_k) \rightarrow n_k = \text{Tr}(\rho \sigma_k)$, become useful to deal with (2.6) for general cases of mixed states transmission. In the following, we will express the fidelity in short as $\mathcal{F}_\Lambda \equiv \mathcal{F}(\rho, \Lambda[\rho])$ assuming the use of the different formulas depending on the nature of the input state ρ .

As a final quotation, note that following a similar development, if $M = \sum_{i=0}^3 b_i \sigma_i$ is a self-adjoint 2×2 matrix ($b_i = b_i^*$), then $\sqrt{M} \equiv \sum_{i=0}^3 c_i \sigma_i$ fulfills (both formulas for each inner sign become equivalent):

$$c_0 = \sqrt{\frac{b_0 \pm \sqrt{b_0^2 - \sum_{i=1}^3 b_i^2}}{2}} \quad (2.10)$$

$$c_i = \sqrt{\frac{b_0 \mp \sqrt{b_0^2 - \sum_{i=1}^3 b_i^2}}{2 \sum_{i=1}^3 b_i^2}}, \quad i = 1, 2, 3 \quad (2.11)$$

As it will be shown in the next chapters of this work, teleportation can be seen as a communication channel and most of the properties found under an indefinite causal order are shown to be applicable for any communication channel. Particularly, we will show that a communication channel behaves as Pauli channel [53]. The properties for the communication channel are represented in Figure 2.1 for the classification of communication channels. Some additional outcomes in the current terms for quantum channels are developed through the next chapters and they are complementary included in the Appendices C and D.

Chapter 3

Teleportation Assisted by Indefinite Causal Order

For the transmission of quantum information, from a place to a different location, it has been pointed out the importance of using a resource called singlet (the entangled resource aimed to assess the teleportation). Such singlet is going to be shared between the two locations (transmitter and receiver), nevertheless, due to the existing imperfections in practice, the teleportation process becomes affected. This imperfect entangled resource can be described from slight variances in relation with a perfect purely Bell state allowing a perfect teleportation to a completely imperfect state that, in principle, messes the teleportation process up. In this sense, some researches have been done and the concept of indefinite causal order has been introduced [22].

In this chapter, an analysis considering a completely imperfect entangled state is studied and some strategies to enhance the fidelity in the teleportation process are featured. Such strategies include the use of quantum teleportation channels in indefinite causal order and the advantages and downsides are presented.

The general aim of this chapter is to make an introduction in order to understand the objectives that will be given in Chapter 4. Note that the work depicted here is a deeper analysis from the work done by [22], thus obtaining the objectives as they are established in Chapter 4.

3.1 Preliminaries for the Teleportation assisted by Indefinite Causal Order

A perfect teleportation process can be reached when the entangled resource assessing the teleportation is purely the Bell state $|\beta_{00}\rangle = \frac{1}{\sqrt{2}}(|00\rangle + |11\rangle)$. However, when performing this teleportation process in some practical models, such entangled state becomes difficult to create exactly as purely as the Bell state $|\beta_{00}\rangle$ and, moreover, it is also difficult to sustain it and, therefore, such singlet could arrive imperfect to the process, thus preventing a perfect teleportation to be achieved. That is why it is more practical to consider a variation of this resource that can be written in the form of the state:

$$|\chi\rangle = \sum_{i=0}^3 \sqrt{p_i} |\beta_i\rangle \quad (3.1)$$

where $|\chi\rangle$ is the representation of the imperfect entangled state as the sum of each one of the possible contributions, $\sqrt{p_i}$ are the probabilities of the superposition (3.1) to be on the Bell state β_i and $|\beta_i\rangle$, is a short notation for the Bell states where $|\beta_0\rangle = |\beta_{00}\rangle$, $|\beta_1\rangle = |\beta_{01}\rangle$, $|\beta_2\rangle = |\beta_{11}\rangle$ and $|\beta_3\rangle = |\beta_{10}\rangle$, with:

$$|\beta_{ij}\rangle = \frac{1}{\sqrt{2}} (|0\ j\rangle) + (-1)^i |1\ j \oplus 1\rangle \quad (3.2)$$

From the notation in (3.1) it can be noticed that the perfect case in quantum teleportation, given when the entangled resource is equal to $|\beta_0\rangle$, is described with $p_0 = 1$ and, therefore, $p_1 = p_2 = p_3 = 0$. Nevertheless, for other cases rather than $|\beta_0\rangle$, when the entangled state is an arbitrary one, and considering the traditional teleportation algorithm running under this resource instead of the perfect case, then the output is going to be equivalent to a quantum channel whose outcome expression in terms of its Kraus operators is given by [54]:

$$\Lambda[\rho] = \sum_{i=0}^3 p_i \tilde{\sigma}_i \rho \tilde{\sigma}_i^\dagger = \sum_{i=0}^3 p_i \sigma_i \rho \sigma_i \quad (3.3)$$

with the Pauli matrices as follows: $\tilde{\sigma}_i = \sigma_i$ if $i = 0, 1, 3$ and $\tilde{\sigma}_2 = i\sigma_2$, and where $\rho = |\psi\rangle\langle\psi|$ is the density matrix of the state to be teleported. Thus, for a single teleportation channel, the corresponding Kraus operators are $K_i = \sqrt{p_i} \sigma_i$. For simplicity, it has been assumed an egalitarian variation with $p_1 = p_2 = p_3 = p$, and the complement $p_0 = 1 - 3p$. This places the constraint $0 \leq p \leq \frac{1}{3}$ on the value of p . This type of channels have been recently studied when they are combined under indefinite causal order [55].

3.2 Redundant case for teleportation with N –channels

In order to get a better understanding of causal order in the quantum teleportation algorithm, the cases where several teleportation channels are applied sequentially will be analysed here. For this case we consider, in general, a set of redundant N –channels teleportation applied in a definite causal order as composition (in addition, we consider for simplicity that each channel is identical to other in the redundant application):

$$(\bigcirc_N \Lambda)[\rho] \equiv \Lambda[\Lambda[\dots \Lambda[\rho] \dots]] = \sum_{i_1, \dots, i_n=0}^3 p_{i_1} \cdots p_{i_n} \sigma_{i_n} \cdots \sigma_{i_1} \rho \sigma_{i_1} \cdots \sigma_{i_n} \quad (3.4)$$

Now, as it has been described in section 3.1, for simplicity and in order to avoid the increasing parameters involved, the values for the entangled state will be described by $p_1 = p_2 = p_3 \equiv p$, and $p_0 = 1 - 3p$, with $0 \leq p \leq \frac{1}{3}$ (notice that when the maximum value for p is reached with $p = \frac{1}{3}$, the Bell state with which the perfect teleportation is achieved ($|\beta_0\rangle$) has no part in this scheme, thus considering a totally imperfect entangled state, and, on the

other hand, the best case is given with $p = 0$ as it has been previously set). From here, we can get the expressions for the corresponding fidelity obtained when the teleportation channels are applied in succession (without the dependence on a quantum switch), obtained from the definition for fidelity given in (2.6) but restricting it to the case for pure states, then it is denoted as:

$$\mathcal{F}_{\bigcirc_N \Lambda} \equiv \text{Tr}(\rho(\bigcirc_N \Lambda)[\rho]) \quad (3.5)$$

Therefore, from equation (3.5), an analysis can be made for the first five cases of redundant sequential applications of teleportation considering the worst case with $p = \frac{1}{3}$ and therefore $p_0 = 0$, in that case the expressions become:

$$\mathcal{F}_{\bigcirc_1 \Lambda} = 1 - 2p \quad (3.6)$$

$$\mathcal{F}_{\bigcirc_2 \Lambda} = 1 - 4p + 8p^2 \quad (3.7)$$

$$\mathcal{F}_{\bigcirc_3 \Lambda} = 1 - 6p + 24p^2 - 32p^3 \quad (3.8)$$

$$\mathcal{F}_{\bigcirc_4 \Lambda} = 1 - 8p + 48p^2 - 128p^3 + 128p^4 \quad (3.9)$$

$$\mathcal{F}_{\bigcirc_5 \Lambda} = 1 - 10p + 80p^2 - 320p^3 + 640p^4 - 512p^5 \quad (3.10)$$

notably, these polynomials have fix points in $p = 0$ and $p = \frac{1}{4}$. From equations (3.6) to (3.10), it can be noticed that those outcomes become independent from the state to be teleported given as a consequence from egalitarian probabilities on the entangled state where $p_1 = p_2 = p_3 = p = \frac{1}{3}$ for this case. In that case, a computational analysis has been developed to get last outcomes for the first five sequential cases and, furthermore, other computational analysis can be done for larger cases.

For a better representation of what happens with the fidelity \mathcal{F} as the number of channels increases, Figure 3.1 exhibits the behavior of the applications of one to five identical teleportation channels sequentially, showing the fidelity obtained as function of p . The gray zone sets the middle point where $\mathcal{F}_{\bigcirc_1 \Lambda} = \frac{2}{3}$ of a fidelity $\mathcal{F}_{\bigcirc_1 \Lambda} \in [\frac{1}{3}, 1]$ given for the specific case $N = 1$ as a reference as it was remarked in [22], being this zone the middle of the fidelity obtained when applying just one teleportation channel and, therefore, an advantage is established when this zone is surpassed or, on the other hand, when the fidelity is inside this zone (under the middle point), there is no advantage on the use of the protocol with the number of given channels.

The single case $N = 1$ sets the expected outcome about the effect of p on $\mathcal{F}_{\bigcirc_1 \Lambda}$, giving the worst value for $p = \frac{1}{3}$ (see Figure 3.1). For $N > 1$ the outcome becomes as could be expected, each application of a new teleportation worsens the output state teleported. Despite, there is certain recovery for $p = \frac{1}{3}$, useful only for low values of N . It can be observed, as the number of N increases, that a convergent value $\mathcal{F}_{N \rightarrow \infty} = \frac{1}{2}$ appears, being this the completely depolarized state.

3.3 Scheme for teleportation with indefinite causal order

The proposed scheme for teleportation under an indefinite causal order scheme is to have N teleportation channels applied back to back and controlled by the state on the control system

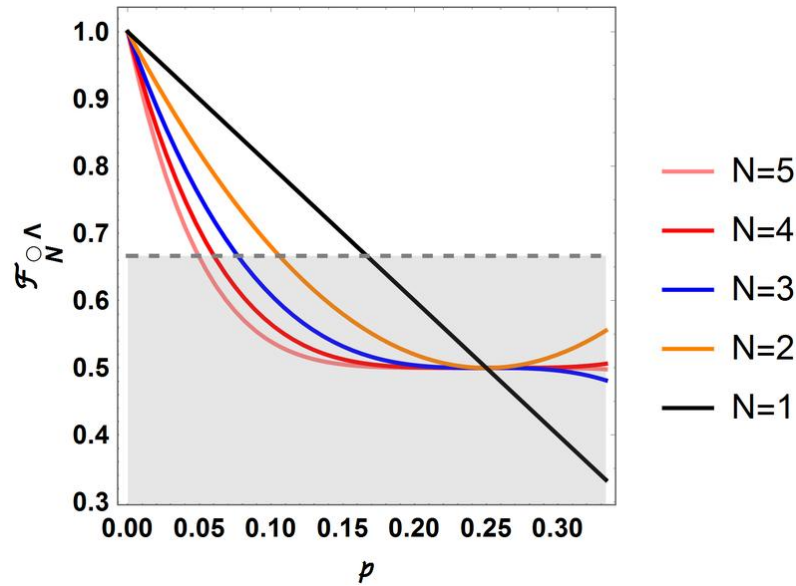


Figure 3.1: Fidelity given by the number of teleportation channels when applied sequentially for the first five sequentially applied channels.

in order to decide which channel is going to be applied first and which one then and so on. For this purpose, Figure 3.2 represents the teleportation channel encapsulated as a box simply named as T , that has only the unknown state as the entrance and at the output the same unknown state.

Now, in order to depict the application of the teleportation channels, Figure 3.3 depicts such process for two quantum teleportation channels, for a) one way of doing the teleportation process followed unambiguously considering the control system on the state $\rho_c = |0\rangle\langle 0|$ (for the specific case depicted in figure, the way followed is T_1 and then T_2), b) the order is contrary to a) when considering the state on the control system as $\rho_c = |1\rangle\langle 1|$ and finally in c) the order followed when the control qubit is a superposition of two states $|0\rangle\langle 0|$ and $|1\rangle\langle 1|$ with certain probabilities for both to succeed given by q_0 and its complement $q_1 = 1 - q_0$, the indefinite causal order depends on the value of the state on the control system.

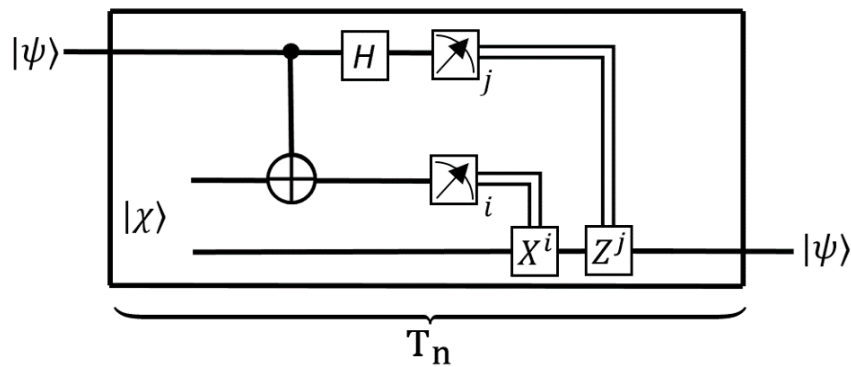


Figure 3.2: Teleportation circuit represented as a teleportation channel.

For the case of two quantum teleportation channels, such scheme considers, for simplicity, two identical teleportation channels applied in superposition and controlled by a control state, thus having T_1 , T_2 and the control state ρ_c as the elements ruling the teleportation.

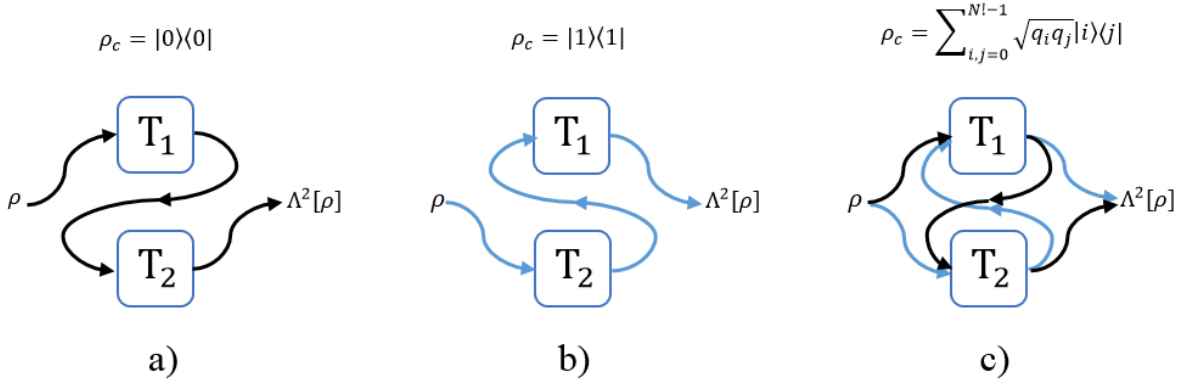


Figure 3.3: Two causal order combinations depending on the control state depicted in: a) when the control state is in $|0\rangle\langle 0|$, b) when it is in $|1\rangle\langle 1|$ and c) when the control state is a superposition of the previous states.

The Kraus operators $K_i = \sqrt{p_i} \sigma_i$ given for one teleportation channel are going to be the same for the other teleportation channel, assuming two identical channels with similar characteristics, The outcome is obtained by a final measurement on the control state, where the perfect teleportation process has been found to be reached when the measurement state is $|+\rangle = \frac{1}{\sqrt{2}}(|0\rangle + |1\rangle)$ [22].

A deeper analysis of the specific case with two teleportation channels using this scheme, which has been taken as an example for the teleportation scheme under indefinite causal order, will be held in the next section.

3.4 Teleportation with $N = 2$ teleportation channels in indefinite causal order

For the analysis of the case with two channels ($N = 2$), the teleportation process assisted by indefinite causal order has been studied and the the outcome for such process when applying two teleportation channels in an indefinite causal order has been discussed in [22, 42], where the features that come with the process are analyzed.

When applying two channels in an indefinite causal order, we will have two combinations with different orders. Thus, we will need a control state with such number of dimensions ($|0\rangle$ sets for the normal sequential order of gates T_1, T_2 and $|1\rangle$ sets the inverted order of gates T_2, T_1) to rule the application of each causal order given by:

$$\rho_c = \left(\sum_{i=0}^1 \sqrt{q_i} |i\rangle_c \right) \left(\sum_{j=0}^1 \sqrt{q_j} \langle j|_c \right) = \sum_{i,j=0}^1 \sqrt{q_i q_j} |i\rangle_c \langle j| \quad (3.11)$$

By constructing the Kraus operators for two consecutive identical teleportation channels

applied in indefinite causal order, but instead of applying a measurement on the control state based on the states $|\pm\rangle$ (as in [22]), a general measurement is applied based on the state:

$$|\psi_m\rangle = \cos\frac{\theta}{2}|0\rangle + \sin\frac{\theta}{2}e^{i\phi}|1\rangle \quad (3.12)$$

and the correspondent orthogonal state $|\psi_m^\perp\rangle = \sin\frac{\theta}{2}|0\rangle - \cos\frac{\theta}{2}e^{-i\phi}|1\rangle$. When the measurement on the control is in the state depicted in (3.12) the unnormalized output can be obtained as:

$$\begin{aligned} \Lambda_{\text{un}}^2[\rho] &= \langle\psi_m| \left(\sum_{i,j=0}^3 W_{ij}(\rho \otimes \rho_c) W_{ij}^\dagger \right) |\psi_m\rangle \\ &= \sum_{i,j=0}^3 p_i p_j \left(\left(\frac{1}{2} + (q_0 - \frac{1}{2}) \cos\theta \right) \sigma_i \sigma_j \rho \sigma_j \sigma_i + \sqrt{q_0 q_1} \sin\theta \cos\phi \sigma_i \sigma_j \rho \sigma_i \sigma_j \right) \end{aligned} \quad (3.13)$$

where $W_{ij} = K_i K_j \otimes |0\rangle_c \langle 0| + K_j K_i \otimes |1\rangle_c \langle 1|$ and the superscript 2 on the Λ refers to two channels in indefinite causal order.

From equation (3.13), we can now get the fidelity as $\mathcal{F} = \text{Tr}(\Lambda^2[\rho]\rho)$ assessing the entire process as a comparative measure between the input and the teleported states as:

$$\mathcal{F}_{\text{un}} = \sum_{i,j=0}^3 p_i p_j \left(\left(\frac{1}{2} + (q_0 - \frac{1}{2}) \cos\theta \right) \mathcal{S}_{ij}^1 + \sqrt{q_0 q_1} \sin\theta \cos\phi \mathcal{T}_{ij}^1 \right) \quad (3.14)$$

and we can also determine the probability of successful measurement as $\mathcal{P} = \text{Tr}(\Lambda^2[\rho])$, thus yielding:

$$\mathcal{P} = \sum_{i,j=0}^3 p_i p_j \left(\left(\frac{1}{2} + (q_0 - \frac{1}{2}) \cos\theta \right) \mathcal{S}_{ij}^0 + \sqrt{q_0 q_1} \sin\theta \cos\phi \mathcal{T}_{ij}^0 \right) \quad (3.15)$$

where $\mathcal{S}_{ij}^k = \text{Tr}(\rho^k \sigma_i \sigma_j \rho \sigma_j \sigma_i)$ and $\mathcal{T}_{ij}^k = \text{Tr}(\rho^k \sigma_i \sigma_j \rho \sigma_i \sigma_j)$ are the forms of the traces needed in the process which involve the Pauli matrices as well as the density matrix of the state to be teleported.

Nevertheless, the value for fidelity in (3.14) is not normalized and therefore it is required to be normalized by dividing it over the probability as follows:

$$\mathcal{F} = \frac{\sum_{i,j=0}^3 p_i p_j \left(\left(\frac{1}{2} + (q_0 - \frac{1}{2}) \cos\theta \right) \mathcal{S}_{ij}^1 + \sqrt{q_0 q_1} \sin\theta \cos\phi \mathcal{T}_{ij}^1 \right)}{\sum_{i,j=0}^3 p_i p_j \left(\left(\frac{1}{2} + (q_0 - \frac{1}{2}) \cos\theta \right) \mathcal{S}_{ij}^0 + \sqrt{q_0 q_1} \sin\theta \cos\phi \mathcal{T}_{ij}^0 \right)} \quad (3.16)$$

following the same reasoning for the values of \mathcal{S}_{ij}^k and \mathcal{T}_{ij}^k described above.

Seen graphically, in [22], it has been shown that when the measurement state on the control is in the basis $|\psi_m\rangle = |+\rangle$ the protocol can occur successfully even though the entangled state is in the worst case, and there is an advantage over just one channel applied. On the other hand, when the measurement state on the control is in the basis $|\psi_m\rangle = |-\rangle$, the protocol fails and no advantage is found there.

Such behavior is depicted in Figure 3.4, where it is notorious an advantage when the entangled state $|\chi\rangle$ is completely contaminated (considering $p = 1/3$ where no contribution of $|\beta_0\rangle$ is given) and it is shown that a fidelity $\mathcal{F} = 1$ can be still reached. The red line represent the behavior when applying just one teleportation channel where no outstanding results are found. The black line represents the sequential application of two teleportation channels, obtaining advantages regarding to just one channel when the singlet tends to be imperfect. The measurements when applying two teleportation channels in superposition of causal order have been done considering the control state with $q_0 = \frac{1}{2}$. The blue dashed lines represent the case when the measurement is with $|\psi_m\rangle = |+\rangle$ and the orange ones have been done considering $|\psi_m\rangle = |-\rangle$. Note in these lines the success of $|\psi_m\rangle = |+\rangle$ over $|\psi_m\rangle = |-\rangle$.

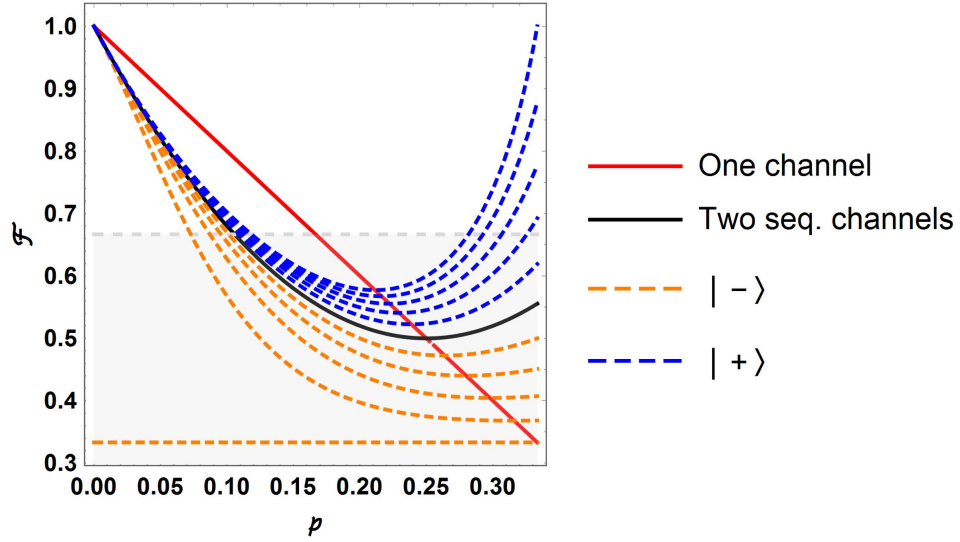


Figure 3.4: Fidelity given for the case of two channels as function of p . The blue dashed upper line corresponds to $|\psi_m\rangle = |+\rangle$ and $q_0 = \frac{1}{2}$ reaching $\mathcal{F} = 1$ in $p = \frac{1}{3}$. The orange dashed line represents the case when the protocol fails with $|\psi_m\rangle = |-\rangle$ and $q_0 = \frac{1}{2}$ and there is no advantage on the application of two channels in superposition of causal order

3.4.1 Two teleportation channels under indefinite causal order considering $p_1, p_2, p_3 \in [0, 1]$

However, for the cases described above, the main consideration has been to have all the values for p equal, except for p_0 which is the complement $p_0 = 1 - p$, and from the Figure 3.4, the best fidelity is only achieved with the worst case for the entangled state with $p = \frac{1}{3}$. However, it is important to analyse the outcomes when $\mathcal{F} = 1$ is not reached: how to make possible a perfect teleportation by varying the parameters and how the probability of success is compromised.

An analysis made considering the fidelity as function of differentiated p_1, p_2 and p_3 is in order. It means in the region with $p_1 \geq 0, p_2 \geq 0$ and $p_3 \geq 0$ and $p_1, p_2, p_3 \leq 1$ and, therefore, $p_0 = 1 - p_1 + p_2 + p_3$, notoriously, this places the constraint that $p_0 + p_1 + p_2 + p_3 = 1$.

Figure 3.5 shows, on a third part of the region, the dependence of the best fidelity from the values for p_1, p_2, p_3 (it implies an optimization was made on the initial control state and

its measurement, it means on the parameters (q_0, θ, ϕ) , the colour bar represents the fidelity (3.16). The blue zone refers to the maximum fidelity achievable when varying the values of p_i , in this case, it is notorious that $\mathcal{F} \approx 1$ can be reached in a large zone when there is no restriction for the values of p_i to be equal.

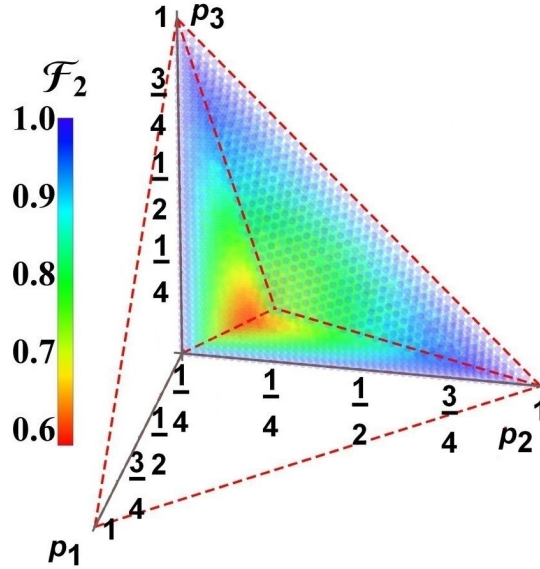


Figure 3.5: Best fidelity \mathcal{F}_2 for the two channels case as function of p_1, p_2, p_3 . Each point inside the polyhedron corresponds to their acceptable values and it is coloured in agreement with its fidelity value (see the color-scale besides); the cut of polyhedron region exhibits the inner structure.

Actually, from Figure 3.5, it seems that when the values of p_i are different, it is better for a best fidelity and not with $p_1 = p_2 = p_3 = p$ as it had been considered in the previous analysis. In fact, note that according to the graph, the cases with the worst fidelity are located in the middle of the line with $p_1 = p_2 = p_3 = p$. All these aspects, for the two cases $p_1 = p_2 = p_3 = p$ or p_i arbitrary within the region, will be analysed extensively in the next chapters together also with a more extensive application of teleportation channels, in order to identify a convenient scheme to improve the quality of teleportation assisted by indefinite causal order.

Chapter 4

Research Questions and Objectives

This chapter is focused on the main enhancements to be tackled and the approaches to be followed in order to reach the objectives aimed to solve the questions. The research questions are regarding the enhancement on the fidelity and probability of measurement. At the end of the chapter, a diagram showing the techniques used to improve the teleportation process is presented.

4.1 Research Questions

The research questions are oriented to seek for the best way to improve the teleportation process when it is assisted by indefinite causal order. These enhancements include the application of different basis in the measurement as different forms for the control state; they also include the use of more than two teleportation channels in a superposition of causal orders. It is considered as well, the analysis of different strategies using the indefinite causal order to assist the teleportation process.

Also, an experimental proposal is suggested at the end. For the last purpose, it is important to consider an experimental model when performing teleportation (e.g. quantum optics). Experimentally, the elements will vary slightly from the theoretical ones (such is the case for the entangled state used as a resource), hence, theoretical as well as experimental models are considered.

4.1.1 Improvement of the teleportation process with arbitrary control states and measurement basis

The teleportation process has been developed in [22] considering two identical channels applied in superposition of causal order with a control state for the superposition of the order. Nevertheless, there the teleportation process is treated with a specific case for the measurement basis (the measurement state $|+\rangle$ which effectively made the protocol succeed) and, moreover, the control state was supposed to have the same probabilities for the orders to happen. But it is important to analyse other control states in order to know if the protocol improves or worsens. Could it be possible to reach $\mathcal{F} = 1$ when either the measurement basis or the control state change? Within the analysis, more characteristics must be analysed, not

only the fidelity but also other aspects such the probability of successful measurement in the process.

Therefore, one of the main interests is to analyse the possibility to find a better teleportation process by changing the measurement basis in order to find an optimal case where fidelity \mathcal{F} is improved without compromise the probability \mathcal{P} . For this process, a general measurement can be analysed (in the form $|\psi_m\rangle = \cos \frac{\theta}{2} |0\rangle + \sin \frac{\theta}{2} e^{i\phi} |1\rangle$) and, by changing the values for θ and ϕ , different states on the Bloch sphere could be considered as potential measurements on the control. Together, the probabilities on the control state depicted in (3.11) can be moved trying other values q_i in the control state (controlling the superposition of orders in the teleportation channels), in order to find optimal cases with different probabilities to those in [22] enhancing the teleportation in terms of fidelity and probability.

4.1.2 Enhancements in teleportation when more than two teleportation channels in indefinite causal order are introduced

The importance of the application of indefinite causal order has been studied in [22, 42], finding the capability of indefinite causal order to aid in the teleportation process when using two channels in indefinite causal order. However, in these cases, although $\mathcal{F} = 1$ can be reached, the probability of reach this outcome is not always high and, moreover, that fidelity is only reached under the assumption of having the worst case on the entangled state described in (3.1) with $p_1 = p_2 = p_3 = p = \frac{1}{3}$.

As comparison, in communication, when a very noisy channel is used in the process (the so called depolarizing channel), all the information is lost and, it has been demonstrated that by using two depolarizing channels in indefinite causal order then the information can be actually transmitted [13, 21], and, even better, when more than two channels in indefinite causal order are applied, communication protocol improves and the quantity of information transmitted increases [23, 14]. Could also a larger number of teleportation channels under indefinite causal orders to improve the teleportation process?

Therefore, an approach based on increasing the number of teleportation channels in an indefinite causal order used in the process can be studied to analyse how the transmission of information is enhanced (in the case of teleportation, how the fidelity of teleportation is improved) as function of such number of channels.

4.2 Research objectives

4.2.1 To explore other control states and measurement control basis to improve \mathcal{F}

The main objective in the research is to improve \mathcal{F} by analysing different strategies involving indefinite causal order as a central support. Alternative intermediate measurement based strategies are also considered.

A first particular objective is to analyse a general control state together with a general basis for the control measurement instead of the measurement based on the states $|\pm\rangle$ (as in [22]) in order to observe the impact on the fidelity and success probability.

For all the cases analysed, considerations on the entangled resource (3.1) are taken into account. Both, values equal for p ($p_0 = p_1 = p_2 = p$) and values different between them ($p_1, p_2, p_3 \in [0, \frac{1}{3}]$) are analysed, so that the behavior of fidelity and success probability can be studied.

4.2.2 To explore the application of a larger number of teleportation channels in indefinite causal order to improve \mathcal{F} in the teleportation process

Since an improvement in quantum communication is given when the number of channels applied in indefinite causal order increases, the second particular objective is to analyse this larger application of N teleportation channels in superposition of causal order to enhance the process in terms of the increasing of \mathcal{F} .

In the same sense, it will be interesting to explore other combinations of indefinite causal order application along with the measurement basis in order to find the best way of doing the teleportation process with the purpose of obtaining better results for fidelity and success probability.

4.2.3 To establish a procedure in order to use indefinite causal order with improved outcomes for \mathcal{F} and \mathcal{P}_m

Strategies presented and followed have shown improvements for the fidelity in the process, nevertheless, the probability of measurement did not result outstanding. That is why this was an additional objective that emerges from a necessity found from the other objectives, where, somehow, the results obtained are optimized, but additionally an improvement on \mathcal{P}_m is sought.

In this sense, some other known elements of quantum theory of communication are necessary to be introduced in order to establish a strategy along with indefinite causal order and post-measurement to obtain an enhanced teleportation process in terms of fidelity and probability of measurement.

4.2.4 To present an insight for an experimental approach for the constructed procedure

In communication, some experimental approaches have come out as well regarding the use of indefinite causal order with partial depolarizing gates, described in theory in [23] and then, there, an improvement has been also demonstrated experimentally [14].

Nevertheless, regarding teleportation, there is a lack of information about the use of indefinite causal order assisting the teleportation process for an experimental approach. Some alternative schemes have been proposed as it is mentioned in [12], but in this case, indefinite causal order is used by trying to maintain the entangled state unaltered when it initially transit through a communication channel (entanglement distribution) to then perform the teleportation process correctly. Despite, some other approaches are necessary to more deeply analyse the use of indefinite causal order in order to improve the teleportation process.

For this reason, it is necessary to review the literature for current experimental approaches in order to analyse whether the theoretical proposal here described can be developed with the known tools. For that, here is provided an experimental proposal to corroborate the quantum teleportation assisted by indefinite causal order based on the current theoretical analysis.

4.3 General diagram for teleportation enhancement

For a more pictorial view of the objectives aimed to do, Figure 4.1 shows a diagram of a summary of the strategies pretended to be explored in order to achieve the objectives previously described, remarking that the main target is to improve the teleportation process in terms of its fidelity \mathcal{F} and probability of successful measurement \mathcal{P}_m .

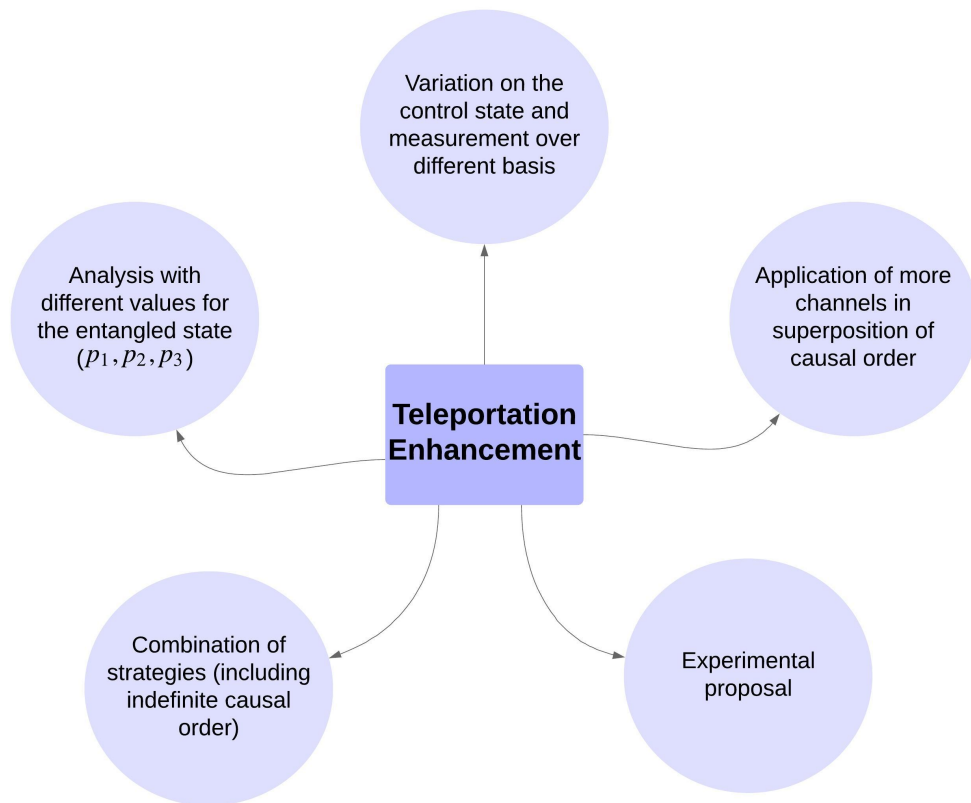


Figure 4.1: Diagram summarizing the research lines to follow in order to improve the teleportation process when it is assisted by indefinite causal order. Each branch represents each one of the main contents in this research report which will be addressed in the next chapters.

In each branch of the diagram, the strategies to follow are presented. This strategies include the analysis of variations on the control state ruling the order of the channels to be applied in teleportation as well as in the measurement state. It is also considered the application of an increasing number of channels in superposition to analyse the feasibility of such protocol. Also, variations on the entangled state assisting the teleportation are analysed and a some

other combinations in strategies including an indefinite causal order along the variation of the parameters previously described in order to enhance the teleportation algorithm. Finally, an experimental proposal is needed to test the analytical development found along the research.

With this proposal, Chapter 5 presents the analysis followed for the case with two channels in superposition of causal order with different scenario on the entangled state. Chapter 6 presents a detailed analysis when the number of channels in indefinite causal order increases. Chapter 7 proposes an experimental approach to test the data obtained in the previous chapters. Finally, the conclusions are given in the last chapter for the following of the research along the objectives proposed.

Chapter 5

Two channels in Indefinite Causal Order

In order to study the feasibility of using causal order in teleportation, here we get started by analysing the use of two channels in an indefinite causal order. In this section we will extend the analysis developed by [22] and presented in Chapter 3 in terms of the use of a more general form for the control state, thus together for the measurement basis used on it.

5.1 Formalism to set quantum teleportation under an indefinite causal order scheme with two channels

The aim is the teleportation of the unknown state:

$$|\psi\rangle = \cos \frac{\theta_0}{2} |0\rangle + \sin \frac{\theta_0}{2} e^{i\phi_0} |1\rangle \quad (5.1)$$

with the density matrix $\rho = |\psi\rangle\langle\psi|$. The imperfect entangled state assessing the teleportation $|\chi\rangle = \sum_{i=0}^3 \sqrt{p_i} |\beta_i\rangle$ is the sum of the Bell states with their corresponding probabilities p , where, for simplicity, let us start considering $p_1 = p_2 = p_3 = p$ with $p \in [0, \frac{1}{3}]$ and p_0 as the complement $p_0 = 1 - 3p$, thus allowing to have different contributions from each one of the Bell states ($|\beta_0\rangle, |\beta_1\rangle, |\beta_2\rangle$ and $|\beta_3\rangle$).

If the Bell state $|\beta_0\rangle$ is used as the successful entanglement resource, the general output of the channel is given by (3.3) with $p_0 = 1, p_1 = p_2 = p_3 = 0$ getting the perfect teleportation process. Otherwise, we can use formulas for \mathcal{F} and \mathcal{P} described in (3.14) and (3.15) [42] in order to analyse the behavior of the scheme with two channels under indefinite causal order for general cases.

The formulas given for the fidelity with two channels (\mathcal{F}_2) and the probability of the successful measurement (\mathcal{P}_m) given in (3.16) and (3.15) respectively, become reduced for pure states $\rho = |\psi\rangle\langle\psi|, |\psi\rangle = \alpha|0\rangle + \beta|1\rangle$ and $p_0 = 1 - 3p, p_1 = p_2 = p_3 = p$ considering:

$$\sum_{i,j=0}^3 p_i p_j \text{Tr}(\rho \sigma_i \sigma_j \rho \sigma_j \sigma_i) = 1 - 4p + 8p^2 \quad (5.2)$$

$$\sum_{i,j=0}^3 p_i p_j \text{Tr}(\sigma_i \sigma_j \rho \sigma_j \sigma_i) = 1 \quad (5.3)$$

$$\sum_{i,j=0}^3 p_i p_j \text{Tr}(\rho \sigma_i \sigma_j \rho \sigma_i \sigma_j) = (1 - 2p)^2 \quad (5.4)$$

$$\sum_{i,j=0}^3 p_i p_j \text{Tr}(\sigma_i \sigma_j \rho \sigma_i \sigma_j) = 1 - 12p^2 \quad (5.5)$$

Note the combination of formulas (5.2) and (5.3) gives the sequential case in (3.7). Other two terms correspond to the interference terms. Formulas (5.2) and (5.4) can be demonstrated noting that:

$$\begin{aligned} \rho &= \frac{1}{2}(\sigma_0 + \hat{n} \cdot \vec{\sigma}) \\ \text{with : } \hat{n} &= (|\alpha|^2 - |\beta|^2, \alpha\beta^* + \alpha^*\beta, i(\alpha\beta^* - \alpha^*\beta)), \\ \vec{\sigma} &= (\sigma_1, \sigma_2, \sigma_3) \end{aligned} \quad (5.6)$$

5.2 Quantum teleportation ruled by an arbitrary control state for two channels under indefinite causal order

Let us start considering the values for the probabilities of the control q_0 (described in (3.11)) different from $\frac{1}{2}$, that is $0 \leq q_0 \leq 1$ and the correspondent complement $q_1 = 1 - q_0$, in order to find the best possible basis for the control to obtain a successful teleportation. Therefore, some other measurement basis for the control state rather than $\{|-\rangle, |+\rangle\}$ cases proposed in [22] will be considered.

The fidelity for the quantum teleportation under a two channels scheme in an indefinite causal order has been described in section 3.4 with formula (3.16) for the fidelity. We can still simplify formula (3.16) using the Pauli matrices and the trace operation properties: $\text{Tr}(\sigma_i \sigma_j \rho \sigma_j \sigma_i) = 1$ and $\text{Tr}(\sigma_i \sigma_j \rho \sigma_i \sigma_j) = \delta_{ij} + (1 - \delta_{ij})(1 - 2\text{sgn}(ij)) = 1 - 2\text{sgn}(ij)(1 - \delta_{ij})$, with $\text{sgn}(ij)$ the sign function resulting on the formula:

$$\mathcal{F}_2 = \frac{\sum_{i,j=0}^3 p_i p_j \left(\left(\frac{1}{2} + (q_0 - \frac{1}{2}) \cos \theta \right) \mathcal{S}_{ij}^1 + \sqrt{q_0 q_1} \sin \theta \cos \phi \mathcal{T}_{ij}^1 \right)}{\sum_{i,j=0}^3 p_i p_j \left(\left(\frac{1}{2} + (q_0 - \frac{1}{2}) \cos \theta \right) + \sqrt{q_0 q_1} \sin \theta \cos \phi (1 - 2\text{sgn}(ij)(1 - \delta_{ij})) \right)} \quad (5.7)$$

Now, it can be shown that for the worst case where $p_1 = p_2 = p_3 = p = \frac{1}{3}$ and $p_0 = 0$ it is possible to reach a perfect teleportation ($\mathcal{F} = 1$) not only with a measurement state $|+\rangle$ but also by choosing adequately the measurement state (3.12). It can also be analysed the

case where the probabilities on the control are not equal ($q_0 = \frac{1}{2}$), but taking values for q_0 in $0 \leq q_0 \leq 1$ and $q_1 = 1 - q_0$. It can be solved numerically the optimization problem by fixing q_0 , the last p_i values and then finding the best θ and ϕ in (3.12) maximizing \mathcal{F} in (3.16).

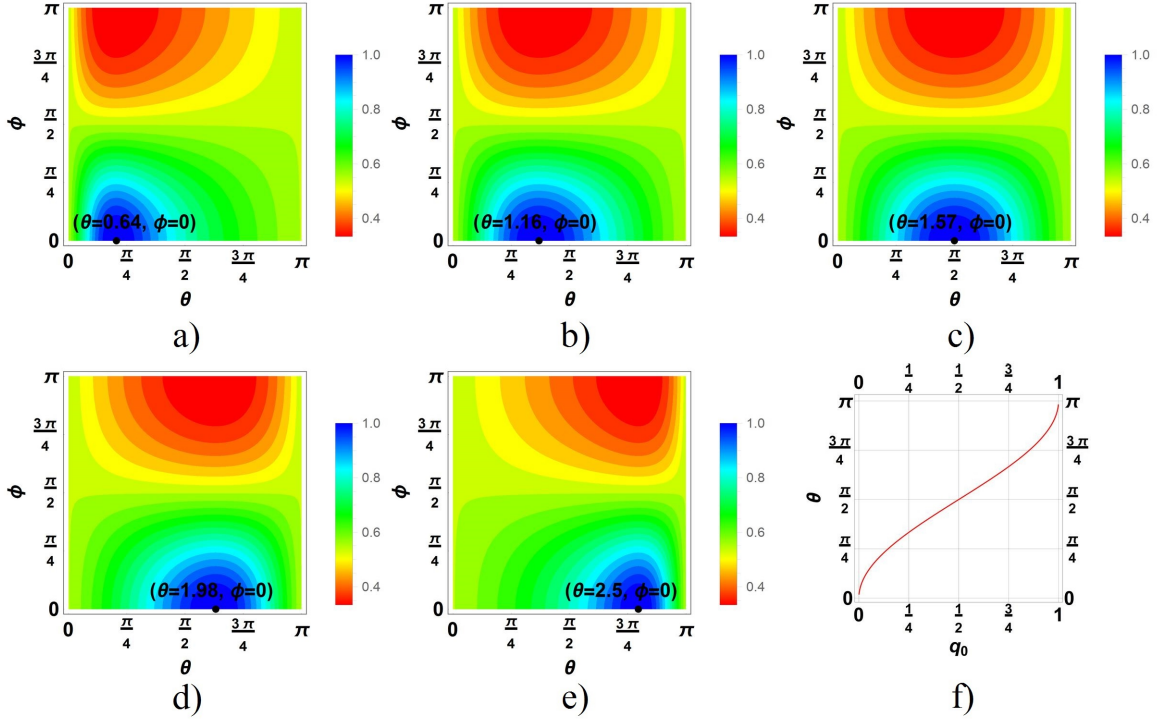


Figure 5.1: In the contour plots a) - e) for \mathcal{F}_2 , it is indicated the values for θ and ϕ such that $\mathcal{F}_2 = 1$ is reached ($q_0 = 0.1, 0.3, 0.5, 0.7, 0.9$ and $\mathcal{P} = 0.12, 0.28, 0.33, 0.28, 0.12$ respectively). Color bar shows the values of fidelity. Plot f) exhibits the relation between θ and q_0 under the election of the best control measurement ($\phi = 0$ always).

Figure 5.1 shows some illustrative graphs where $\mathcal{F}_2 = 1$ is reached by varying the measurement state. Contour plots a) - e) correspond to different values on the control state ruling the order in superposition with $q_0 = 0.1, 0.3, 0.5, 0.7$ and 0.9 deploying the fidelity values for the entire measurement states (3.12) in the Bloch representation in agreement with the color bar besides. The best state ($\mathcal{F}_2 = 1$) is marked with a black dot stating the corresponding values of θ and ϕ . The case in [22] has the best $\mathcal{P} = 0.33$. Note 5.1c corresponds to the case analyzed in [22] where $|\psi_c\rangle = |+\rangle$ as optimal measurement. Plot 5.1f shows θ versus q_0 (note $\phi = 0$ in all cases), despite it has been obtained numerically, it can be inferred that the relation between θ and q_0 is:

$$q_0 = \frac{1}{2}(1 - \cos \theta) \quad (5.8)$$

and if (5.8) is substituted in (5.7), the value for fidelity is effectively 1, therefore, $\mathcal{F}_2 = 1$ can be still reached even though the values on the control are not necessarily $q_0 = \frac{1}{2}$ and the measurement state in the basis $|\pm\rangle$, but also by choosing correctly those values. In this case, the value of \mathcal{P}_m is:

$$\mathcal{P}_m = \frac{4}{3}q_0(1 - q_0) \quad (5.9)$$

which the maximum value is $\mathcal{P}_m = \frac{1}{3}$ for $q_0 = \frac{1}{2}$ (the value reported by [22]). Let us remark that in all cases in the Figure 5.1, the values p for the entangled state are equal to $\frac{1}{3}$, for that, the case where $p \neq \frac{1}{3}$ will be analysed in the following.

5.3 Two quantum channels in indefinite causal order with an entangled state with $p \in [0, \frac{1}{3}]$

It can be asked about the best performance for cases where $p \neq \frac{1}{3}$. Unfortunately, the situation is not optimal there. Plot 5.2a shows the best fidelity found for a case in this situation with $p = \frac{1}{6}$ and $q_0 = \frac{1}{4}$ where $\mathcal{F} = 0.60$ is obtained with a respective probability $\mathcal{P} = 0.28$, thus obtaining that the optimal case does not give $\mathcal{F}_2 = 1$. In fact, surprisingly the outcome is independent from q_0 : once selected the p -value, the best fidelity becomes fixed. Thus, Figure 5.2b reproduces the curve reported in Figure 2 of [22] for the $q_0 = \frac{1}{2}$ case. Nevertheless, for other values for q_0 rather than $q_0 = \frac{1}{2}$, the scheme does not improve, even though using the optimal measurement basis, and, therefore, \mathcal{F}_2 is not better for other values of q_0 . The dependence of θ with p and q_0 is reported in the Figure 5.2b, the same than in Figure 5.1f which denotes the independence from p .

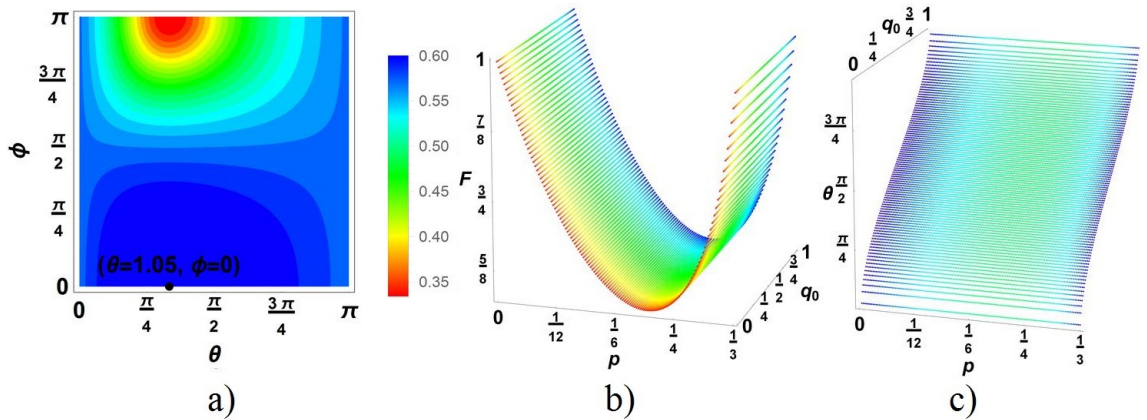


Figure 5.2: Outcomes for the fidelity \mathcal{F} for other values of p different from $\frac{1}{3}$. a) Shows the contour plot for \mathcal{F} for $p = \frac{1}{6}$ and $q_0 = \frac{1}{4}$; b)-c) depicts the dependence of \mathcal{F} and θ from p and q_0 .

However, for the case $N = 2$, [42] has shown that for different values of $q_0 = \frac{1}{2}$, other measurements $|\psi_m\rangle = \cos \frac{\theta}{2} |0\rangle + \sin \frac{\theta}{2} e^{i\phi} |1\rangle$ are possible in order to achieve $\mathcal{F}_2 = 1$ when $p = \frac{1}{3}$ giving $\phi = 0$ and θ distributed as in the Figure 5.3 as function of q_0 . Thus, best fidelities \mathcal{F}_2 depends entirely from p (see the color-scale besides in Figure 5.3) but the corresponding values of \mathcal{P}_m go down far from $q_0 = \frac{1}{2}$ ($\theta = \frac{\pi}{2}$). The red dotted line is the threshold setting the minimum fidelity reached in the optimal case for $p = \frac{3-\sqrt{3}}{6}$, $\mathcal{F}_2 = \frac{1}{\sqrt{3}}$. Thus, the conclusion

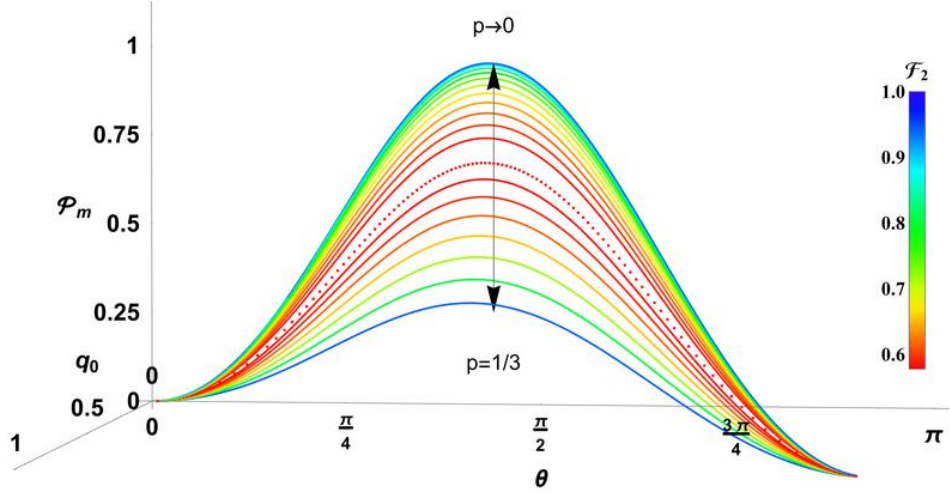


Figure 5.3: Condensed outcomes for the case $N = 2$. The respective probability \mathcal{P}_m of measurements are included as function of q_0 and θ in $|\psi_m\rangle = \cos \frac{\theta}{2} |0\rangle + \sin \frac{\theta}{2} e^{i\phi} |1\rangle$ ($\phi = 0$ in the optimal measurement). Fidelity depends entirely from p and \mathcal{P}_m goes down while $p \rightarrow \frac{1}{3}$.

is that for $p = p_1 = p_2 = p_3$, the best state for the control is $q_0 = \frac{1}{2}$ in order to maximize \mathcal{P}_m , despite only for $p = \frac{1}{3}$ and $p \rightarrow 0$ it is possible to approach $\mathcal{F}_2 \rightarrow 1$.

In these schemes, all the cases are considered to have $p_1 = p_2 = p_3 = p$ and their values are considered both equal to $\frac{1}{3}$ and in the interval $[0, 1]$, but all the values remain the same for the three p , then, it is important to analyse other values where p are different between them.

5.4 Two quantum channels in indefinite causal order with an entangled state with $p_1, p_2, p_3 \in [0, 1]$

Fidelity (3.16) can be still analysed for independent values of p_1, p_2, p_3 . Figure 5.4 shows a numerical analysis to search the best possible fidelity (achieved for certain teleported state) $\max_{|\psi_m\rangle, q_0}(\mathcal{F}_2)$ for all possible $|\psi_m\rangle$ and $0 \leq q_0 \leq 1$. The value of fidelity \mathcal{F}_2 is represented in color in agreement with the color-scale bar besides. Figure 5.4a shows a cut from the entire plot showing the inner core where fidelity goes down (three parts are almost symmetric). The higher values of fidelity on the faces of polyhedron suggest that better solutions can be reached for other cases with unequal values of $p_i, i = 1, 2, 3$. The case $p_1 = p_2 = p_3 \equiv p$ falls in the central red dashed division crossing the clearer core reflecting the outcome in Figure 3.4 where not good values of \mathcal{F}_2 are inevitably obtained far from $p = 0$ and $p = \frac{1}{3}$.

In addition, complementary information for such cases is given by \mathcal{P}_m in Figure 5.4b, the probability to reach the corresponding higher fidelity in each process assisted by an intermediate optimal measurement on the control qubit. Plot depicts disperse outcomes barely around of $\mathcal{P}_m \approx 0.5$. By performing a numerical statistics of our outcomes for each \mathcal{P}_m , we get an approximation to its statistical distribution $\rho_{\mathcal{P}_m}$ included in the upper inset. This distribution shows a symmetric behavior around of $\mathcal{P}_m = 0.5$ as it could be expected.

All in all, even though a $\mathcal{F}_2 = 1$ can be reached with two quantum channels in superposition of causal order, the probability of measurement \mathcal{P}_m is compromised as it has been

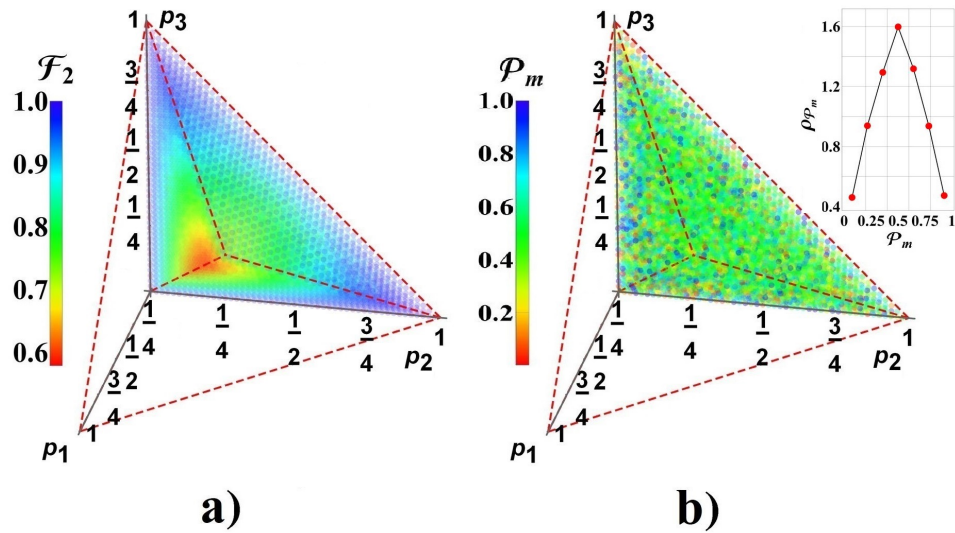


Figure 5.4: a) Best fidelity \mathcal{F}_2 for the two channels case as function of p_1, p_2, p_3 . Each point inside the polyhedron corresponds to their acceptable values and it is coloured in agreement with its fidelity value (see the color-scale besides); the cut of polyhedron region exhibits the inner structure; b) The corresponding values for measurement probabilities \mathcal{P}_m denoting disperse values around 0.5. The upper inset confirms the statistical distribution $\rho_{\mathcal{P}_m}$ exhibiting symmetry around $\mathcal{P}_m = 0.5$.

shown in Figure 5.4 to be around $\mathcal{P}_m = 0.5$ and, therefore, some other schemes for enhancing the teleportation process must be considered using more gates in superposition of causal order, which will be part of the next chapter. It can also be considered the same scheme with two channels but implementing additional modifications to the simply application of causal order.

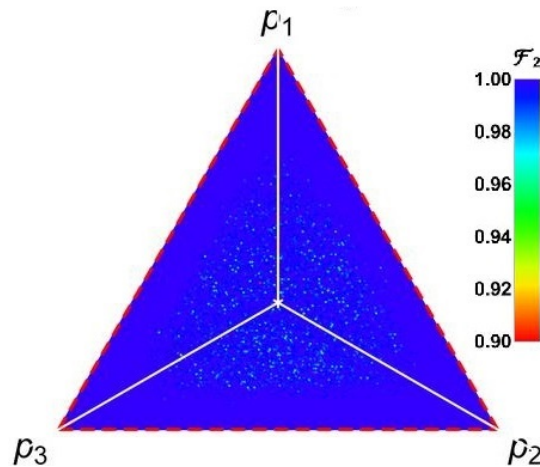


Figure 5.5: Best fidelity \mathcal{F}_2 for the two channels case as function of p_1, p_2, p_3 in the frontal face.

Actually, a numerical analysis for the two teleportation channels scenario in superposition of causal order can be realized. Figure 5.5 shows 10^5 states covering the frontal face, thus, the best fidelity is obtained using two teleportation channels under indefinite causal order by taking the optimal measurement on the control state together with the best state able to be teleported. It can be then inferred from Figure 5.5 that the most of the values at the frontal face are $\mathcal{F}_2 \approx 1$, thus representing the best possible scenario. Therefore, an analysis based only on the frontal face can be considered in particular related to the values of \mathcal{P}_m . This same result found for two channels also occurs for N -channels in superposition of causal order.

From here, note that the perfect teleportation can be reached with the application of two channels under an indefinite causal order, unfortunately, \mathcal{P}_m reduces as the value of p rises, therefore it is necessary a deeper analysis with other approaches in order to improve \mathcal{P}_m but without compromise the fidelity.

Chapter 6

N -channels in Indefinite Causal Order

Now the aim is to continue applying the idea when two channels are applied under an indefinite causal order controlled by a control system. In this case, when more than two channels are applied is studied in order to look for enhancements to \mathcal{P}_m but maintaining the best fidelity possible, since it has been shown that a perfect teleportation can be reached with only $N = 2$ channels in superposition of indefinite causal order but \mathcal{P}_m can be compromised.

6.1 Preliminaries to the analysis of the teleportation process with N -channels under indefinite causal order

When applying N channels in an indefinite causal order, there will be $N!$ combinations with different orders and, for this case, the control for the process will have such $N!$ number of dimensions to rule the application of each one of the orders (where particularly $|0\rangle$ will denote the normal sequential order of gates T_1, T_2, \dots, T_N). Similarly to (3.11) but now for N -channels, the control ruling the application of each causal order is given by:

$$\rho_c = \left(\sum_{i=0}^{N!-1} \sqrt{q_i} |i\rangle_c \right) \left(\sum_{j=0}^{N!-1} \sqrt{q_j} \langle j|_c \right) = \sum_{i,j=0}^{N!-1} \sqrt{q_i q_j} |i\rangle_c \langle j| \quad (6.1)$$

By defining a causal order of teleportation channels $T_{i_1}, T_{i_2}, \dots, T_{i_N}$ that are given by the element $\pi_k \in \Sigma_N$ in the symmetric group of permutations Σ_N , the effect will be:

$$\pi_k = \begin{pmatrix} T_{i_1} & T_{i_2} & \dots & T_{i_N} \\ T_{i_{j_1}} & T_{i_{j_2}} & \dots & T_{i_{j_N}} \end{pmatrix} \rightarrow \pi_k(K_{i_1} K_{i_2} \dots K_{i_N}) = K_{i_{j_1}} K_{i_{j_2}} \dots K_{i_{j_N}} \quad (6.2)$$

and symbolically corresponding to the control state $|k\rangle_c$, the corresponding Kraus operators W_{i_1, i_2, \dots, i_N} are:

$$W_{i_1, i_2, \dots, i_N} = \sum_{k=0}^{N!-1} \pi_k(K_{i_1} K_{i_2} \dots K_{i_N}) \otimes |k\rangle_c \langle k| \quad (6.3)$$

where $\pi_0(K_{i_1} K_{i_2} \dots K_{i_N}) = K_{i_1} K_{i_2} \dots K_{i_N}$. Thus, using (6.3) the output for N -channels in superposition of causal order is given by:

$$\begin{aligned}
\Lambda^N [\rho \otimes \rho_c] &= \sum_{i_1, \dots, i_N} W_{i_1, i_2, \dots, i_N} \rho \otimes \rho_c (W_{i_1, i_2, \dots, i_N})^\dagger \quad (6.4) \\
&= \sum_{i_1, \dots, i_N} \left(\sum_k \pi_k (K_{i_1} K_{i_2} \dots K_{i_N}) |k\rangle \langle k| \right) \rho \otimes \rho_c \left(\sum_{k'} \pi_{k'} (K_{i_1} K_{i_2} \dots K_{i_N}) |k'\rangle \langle k'| \right)^\dagger \\
&= \sum_{i_1, \dots, i_N} p_{i_1} \dots p_{i_N} \left(\sum_k \pi_k (\sigma_{i_1} \dots \sigma_{i_N}) |k\rangle \langle k| \right) \rho \otimes \rho_c \left(\sum_{k'} \pi_{k'}^\dagger (\sigma_{i_1} \dots \sigma_{i_N}) |k'\rangle \langle k'| \right) \\
&= \sum_{\substack{i_1, \dots, i_N \\ k, k'}} p_{i_1} \dots p_{i_N} \sqrt{q_k q_{k'}} |k\rangle \langle k'| \otimes \pi_k (\sigma_{i_1} \dots \sigma_{i_N}) \rho \pi_{k'}^\dagger (\sigma_{i_1} \dots \sigma_{i_N}) \quad (6.5)
\end{aligned}$$

hereafter, the tensor product \otimes will be suppressed in the notation for simplicity. Still, using the combinatorics and the properties of Pauli matrices, we can address last formula to reach a simpler expression, by noting that the i_j , with $j = 1, 2, \dots, N$, indices can allow to reorder the sums by putting them together. For instance, for the case $N = 2$ with $K_0 K_0$ it will result in $t_0 = 2, t_1 = 0, t_2 = 0$ and $t_3 = 0$. This case is explained with $N = 2$, because when working with $N > 2$ it would be very large. Actually, by noting that the sum in (6.5) including all different values given to i_1, i_2, \dots, i_N can be changed as follows:

$$\sum_{i_1=0}^3 \sum_{i_2=0}^3 \dots \sum_{i_N=0}^3 \rightarrow \sum_{t_1=0}^N \sum_{t_2=0}^{N-t_1} \sum_{t_3=0}^{N-t_1-t_2} \sum_{p=1}^{N'} \quad (6.6)$$

where t_j is the number of scripts in i_1, i_2, \dots, i_N equal to j ($t_0 = N - t_1 - t_2 - t_3$). Sum over p runs on the distinguishable arrangements obtained with a fix number t_j of operators σ_j and $N' = \frac{N!}{t_0! t_1! t_2! t_3!}$ by means of a certain permutation $\pi_{k_p^{t_1, t_2, t_3}}$. In such case, formula (6.5) can be written as:

$$\begin{aligned}
\Lambda^N [\rho \otimes \rho_c] &= \sum_k \sum_{k'} \sqrt{q_k q_{k'}} |k\rangle \langle k'| \sum_{t_1=0}^N \sum_{t_2=0}^{N-t_1} \sum_{t_3=0}^{N-t_1-t_2} \prod_{j=0}^3 p_j^{t_j} \otimes \quad (6.7) \\
&\quad \sum_{p=1}^{N'} \pi_k \left(\pi_{k_p^{t_1, t_2, t_3}} (\sigma_0^{t_0} \sigma_1^{t_1} \sigma_2^{t_2} \sigma_3^{t_3}) \right) \rho \left(\pi_{k'} \left(\pi_{k_p^{t_1, t_2, t_3}} (\sigma_0^{t_0} \sigma_1^{t_1} \sigma_2^{t_2} \sigma_3^{t_3}) \right) \right)^\dagger
\end{aligned}$$

which provides a formula for $\Lambda^N [\rho \otimes \rho_c]$ in terms of a definite number of sums and with the teleported state almost separated from the control state. Note in this notation, the superscript N in Λ refers to N channels in indefinite causal order. Using the properties of Pauli matrices algebra, it is clear that both permutation terms besides ρ in (6.7) becomes equal until a sign and in addition each one are in the set $\{\sigma_j | j = 0, 1, 2, 3\}$. Thus, (6.7) becomes a mixed state obtained as a linear combination of syndromes $\sigma_j \rho \sigma_j$, $j = 0, 1, 2, 3$ together and normally entangled with the control state.

Following to [22], then we select an adequate basis to perform a measurement for the control state, which for the general case will be given for $\mathcal{B} = \{|\psi_{M_i}\rangle | i = 1, 2, \dots, N!\}$. In

such basis we hope to find a privileged state $|\psi_m\rangle \in \mathcal{B}$ to maximize the fidelity in a process with N -channels in superposition of causal order given by:

$$\mathcal{F}_N = \frac{\text{Tr}(\rho\langle\psi_m|\Lambda^N[\rho \otimes \rho_c]|\psi_m\rangle)}{\mathcal{P}_m} \quad (6.8)$$

and with probability of successful measurement \mathcal{P}_m , also for N -channels in an indefinite causal order, given by:

$$\mathcal{P}_m = \text{Tr}(\langle\psi_m|\Lambda^N[\rho \otimes \rho_c]|\psi_m\rangle) \quad (6.9)$$

Such process for N -channels is depicted by Figure 6.1 where $N!$ causal orders are considered to arrive to the pictorial representation of a complete superposition of causal orders on the right. Each teleportation channel is represented by T_i and each causal order corresponds to a definite order in the application of channels T_i ruled by the control state ρ_c above it.

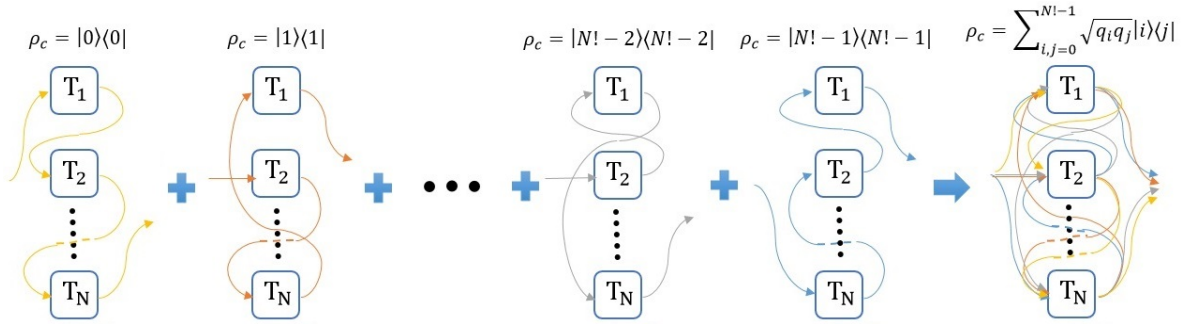


Figure 6.1: $N!$ causal order combinations for N identical teleportation channels T_i , $i = 1, 2, \dots, N$ conforming finally a superposition of those causal orders. Each one is ruled by the control state above.

In (6.9), \mathcal{P}_m sets the probability of success of the process. If the measurement of control does not conduct to $|\psi_m\rangle$ then other undesired teleportation outcome will be obtained. Then, if the desired outcome is not obtained, we disregard the output state.

6.2 Analysis of quantum teleportation when increasing the number of channels applied

Formula (6.7) exhibits superposition of terms finally involving the states $\rho, \sigma_1\rho\sigma_1, \sigma_2\rho\sigma_2$ and $\sigma_3\rho\sigma_3$ while they become entangled with the control state ρ_c . In the next sections we deal with two cases of interest for the use of the teleportation algorithm under indefinite causal order.

6.2.1 Case $p_1 = p_2 = p_3 \equiv p$

We will address first the case with $p = p_1 = p_2 = p_3$ widely used in the literature for its simplicity. In [22], it has been suggested that for $|\psi_m\rangle$ having one of the following forms:

$$|\varphi_m^\pm\rangle \equiv \frac{1}{\sqrt{N!}} \sum_{i=0}^{N!-1} (\pm 1)^{\sigma(\pi_i)} |i\rangle \quad (6.10)$$

the teleportation fidelity becomes optimal. There, σ is the signature of the parity of each order $|i\rangle$. By considering (6.7) together with (6.10) and the control state with $q_k = \frac{1}{N!} \forall k = 0, 1, \dots, N! - 1$:

$$\begin{aligned} \langle \varphi_m^\pm | \Lambda^N [\rho \otimes \rho_c] | \varphi_m^\pm \rangle &= \sum_k \sum_{k'} \frac{1}{N!^2} (\pm 1)^{\sigma(\pi_k) + \sigma(\pi_{k'})} \sum_{t_1=0}^N \sum_{t_2=0}^{N-t_1} \sum_{t_3=0}^{N-t_1-t_2} \prod_{j=0}^3 p_j^{t_j} \cdot \\ &\sum_{p=1}^{N'} \pi_k \left(\pi_{k_p}^{t_1, t_2, t_3} \left(\sigma_0^{t_0} \sigma_1^{t_1} \sigma_2^{t_2} \sigma_3^{t_3} \right) \right) \rho \left(\pi_{k'} \left(\pi_{k_p}^{t_1, t_2, t_3} \left(\sigma_0^{t_0} \sigma_1^{t_1} \sigma_2^{t_2} \sigma_3^{t_3} \right) \right) \right)^\dagger \end{aligned} \quad (6.11)$$

Then, we have developed the formulas (6.5) and (6.8) with $|\psi_m\rangle = |\varphi_m^\pm\rangle$ in (6.10) to get both \mathcal{F}_N and \mathcal{P}_N for $N = 2, 3, 4$, those formulas (reported in Appendix A) have been plotted, the outcomes are shown in Figure 6.2 showing that a perfect fidelity $\mathcal{F}_N = 1$ for $p = \frac{1}{3}$ is achieved when $|\varphi_m^\pm\rangle$ meets with the same parity to N (p is indicated in the color-scale besides). Despite, for $p = \frac{1}{3}$ the success probabilities \mathcal{P}_m decrease while N increases. For $|\varphi^- \rangle$ and $N = 4$, we get $\mathcal{P}_m = 0$, thus \mathcal{F}_4 becomes undefined in such case. While $p \in [0, \frac{1}{6}]$ the best election is the single teleportation channel, for $p \in [\frac{1}{6}, \frac{1}{3}]$, the assistance of the causal order becomes an alternative to enhance the fidelity of teleportation, particularly with $N = 3$ channels.

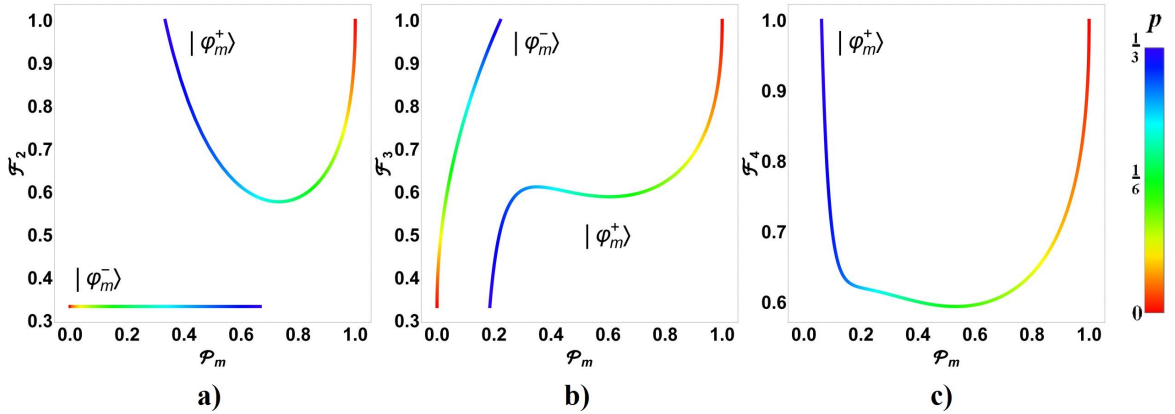


Figure 6.2: Probability \mathcal{P}_m to obtain different values of fidelity \mathcal{F}_N when the measurement states $|\varphi_+\rangle$ or $|\varphi_-\rangle$ are applied for cases a) $N = 2$, b) $N = 3$ and c) $N = 4$. Color-scale bar depicts the respective value for p for $N = 2, 3, 4$.

Figure 6.3 compares again the fidelity \mathcal{F}_N versus p for both measurements compared with the corresponding sequential case showing the alternated optimization of \mathcal{F}_N as function of the parity of N and $|\varphi_m^\pm\rangle$. Despite, the outcomes in Figure 5.4 suggest to analyse the behavior of \mathcal{F}_N for independent values of p_1, p_2, p_3 .

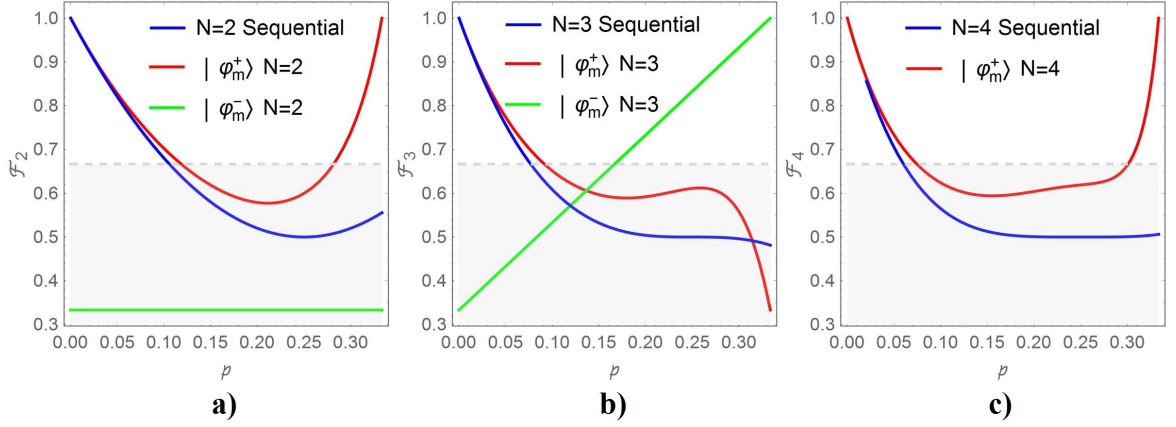


Figure 6.3: Comparison of Fidelity obtained when the channels are applied sequentially and with causal order depending on the measurement state.

6.2.2 Case $p_j \ll 1$, $j = 1, 2, 3$

In some practical models, the expected values for the entangled resource $|\chi\rangle$ vary slightly from a perfect entangled state: $p_j \ll 1$ for $j = 1, 2, 3$. Thus, the outcome described through formula (6.7) becomes in this case (developing to first order for p_j , $j = 1, 2, 3$ the factor $\prod_{j=0}^3 p_j^{t_j}$ there):

$$\Lambda^N[\rho \otimes \rho_c] \approx \left[\left(1 - N \sum_{j=1}^3 p_j \right) \rho + N \sum_{j=1}^3 p_j \sigma_j \rho \sigma_j \right] \otimes \rho_c \equiv \rho_{out} \otimes \rho_c \quad (6.12)$$

note that under this approximation, ρ_c becomes unaltered and uncoupled from the system state. Thus, the optimal way to teleport the state implies to measure the control state considering $|\psi_m\rangle = \sum_k \sqrt{q_k} |k\rangle$. In the following we assume such optimal measurement made on the control state.

For the particular case where $p_j = \frac{1}{4N}$ with $j = 1, 2, 3$, last formula can be written as:

$$\Lambda^N[\rho \otimes \rho_c] \approx \frac{1}{2} \sigma_0 \otimes \rho_c \quad (6.13)$$

obtaining the totally depolarized state $\frac{1}{2} \sigma_0$. Notice it is only applicable for very large values of N (due to the assumption $p_j \ll 1$, $j = 1, 2, 3$). This aspect is advised in the Figure 6.2 where the fidelity drops more rapidly to $\frac{1}{2}$ when N grows.

In general, the probability and fidelity given in (6.12) will become respectively (developing to first order in p_j , $j = 1, 2, 3$):

$$\mathcal{P}_m \approx \text{Tr}[\rho_{out}] = 1 \quad (6.14)$$

$$\begin{aligned} \mathcal{F}_N &\approx \frac{\text{Tr}[\rho\rho_{out}]}{\mathcal{P}_m} = 1 - N \sum_{j=1}^3 p_j(1 - n_j^2) \\ &\equiv 1 - N p_{ts} \sum_{j=1}^3 \alpha_j(1 - n_j^2) \equiv 1 - N p_{ts} \Delta_{\theta,\phi}^{\alpha_1,\alpha_2,\alpha_3} \end{aligned} \quad (6.15)$$

where the quantity $\Delta_{\theta,\phi}^{\alpha_1,\alpha_2,\alpha_3} = \sum_{j=1}^3 \alpha_j(1 - n_j^2)$ represents a variation depending on the values $\alpha_1, \alpha_2, \alpha_3, \theta$ and ϕ , and ρ was written as in (5.6). We have introduced the reduced parameters $\alpha_j \in [0, 1]$ and the threshold probability $p_{ts} \ll 1$ to limit the validity of the current approximation ($p_j = p_{ts}\alpha_j \ll 1, j = 1, 2, 3$). We note in any case that an increasing of N worsens the fidelity. Note each term in the sum in (6.15) is non-negative, thus the fidelity becomes commonly reduced. Because only one of $n_j^2, j = 1, 2, 3$ could be one at the time, then it is necessary two p_j become zero to get $\mathcal{F}_N = 1$. Otherwise, $\mathcal{F}_N < 1$ with a near decreasing if N is large. The outcome in (6.14) exhibits a combinations of the three error-syndromes $\sigma_1\rho\sigma_1, \sigma_2\rho\sigma_2, \sigma_3\rho\sigma_3$ reflected through the terms $\alpha_j(1 - n_j^2)$ as function of α_j . Thus, for each syndrome $\sigma_j\rho\sigma_j$ the best states being teleported are those closer to the eigenstates of σ_j , otherwise while several $\alpha_j \neq 0$ the teleportation capacity becomes reduced.

Considering $\rho = |\psi\rangle\langle\psi|$ with $|\psi\rangle = \cos\frac{\theta}{2}|0\rangle + \sin\frac{\theta}{2}e^{i\phi}|1\rangle$ on the Bloch sphere: $n_1 = \sin\theta\cos\phi, n_2 = \sin\theta\sin\phi, n_3 = \cos\theta$. Then, we analyse each syndrome and its impact on the fidelity through the quantity $\Delta_{\theta,\phi}^{\alpha_1,\alpha_2,\alpha_3}$, as lower it becomes, higher becomes \mathcal{F}_N . Figure 6.4a shows the simple behavior of $\Delta_{\theta,\phi}^{\alpha_1,\alpha_2,\alpha_3}$ for each state on the Bloch sphere under each syndrome: $p_1 = 1, p_2 = p_3 = 0, p_2 = 1, p_1 = p_3 = 0$ and $p_3 = 0, p_1 = p_2 = 0$ in such order. We are denoted as $|0_j\rangle$ and $|1_j\rangle$ to the eigenstates of $\sigma_j, j = 1, 2, 3$. Note the behavior commented in the previous paragraph.

Despite, the most interesting issue is centered in the fact that the entanglement resource $|\chi\rangle$ is normally unknown but with a tiny variation of $|\beta_0\rangle$ through the deformation parameters p_1, p_2, p_3 . By calculating the average and the standard deviation of $\Delta_{\theta,\phi}^{\alpha_1,\alpha_2,\alpha_3}$ on the parameters $\alpha_1, \alpha_2, \alpha_3 \in [0, 1]$:

$$\mu_{\Delta_{\theta,\phi}^{\alpha_1,\alpha_2,\alpha_3}} = \int_0^1 \int_0^1 \int_0^1 \Delta_{\theta,\phi}^{\alpha_1,\alpha_2,\alpha_3} d\alpha_1 d\alpha_2 d\alpha_3 = 1 \rightarrow \mu_{\mathcal{F}_N} = 1 - N p_{ts} \quad (6.16)$$

$$\begin{aligned} \sigma_{\Delta_{\theta,\phi}^{\alpha_1,\alpha_2,\alpha_3}} &= \sqrt{\mu_{\Delta_{\theta,\phi}^{\alpha_1,\alpha_2,\alpha_3}}^2 - \mu_{\Delta_{\theta,\phi}^{\alpha_1,\alpha_2,\alpha_3}}^2} \\ &= \frac{1}{8\sqrt{6}} \sqrt{53 + \sin^4(\theta) \cos(4\phi) + 4 \cos(2\theta) + 7 \cos(4\theta)} \end{aligned} \quad (6.17)$$

$$\begin{aligned} &\in \left[\frac{1}{3}, \frac{1}{\sqrt{6}}\right] \\ &\rightarrow \sigma_{\mathcal{F}_N} = N p_{ts} \sigma_{\Delta_{\theta,\phi}^{\alpha_1,\alpha_2,\alpha_3}} \end{aligned} \quad (6.18)$$

we note that the average value of fidelity $\mathcal{F}_N = 1 - N p_{ts}$ becomes independent from the state being teleported. While, the dispersion for $\Delta_{\theta,\phi}^{\alpha_1,\alpha_2,\alpha_3}$ on the values p_1, p_2, p_3 depends from the

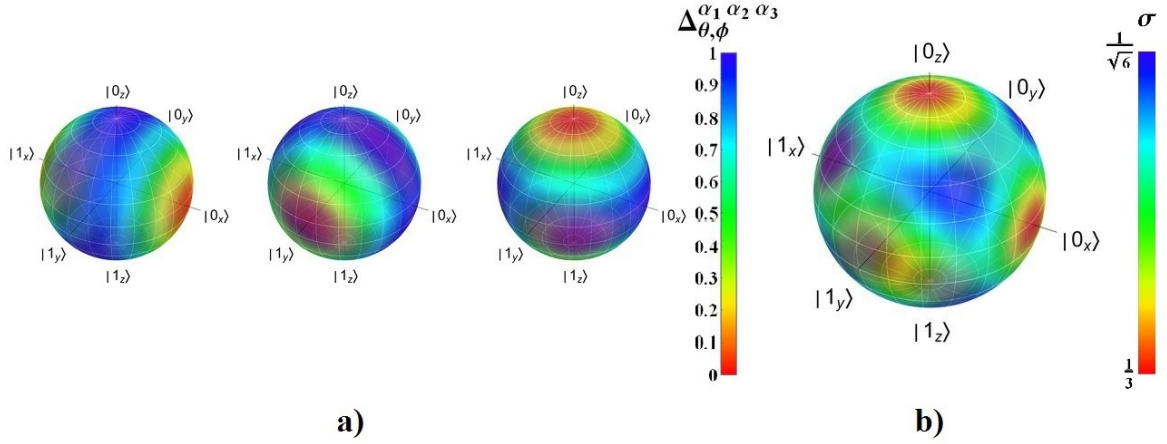


Figure 6.4: Bloch sphere showing under the assumption $p_j \ll 1$, $j = 1, 2, 3$ for each state: a) $\Delta_{\theta,\phi}^{\alpha_1,\alpha_2,\alpha_3}$ in color obtained for each syndrome in (6.12), $\sigma_1\rho\sigma_1$, $\sigma_2\rho\sigma_2$, $\sigma_3\rho\sigma_3$ respectively, and b) the standard deviation $\sigma_{\Delta_{\theta,\phi}^{\alpha_1,\alpha_2,\alpha_3}}$ in (6.18). Red is the best fidelity in a) and the lower dispersion in b).

teleported state and it becomes lowest for the eigenstates of $\sigma_1, \sigma_2, \sigma_3$. In fact, the exact result for the case of $N = 1$ is precisely (6.15) with such value in (3.3): $\mathcal{F}_1 = 1 - \sum_{j=1}^3 p_j(1 - n_j^2)$, thus the values in (6.18) are scaled from it by a factor N . The reason is easily noticed, the ρ_{out} in (6.12) obtained by linearization from (6.8) coincides with the sequential case (3.4) under linearization, so both cases exactly meet under the current limit. It implies that indefinite causal order in teleportation become unpractical in this limit.

So far, as a first conclusion, it can be noticed that, the teleportation process seems to be better for the case with only two channels in superposition of causal order since when applying a larger number of channels, the fidelity worsens. For the case where the values for p in the entangled state are equal, the optimal case is where $p = \frac{1}{3}$ with $p_0 = 0$ so the protocol can proceed successfully, for other cases rather than $p = \frac{1}{3}$, let p be $p \in [0, \frac{1}{3}]$, $\mathcal{F} = 1$ can not be reached. Also, for the case when $p \ll 1$, the results remain the same as the case when the teleportation channels are applied sequentially and, therefore, no advantage is observed. All in all, the best case seems to be to apply two channels in superposition of causal order and, in order to enhance the process, differentiated values on the p have to be proved.

6.2.3 Notable behavior on the frontal face of the parametric region: case $p_0 = 0$

Due to the previous successful outcomes for teleportation when $p = \frac{1}{3} = p_1 = p_2 = p_3$, we extend our analysis to the entire frontal face of the p_j -space where $p_0 = 0$: $p_1 + p_2 + p_3 = 1$. There, we have calculated numerically for 10^5 states covering the frontal face, the best fidelity obtained using two teleportation channels under indefinite causal order by taking the optimal measurement on the control state together with the best state able to be teleported. Thus, it represents naively the best possible scenario.

In the last process, for each $|\chi\rangle$ on the front face, we had taken a sample of 10^2 sets

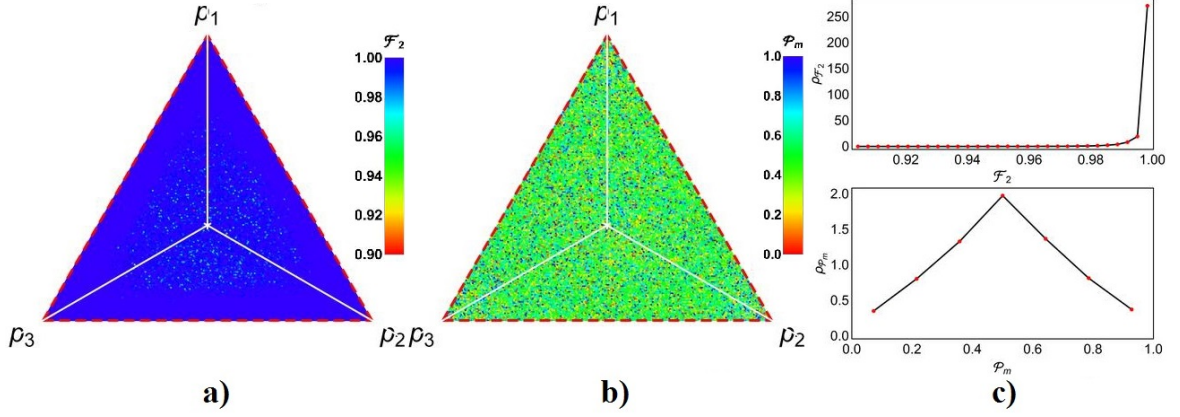


Figure 6.5: Optimal fidelity using two teleportation channels in indefinite causal order followed by an appropriate measurement $|\varphi_m\rangle$. a) The best fidelity obtained for certain teleported state if optimal control measurement is obtained, b) the probability \mathcal{P}_m of success for the last process, and c) the statistical distribution for \mathcal{F}_2 and \mathcal{P}_m .

of values for $q_0 \in [0, 1]$ (the initialization value for the control state for $N = 2$), $\theta \in [0, \pi]$, $\phi \in [0, 2\pi]$ for $|\psi_m\rangle$ and $\theta_0 \in [0, \pi]$, $\phi_0 \in [0, 2\pi]$ for the teleported state $|\psi\rangle = \cos \frac{\theta_0}{2} |0\rangle + \sin \frac{\theta_0}{2} e^{i\phi_0} |1\rangle$. Each value is used as initial condition to find a local maximum for the fidelity \mathcal{F}_2 and then those values are used to predict the global maximum of \mathcal{F}_2 for each point on the front face. Figure 6.5a shows the best fidelity on the face together with the statistical distribution of the fidelities on the front face in the upper image of Figure 6.5c, which suggest that $\mathcal{F}_2 = 1$ could be obtained on the face always (the little dispersion with lower values of $\mathcal{F}_2 \in [0.9, 1]$ are surely due to the numerical procedure followed). The same follows for \mathcal{P}_m (Figures 6.5b and 6.5c lower) but denoting that such probabilities of success are centrally distributed around $\frac{1}{2}$ (note they are not the best probabilities because the process is centred on maximize \mathcal{F}_2).

This outcome suggest that the case with $N = 2$ could become optimal if we limit the $|\chi\rangle$ state to $p_0 = 0$. But this is precisely the opposite case to the perfect situation $p_0 = 1$, which suggest an alternative strategy to reach one or another scenario. We explore such possibility in the next chapter.

In order to analyse deeply the case $p_0 = 0$ previously presented by means of a numerical approach, we take a more critical view of formulas (3.16) and (3.15) and referring to [42] which numerically suggests that $q_0 = \sin^2 \frac{\theta}{2} = \frac{1}{2}(1 - \cos \theta)$, $\phi = 0$ is related with the optimal case for the case $p = p_1 = p_2 = p_3 = \frac{1}{3}$. In fact, in such case, last formulas become reduced to:

$$\mathcal{F}_2 = \frac{\sum_{i,j=0}^3 p_i p_j (\text{Tr}(\rho \sigma_i \sigma_j \rho \sigma_j \sigma_i) + \text{Tr}(\rho \sigma_i \sigma_j \rho \sigma_i \sigma_j))}{\sum_{i,j=0}^3 p_i p_j (\text{Tr}(\sigma_i \sigma_j \rho \sigma_j \sigma_i) + \text{Tr}(\sigma_i \sigma_j \rho \sigma_i \sigma_j))} \quad (6.19)$$

$$\mathcal{P}_m = \frac{\sin^2 \theta}{2} \sum_{i,j=0}^3 p_i p_j (\text{Tr}(\sigma_i \sigma_j \rho \sigma_j \sigma_i) + \text{Tr}(\sigma_i \sigma_j \rho \sigma_i \sigma_j)) \quad (6.20)$$

Last formula explains why the case $\theta = \frac{\pi}{2}$ is optimal for \mathcal{P}_m . Moreover, on the frontal

face $p_0 = 0$, then they clearly become (by splitting the cases $i = j$ from $i \neq j$, noting for the last case $\sigma_i \sigma_j = -\sigma_j \sigma_i$ and we are dealing with pure states):

$$\mathcal{F}_2 = 1 \quad (6.21)$$

$$\mathcal{P}_m = \sin^2 \theta \sum_{i=1}^3 p_i^2, \quad \text{with } \sum_{i=1}^3 p_i = 1 \quad (6.22)$$

Thus, last conditions make the teleportation optimal not only for $p = p_1 = p_2 = p_3 = \frac{1}{3}$ but instead for the entire cases on the front face and it is independent from the teleported state. Nevertheless, the probability of success depends entirely from the values of p_i (despite considering the best case $\theta = \frac{\pi}{2}$). Figure 6.6 shows the distribution of \mathcal{P}_m (in some cases we will denote this probability in the frontal face by $\mathcal{P}_{m,N=2}^{\{p_i\}}$ to state $\theta = \frac{\pi}{2}$, $p_0 = 0$ and p_i arbitrary but fulfilling $p_1 + p_2 + p_3 = 1$) on the frontal face, which ranges on $[\frac{1}{3}, 1]$. In fact, the case $p = p_1 = p_2 = p_3 = \frac{1}{3}$ corresponds to the worst case for \mathcal{P}_m in the center of the face. We have constructed the norm on the frontal face to report such distribution. The mean $\mu_{\mathcal{P}_m} = \frac{1}{2}$ and the standard deviation $\sigma_{\mathcal{P}_m} \approx 0.13$ were calculated using such distribution.

Last analysis suggests for arbitrary N that the procurement of an analytical formula for (6.7) is in order at least for the case $p_0 = 0$, which implies $t_0 = 0$:

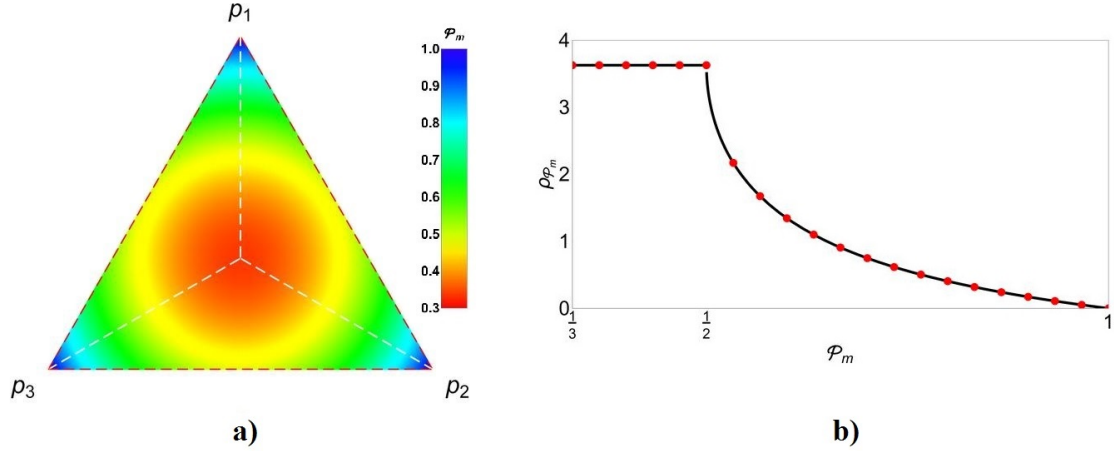
$$\Lambda^N [\rho \otimes \rho_c] = \sum_k \sum_{k'} \sqrt{q_k q_{k'}} |k\rangle \langle k'| \sum_{t_1=0}^N \sum_{t_2=0}^{N-t_1} \prod_{j=1}^3 p_j^{t_j} \otimes \sum_{p=1}^{N'} \pi_k \left(\pi_{k_p}^{t_1, t_2, t_3} \left(\sigma_1^{t_1} \sigma_2^{t_2} \sigma_3^{t_3} \right) \right) \rho \left(\pi_{k'} \left(\pi_{k'_p}^{t_1, t_2, t_3} \left(\sigma_1^{t_1} \sigma_2^{t_2} \sigma_3^{t_3} \right) \right) \right)^\dagger \quad (6.23)$$

$$= \sum_k \sum_{k'} \sqrt{q_k q_{k'}} |k\rangle \langle k'| \sum_{t_1=0}^N \sum_{t_2=0}^{N-t_1} \prod_{j=1}^3 p_j^{t_j} \otimes \sum_{p=1}^{N'} \sum_{k_p}^k \sum_{k'_p}^{k'} \left(\sigma_1^{t_1} \sigma_2^{t_2} \sigma_3^{t_3} \right) \rho \left(\sigma_1^{t_1} \sigma_2^{t_2} \sigma_3^{t_3} \right)^\dagger \quad (6.24)$$

and $t_3 = N - t_1 - t_2$. As it was previously mentioned, factors generated by π_k and $\pi_{k'}$ are equal until a sign. In addition, they evolve to $\sigma_0, \sigma_1, \sigma_2$ or σ_3 . Thus, those factors and their signs state the introduction of syndromes on ρ together with interference among them and the different paths on the indefinite causal order. Such interference could be manipulated through the parameters q_k, p_j .

Despite, this formula is not easy to address in order to get a simpler closed result because the sign $\sum_{k_p}^k, \sum_{k'_p}^{k'}$ introduced in the permutation with respect $\sigma_1^{t_1} \sigma_2^{t_2} \sigma_3^{t_3}$ cannot be advised easily. Nevertheless, we can still to analyse the cases for the lowest values of N computationally (analytical cases addressed by computer aided methods due to the factorial increasing number of terms).

Actually, the suggested results in this chapter for the communication channels have the same properties for the frontal face, as long as the channel can be represented as it was shown

Figure 6.6: Distribution of \mathcal{P}_m on the frontal face.

in (3.3), which can actually correspond to communication channels outside the context of teleportation.

These communication channels are known as Pauli channels. Although those Pauli channels are not the main topic of the present thesis project, parallel to this, it has been developed an analysis for classification of quantum channels under indefinite causal order, showing particularly the behavior on the frontal face where $p = 0$, since \mathcal{F} has pure states as well as mixed states, on the frontal face, $\mathcal{F} = 1$ (see discussion in Appendix B).

For the cases in the frontal face, a value for the probability of measurement is defined as $\mathcal{P}_{m,N}^{\text{ff},\{p_i\}}$. Formulas for $\mathcal{P}_{m,N}^{\text{ff},\{p_i\}}$ and \mathcal{F} for N larger than two can be obtained using a computational treatment. As in our previous discussion for the case $p_1 = p_2 = p_3 = p$ in the section 6.2.1, $\mathcal{F} = 1$ is obtained for all cases on the frontal face if the measurement in the indefinite causal order becomes $|\varphi_m^+\rangle$ for $N = 2, 4$ and $|\varphi_m^-\rangle$ for $N = 3$ independently of the teleported state with a probability of successful measurement given by:

$$\mathcal{P}_{m,N=2}^{\text{ff},\{p_i\}} = p_1^2 + p_2^2 + p_3^2 \quad (6.25)$$

$$\mathcal{P}_{m,N=3}^{\text{ff},\{p_i\}} = 6p_1p_2p_3 \quad (6.26)$$

$$\mathcal{P}_{m,N=4}^{\text{ff},\{p_i\}} = p_1^4 + p_2^4 + p_3^4 + \frac{2}{3}(p_1^2p_2^2 + p_1^2p_3^2 + p_2^2p_3^2) \quad (6.27)$$

For complementary cases using other measurement outcome we get $\mathcal{F} \neq 1$ depending from p_1, p_2, p_3 or still undefined, and additionally depending from the teleported state. The formulas obtained in the analysis are reported in Appendix E. Actually, a direct analysis made aided by computer until $N = 9$, shows that $\mathcal{F} = 1$ can be reached for values of N when the correct measurement state is obtained, namely, when the measurement state is $|\psi_m\rangle = |\psi_m^+\rangle$ for N even and $|\psi_m\rangle = |\psi_m^-\rangle$ for N odd, nevertheless, the value for \mathcal{P}_m decreases when N increases. Therefore, so far, the best case so we can obtain $\mathcal{F} = 1$ with the best probability of measurement is for $N = 2$, since, as it has been mentioned, even though $\mathcal{F} = 1$ can be

reached with larger number N the probability of successful measurement rapidly decreases when N increases.

In spite the previous outcomes, we guess the indefinite causal order could not work properly in any point inside of region depicted in the Figure 5.4. Nevertheless, due to the outcomes in [22] for the case $p = p_1 = p_2 = p_3$ and those exhibited in the Figure 5.4, the teleportation process assisted by indefinite causal order (at least for two channels) becomes optimal on $p_0 = 0$ and $p_0 = 1$ (the origin and the frontal face in Figure 5.4a). Then, we propose, on the next chapter, an alternative strategy beginning with a weak measurement on the entangled resource in order to reduce it to each one of the optimal cases found, using this results but enhancing the probability of success.

Chapter 7

Teleportation assisted by weak measurement

Given the previous results with $\mathcal{F} = 1$ both in the origin ($p_0 = 1$) as in the frontal face ($p_0 = 0$), it can be noticed the importance of adopting a strategy to get the entangled resource $|\chi\rangle$ projected on any of those states. In this chapter, it is developed a strategy to reach this projection by using a weak measurement.

7.1 General case for $N = 2$ assisted by a weak measurement

It is first considered a weak measurement on the entangled resource $|\chi\rangle$. Then, the post-measurement states are obtained and their probabilities of occurrence as:

$$P_0 = |\beta_0\rangle\langle\beta_0| \rightarrow |\chi_0\rangle = (P_0|\chi\rangle)_{\text{norm}} = |\beta_0\rangle, \quad \tilde{p}_0 = p_0 \quad (7.1)$$

$$P_1 = \mathbb{I} - P_0 \rightarrow |\chi_1\rangle = (P_1|\chi\rangle)_{\text{norm}} = \sum_{i=1}^3 \sqrt{\frac{p_i}{\tilde{p}_1}} |\beta_i\rangle \equiv \sum_{i=1}^3 \sqrt{p'_i} |\beta_i\rangle \quad (7.2)$$

$$\text{with : } \tilde{p}_1 = \sum_{i=1}^3 p_i$$

which projects the entangled state on one of the two states $|\chi_0\rangle, |\chi_1\rangle$ with probabilities \tilde{p}_0, \tilde{p}_1 . Each state is located on the origin or otherwise on the frontal face of region shown in Figure 5.4. Then, if $|\chi_0\rangle$ is obtained, the teleportation process can go as in the Figure 1.1, otherwise, if $|\chi_1\rangle$ is obtained, we can try the teleportation assisted by indefinite causal order (at this point the reader could note that clearly they are needed two entangled resources). In fact, the feasibility of last strategy for $N = 2$ can be advised in the Figure 6.5 (renaming p'_i as p_i again, with $p_1 + p_2 + p_3 = 1$).

The entire process is depicted in the Figure 7.1. Given certain state to teleport, we use certain entangled resource $|\chi_a\rangle$. It goes through the weak measurement in (7.1) to get $|\chi_{a0}\rangle = |\beta_0\rangle$ with probability p_0 then we perform a single teleportation. Instead, by obtaining $|\chi_{a1}\rangle$ with probability $1 - p_0 = p_1 + p_2 + p_3$, then we prepare a second entangled resource $|\chi_b\rangle$ repeating with them the same procedure, if after of the weak measurement $|\chi_{b0}\rangle = |\beta_0\rangle$ is

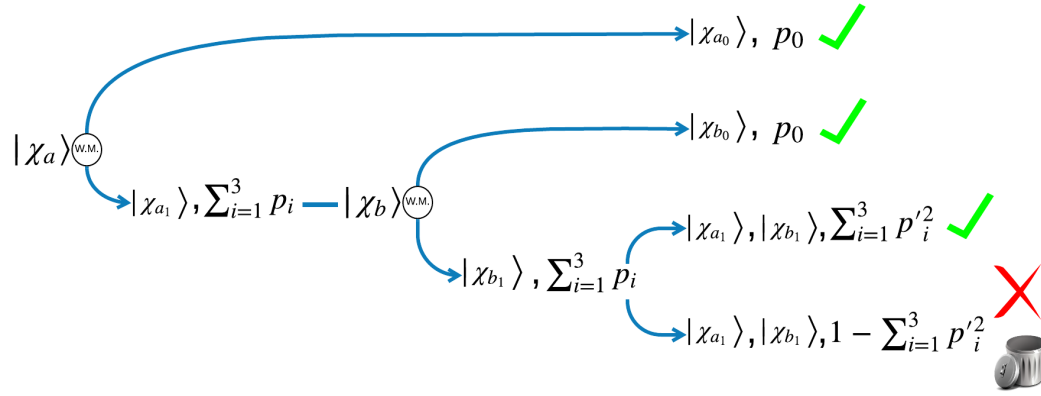


Figure 7.1: Schematic teleportation process assisted by weak measurement.

obtained with probability p_0 , we disregard $|\chi_{a_1}\rangle$ proceeding with a single teleportation using such state. Otherwise, if $|\chi_{b_1}\rangle$ is obtained, we perform a two-channel teleportation assisted by indefinite causal order. There, the teleportation will become successful with probability $p_1'^2 + p_2'^2 + p_3'^2$, otherwise it become unsuccessful. Thus, the global probability of success is:

$$\mathcal{P}_{\text{Tot}} = p_0 + (1 - p_0)p_0 + (1 - p_0)^2 \sum_{i=1}^3 p_i' = 1 - 2(p_1p_2 + p_2p_3 + p_3p_1)$$

Last function has been represented in the plots of Figure 7.2. For each initial set

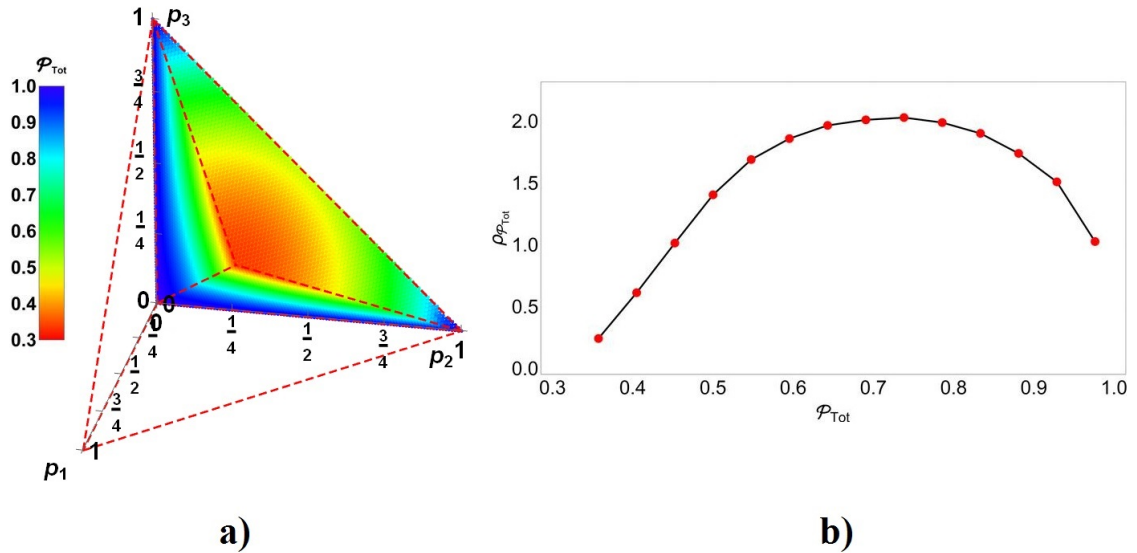


Figure 7.2: Distribution of \mathcal{P}_{Tot} : a) as function of (p_1, p_2, p_3) , and b) as statistical distribution by itself obtained numerically from the data of a).

(p_1, p_2, p_3) of the entangled resources (assumed identical), \mathcal{P}_{Tot} is plotted in color in agreement with the bar besides in the Figure 7.2a. One third of the plot has shown due to this symmetry to exhibit its inner structure. The corresponding statistical distribution is obtained numerically in the Figure 7.2b by sampling uniformly the space in the figure on the left. The mean value of \mathcal{P}_{Tot} becomes 0.70 and their standard deviation 0.16.

7.2 General case for $N \geq 2$ assisted by a weak measurement

In order to improve \mathcal{P}_{Tot} , for $N \geq 2$, the procedure follows as in the previous section by introducing N imperfect entangled resources, $|\chi_i\rangle$ (assumed identical for simplicity) but in each step, we decide if after of the weak measurement, the state $|\chi_{j0}\rangle = |\beta_0\rangle$ is used to perform the teleportation or if we continue the process of weak measurement N times on identical entangled resources $|\chi_j\rangle$ to finally get $|\chi_{N1}\rangle = \sum_{i=1}^3 p'_i |\beta_i\rangle$ as in the Figure 7.1. The corresponding situation is now depicted for the general case in the Figure 7.3. In this case, the global probability of success becomes:

$$\mathcal{P}_{\text{Tot}N} = \sum_{j=1}^N p_0 (1 - p_0)^{j-1} + (1 - p_0)^N \mathcal{P}_{m,N}^{\text{ff},\{p'_i\}} \quad (7.3)$$

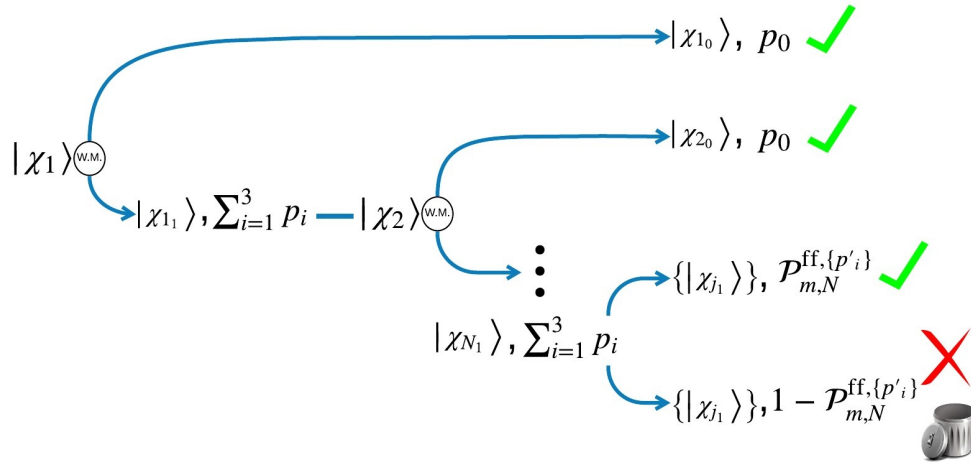


Figure 7.3: Schematic teleportation process assisted by indefinite causal order using N -teleportation channels and weak measurement.

Then, we can get the outcomes for global probability $\mathcal{P}_{\text{Tot}N}$ for the last cases with $\mathcal{F} = 1$:

$$\mathcal{P}_{\text{Tot}2} = 1 - 2(p_1 p_2 + p_1 p_3 + p_2 p_3) \quad (7.4)$$

$$\mathcal{P}_{\text{Tot}3} = 1 - (p_1^3 + p_2^3 + p_3^3) - 3(p_1^2(p_2 + p_3) + p_2^2(p_1 + p_3) + p_3^2(p_1 + p_2)) \quad (7.5)$$

$$\begin{aligned} \mathcal{P}_{\text{Tot}4} = & 1 - 4(p_1^3(p_2 + p_3) + p_2^3(p_1 + p_3) + p_3^3(p_1 + p_2)) \\ & - 12p_1 p_2 p_3 (p_1 + p_2 + p_3) - \frac{16}{3}(p_1^2 p_3^2 + p_2^2 p_3^2 + p_1^2 p_2^2) \end{aligned} \quad (7.6)$$

Now we can visualize last outcomes for \mathcal{P}_{Tot} in Figure 7.4. Again, all the entangled states used for the teleportation process are assumed to be identical by simplicity. Figures 7.4a-c depict the probability $\mathcal{P}_{\text{Tot},N}$ to reach $\mathcal{F} = 1$ in the entire process represented by the coloring. Each

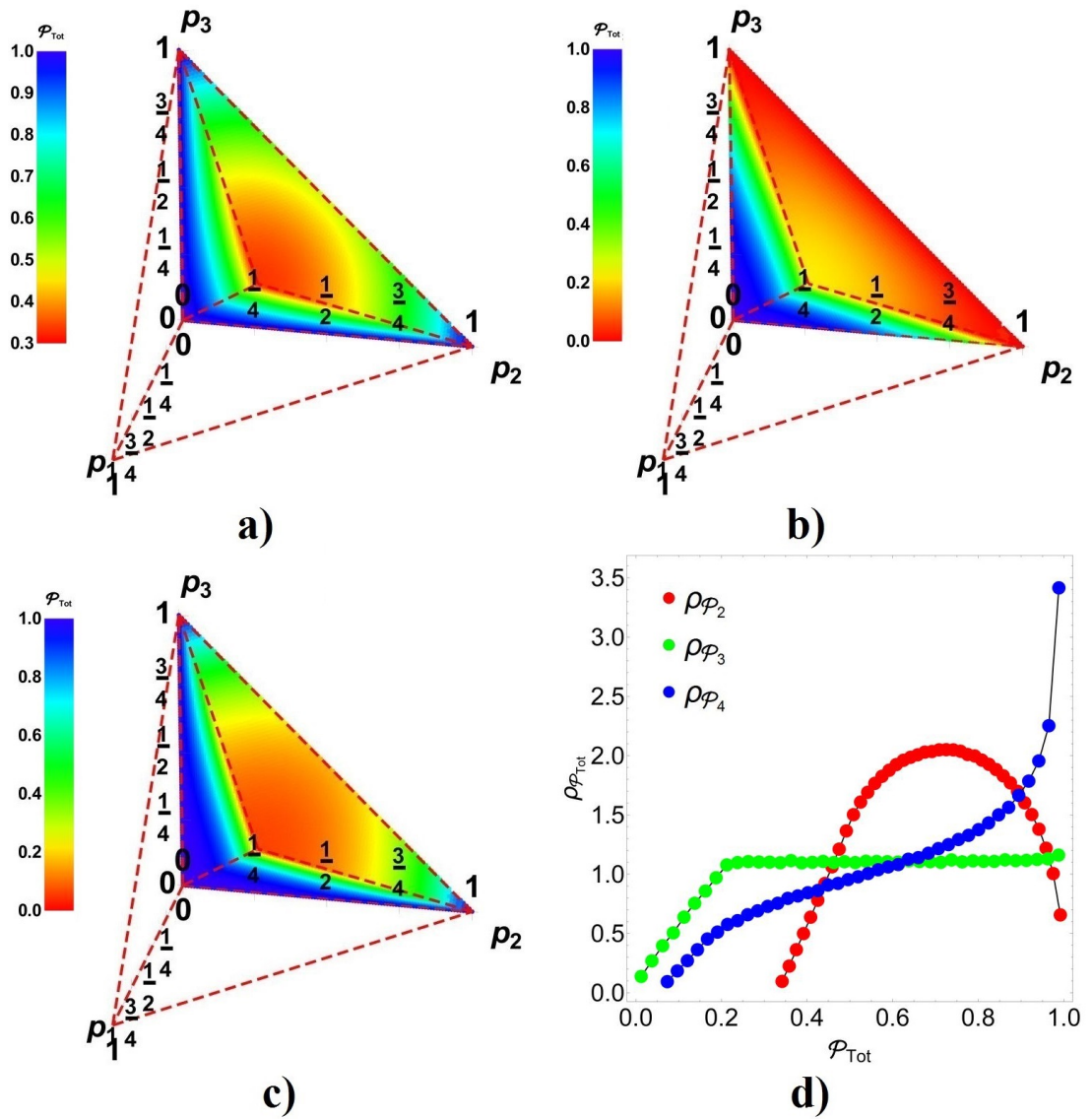


Figure 7.4: a) to c) values of \mathcal{P}_{Tot} as function of (p_1, p_2, p_3) , for N_2 , N_3 and N_4 respectively. d) statistical distribution numerically obtained for $\mathcal{P}_{\text{Tot}2}$, $\mathcal{P}_{\text{Tot}3}$ and $\mathcal{P}_{\text{Tot}4}$.

color bar shows the entire range of values for such probabilities on the graphs. According to the color, the blue zone represents the region where $\mathcal{P}_{\text{Tot}} \rightarrow 1$, observing for the case $N = 4$ a larger blue area, suggesting the goodness of increase the number of teleportation channels under indefinite causal order.

Figure 7.4d depicts a numerical analysis of statistical distribution for the cases $N = 2, 3, 4$. Note that for $N = 3$, all greater values for the probability occur almost evenly. For the case $N = 4$, it is observed a larger amount of success probabilities than failure probabilities compared with $N = 3$. Despite, $\mu_{\mathcal{P}_{\text{Tot}2}} \approx 0.702$, $\sigma_{\mathcal{P}_{\text{Tot}3}} \approx 0.158$ and $\mu_{\mathcal{P}_{\text{Tot}4}} \approx 0.667$, $\sigma_{\mathcal{P}_{\text{Tot}4}} \approx 0.249$ (because for $N = 2$ there is a large distribution for medium success probabilities). In any case, the most successful outcomes of teleportation appear for $N = 4$.

Chapter 8

Experimental Implementation

In this chapter, some of main experimental developments for the deployment of indefinite causal order in teleportation are commented. The Chapter begins with the procedure to set the weak measurement used in section 7.1. After that, some elements and experimental developments are taken in order to propose the experimental implementation of the theoretical proposal presented before.

8.1 Weak measurement to project $|\chi\rangle$

In section 7.1, it was stated the implementation of a weak measurement to project $|\chi\rangle$ conveniently onto $|\chi_0\rangle = |\beta_0\rangle$ or $|\chi_1\rangle = \sum_{i=1}^3 p'_i |\beta_i\rangle$. Despite, in the experimental approach, there are certain differences due to the resources been used. In this section, we present how to afford the weak measurement stated in (7.1). An ancilla qubit $|0_a\rangle$ is used to do the measurement minimizing the impact on $|\chi\rangle$ as is desired. In this implementation, we will use as central resource the Toffoli gate. In order to prepare the $|\chi\rangle$ stated properly for such measurement, we combine it with the ancilla. Then, we send the combined system into the circuit presented in Figure 8.1a. This circuit employs the Toffoli gate $\mathcal{T}_{1,2,a}$ on channels 1, 2 for $|\chi\rangle$ and a for $|0_a\rangle$ together with the C^1Not_2 gate (developed for ions [56, 57] and photons [58]). In fact, it is well known that Toffoli gate can be performed using $CNot$ gates and single qubit gates [38] or by means of the Sleator-Weinfurter construction [59], despite other more efficient developments are known for ions [60] and photons [61]. Some single qubit gates as Hadamard (\mathcal{H}) and Not (\mathcal{X}) are also used. In the following development we write $|\chi\rangle = \sum_{i=0}^3 \sqrt{p_i^*} |\beta_i\rangle$ as the imperfect entangled resource (* does not mean complex conjugation in this case). Thus, all necessary quantum gates have been experimentally developed in our days at least in quantum optics.

A direct calculation shows that this circuit performs the following transformation on $|\psi_0\rangle = |\chi\rangle \otimes |0_a\rangle$ into:

$$|\psi_1\rangle = \sqrt{p_0} |\beta_0\rangle \otimes |1_a\rangle + (\sqrt{p_1} |\beta_1\rangle + \sqrt{p_2} |\beta_2\rangle + \sqrt{p_3} |\beta_3\rangle) \otimes |0_a\rangle \quad (8.1)$$

$$\text{with : } \begin{aligned} \sqrt{2p_0} &= \sqrt{p_0^*} - \sqrt{p_3^*}, & \sqrt{2p_1} &= \sqrt{p_1^*} - \sqrt{p_2^*}, \\ \sqrt{2p_2} &= \sqrt{p_0^*} + \sqrt{p_3^*}, & \sqrt{2p_3} &= \sqrt{p_1^*} + \sqrt{p_2^*} \end{aligned} \quad (8.2)$$

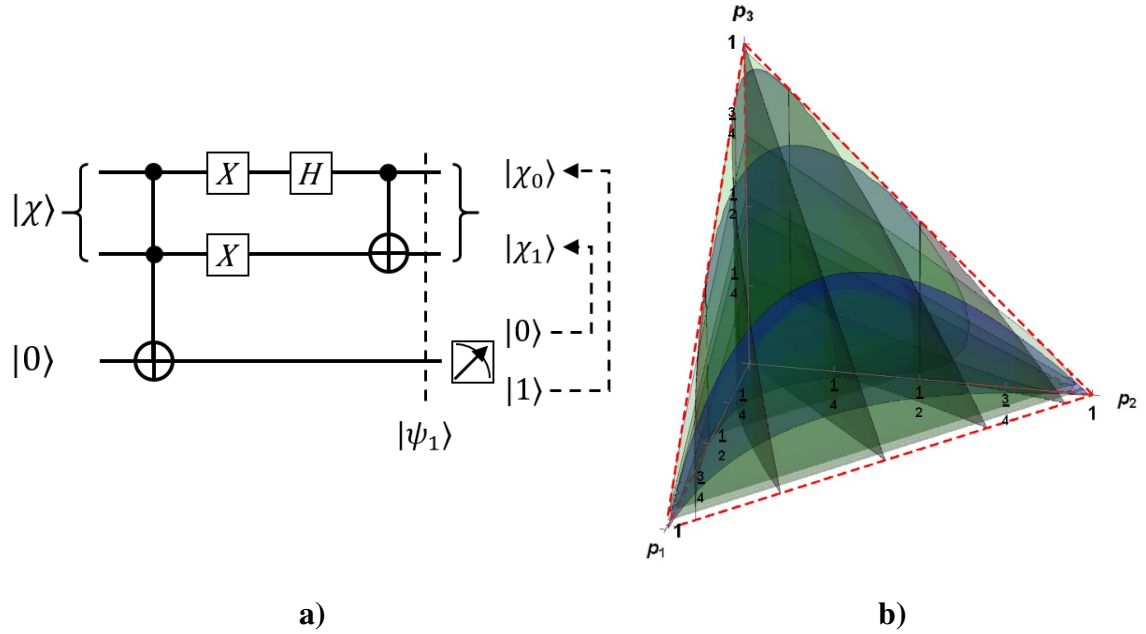


Figure 8.1: a) Quantum circuit generating the weak measurement on $|\chi\rangle$, and b) contour plots for the map on the region (p_1, p_2, p_3) between those probabilities and p_1^* (red), p_2^* (green) and p_3^* (blue).

just before of the projective measurement on the qubit a shown in the Figure 8.1a. Clearly, after of measurement, two possible outcomes arise in the qubit a , $|1_a\rangle, |0_a\rangle$ while on qubits 1, 2 the outcomes are $|\chi_0\rangle = |\beta_0\rangle$, $|\chi_1\rangle = \sum_{i=1}^3 \sqrt{p_i} |\beta_i\rangle$ respectively as in the section 7.1 completing the weak measurement. The only difference with respect our previous development is that this coefficients are not the original $\{p_i^*\}$. Despite, in the event such coefficients are unknown, this fact is not important, the really outstanding outcome is that this procedure projects the state into the perfect Bell state to perform the teleportation $|\beta_0\rangle$ or otherwise on the frontal face if this resource is planned to be used under indefinite causal order and measurement as it was previously depicted in the procedure of section 7.1. Anyway, Figure 8.1b shows the contour plots of p_1^* (red), p_2^* (green) and p_3^* (blue) in the region (p_1, p_2, p_3) as a reference of the involved geometric transformations.

8.2 An insight about teleportation implementing indefinite causal orders experimentally with light

Formula (3.3) regards the teleportation algorithm as a quantum communication channel. Despite this formula is a useful simplification for theoretical analysis, it expresses the teleportation channel with the input and output through the same system, which is not precisely the real experimental situation. Then, as it was true for the original implementation of the original teleportation proposal [1] in [3], the deployment should be modified to have a correct

approach to the theory. In this section we discuss an insight view about its experimental deployment together with indefinite causal order based on current techniques and experimental developments.

A possible implementation with light should to consider and initial state with at least three initial photons exhibiting each one at least a pair of quantum variables as polarization, frequency or spatial (\mathbf{k} -vector state) among other as in the original experimental teleportation proposal [62]: $|\psi_0\rangle = |v\rangle_1 \otimes |v\rangle_a \otimes |v\rangle_b$, using polarization in the vertical direction as instance. Those photons, represented at the beginning on Figure 8.2, should be then converted into five photons by splitting the last two into entangled pairs using Spontaneous Parametric Down Conversion (SPDC) [63] as instance, while the first is arbitrarily rotated by a quartz polarization rotator (QPR) [64] (it can be visualized in Figure 8.2 represented by the letter R) -to generate the state to teleportate-: $|\psi_1\rangle = (\alpha|v\rangle_1 + \beta|h\rangle_1) \otimes \frac{1}{\sqrt{2}}(|v\rangle_2|h\rangle_3 + |h\rangle_2|v\rangle_3) \otimes \frac{1}{\sqrt{2}}(|v\rangle_4|h\rangle_5 + |h\rangle_4|v\rangle_5)$. After, five photons should be sent together into two alternative directions (through a dichroic beamsplitter -a splitting wavelength dependent- instead a polarization beamsplitting) coincidentally, not independently (it means five photons will travel through corresponding paths labeled by p_A or p_B). This beamsplitter (corresponding to the box with the BS in Figure 8.2) works as our control state superposing the two path states (the two causal orders further). Last effect should be solved based on the frequency of original photons which should be quantum generated to let a quantum splitting of all beams, or otherwise based on the previous generation of a GHZ state [65]). This necessary beamsplitter is still a cutting-edge technology. Such spatial quantization introduces an additional quantum variable thus converting the initial state into:

$$\begin{aligned}
|\psi_2\rangle = & \frac{1}{\sqrt{8}} \left((\alpha|v\rangle_1 + \beta|h\rangle_1) |p_A\rangle_1 (|v\rangle_2|h\rangle_3 + |h\rangle_2|v\rangle_3) |p_A\rangle_2 |p_A\rangle_3 \otimes \right. \\
& (|v\rangle_4|h\rangle_5 + |h\rangle_4|v\rangle_5) |p_A\rangle_4 |p_A\rangle_5 + (\alpha|v\rangle_1 + \beta|h\rangle_1) |p_B\rangle_1 \otimes \\
& \left. (|v\rangle_2|h\rangle_3 + |h\rangle_2|v\rangle_3) |p_B\rangle_2 |p_B\rangle_3 (|v\rangle_4|h\rangle_5 + |h\rangle_4|v\rangle_5) |p_B\rangle_4 |p_B\rangle_5 \right) \quad (8.3)
\end{aligned}$$

If additionally we introduce certain optical distortion in the SPDC, we get imperfect entangled states then changing each $\frac{1}{\sqrt{2}}(|v\rangle_i|h\rangle_j + |h\rangle_i|v\rangle_j)$ by $|\chi\rangle_{ij}$. In the following, we will change v, h by 0, 1 respectively for simplicity.

Note that teleportation is in certain sense automatically generated due to the non-locality of resource $|\beta_0\rangle$ (or imperfectly $|\chi\rangle$), then collapsed on four adequate outcomes involving an additional correction as function of those outcomes using classical communication (Figure 1.1). In addition, for two sequential teleportation channels, the process can be achieved by post-measurement at the end of both processes. Nevertheless, the implementation of indefinite causal order in teleportation introduces additional challenges due to the connectivity of paths and measurements. In the process, it will be required the implementation of the *SWAP* gate, which has already been experimentally performed in optics [66, 67].

Thus, Figure 8.2 depicts a possible implementation for two teleportation processes assisted by indefinite causal order. The first photon goes to the QPR (the box with a letter R in Figure 8.2) and then the five photons go through the coordinated BS. The proposed process can be then followed in the Figure 8.2 with paths labeled by p_A in green and p_B in red. For

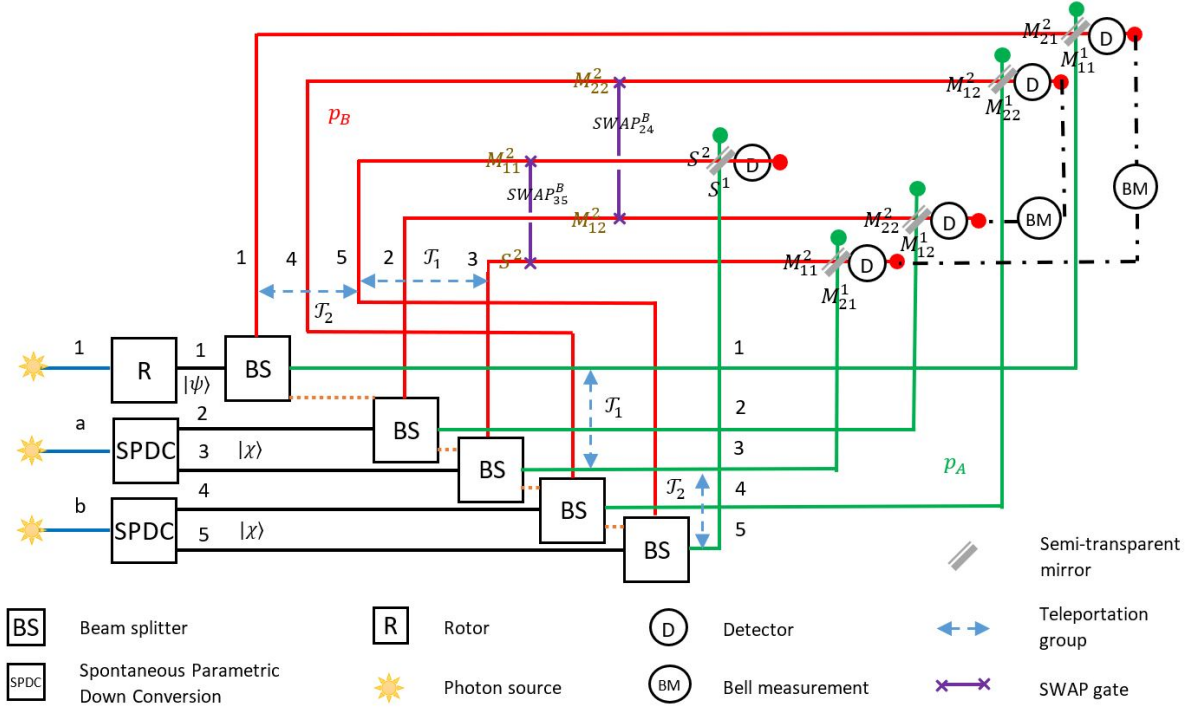


Figure 8.2: Diagram for an implementation of teleportation with causal ordering as it is discussed in the text. Photons are splitted on two different set of paths to superpose the two causal orders of two sequential teleportation process. In this diagram, photon 1 works as the target qubit while photons a and b works as the target qubits. SWAP gates are used to move information from one red path to another one letting to meet the information on the corresponding green path (on the same system) at the end of the circuit upon the recombination.

simplicity, teleportation processes are assumed to perform measurements on the Bell states basis as in Figure 8.3, thus avoiding the use of H and $CNOT$ gates in the analysis. Due to the above (post-measurement and measurement assumed on the Bell basis), almost no gates are present in the process, just two $SWAP$ gates stating the causal connections. At the end of each path, a semi-transparent mirror should mix again the paths (but not the polarization) by pairs into the basis $|\pm\rangle_i = \frac{1}{2}(|p_A\rangle_i \pm |p_B\rangle_i)$ for each photon i , in order to erase the path followed information. We are labeled each path (or the information being carried on it) by M_{ij}^k (in case that photon carries the information of one of the complementary systems not containing the output of teleportation) remarking the path typr followed $k = A, B, +, -$, the final belonging teleportation process $i = 1, 2$, and the number of sequential qubit to be measured there: $j = 1$ for the former input and $j = 2$ for the correspondent to the first qubit of the original entangled resource. Instead, the final outputs are labeled by S^k ($k = A, B, +, -$). By following the color, the reader should easily identify each path considering additionally the effect of the intermediate use of $SWAP$ gates which is discussed below.

By ignoring first the $SWAP$ gates in the Figure 8.2, we can realize that the circuit has not any effect. We are indicated each optical element described before. The dotted line connecting the BS 's denotes the not independent functioning, all together should send the five photons on the green paths or on the red ones. States $|\psi\rangle$ and $|\chi\rangle$ are remarked on photons 1

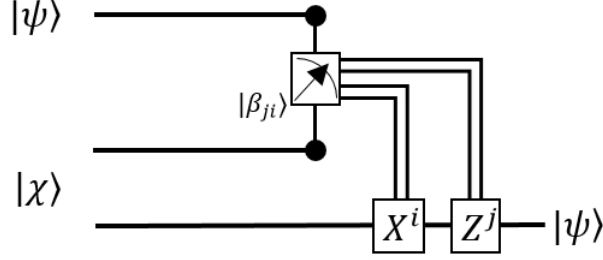


Figure 8.3: Teleportation processes are assumed to perform measurements on the Bell states basis.

and 2, 3, 4, 5 respectively. Each path (green or red) is labeled from 1 to 5 in agreement with the photon carried out. Blue arrows remarks the group of photons involved in each teleportation process \mathcal{T}_1 or \mathcal{T}_2 on each path (the first subscript in M_{ij}^k): 1, 2, 3 and 3, 4, 5 respectively for green paths, and 1, 4, 5 and 5, 2, 3 respectively for red ones. On each path, we are reported the associated label for each system S^k or M_{ij}^k as was depicted before. Note that brown labels correspond to the information being carried before of *SWAP* gates, while black labels are the final states reported there at the end of the path but before of the recombining in the semi-transparent mirrors. The reason for the *SWAP* gate between the paths 3 and 5 should be clear, we need get the teleportation outputs on the same photon to generate the superposition of information. The *SWAP* gate on the red paths 2 and 4 exchanges the information on those paths in order to generate the superposition at the end among path information M_{ij}^1 and $M_{i'j}^2$ with $i \neq i', j = 1, 2$ thus mixing both. Note that the set of states in M_{ij}^k are those to be measured in the teleportation process (here in the Bell basis by pairs) in order to correct the output states. The reader should advise this process does not reproduce exactly that depicted by (3.3) because such formula assumes the measurements are internal generating a mixed state coming from the corresponding projections and corrections. In this approach, we have the possibility to measure only four qubits instead eight. Despite, we will note this procedure still reproduces some main previous features. At the end of the process each semi-transparent mirror (diagonal in grey) mixes the information on the states $|\pm\rangle_i$ for each photon i on the red and green edges (with information M_{ij}^\pm or S^\pm respectively -red and green-, not represented in the Figure 8.2). On the red edges, a detector first decides if the photon exits through them (they are the projective measurement on $|\varphi_m^\pm\rangle$ states in our development). In addition, a Bell measurement is then performed on each pair 1, 3 and 2, 4 in order to inquire the information codified in the output S^+ .

A direct but large calculation to expand (8.3) then applying the *SWAP* gates and projecting on $|+\rangle_i, i = 1, \dots, 5$ was performed. Finally, this output was written in terms of $|\beta_i\rangle_{1,3} \otimes |\beta_j\rangle_{2,4}, i, j = 0, \dots, 3$ to ease the identification of final successful measurements. If $p_0 = 1$ or $p_0 = 0$, upon the measurement of $|\beta_i\rangle_{1,3} \otimes |\beta_j\rangle_{2,4}$ and then the application of $\sigma_i \sigma_j$ as correction, the output S^+ becomes $|\psi\rangle$ faithfully in the following cases:

- If $p_0 = 1$ for all $i, j = 0, \dots, 3$ cases with a global successful probability of $\frac{1}{16}$.
- If $p_0 = 0$ for the cases $i = 0, \dots, 3$ and $j = 2$ with a global successful probability of $\frac{(p_1 - p_2 + p_3)^2}{64}$.

which clearly resembles our main outcomes. For the second case, other measurement outcomes give an imperfect teleportation. Then, additional experimental proposals should be developed to approach them into the ideal case considered in our theoretical results.

Chapter 9

Conclusions and future work

Quantum teleportation has an important role in quantum processing for the transmission of quantum information. In this context, many approaches have surged in order to make the teleportation process more reliable in terms of fidelity and probability of measurement. Nevertheless there are several possible issues preventing the outcome process to occurs successfully, such as those on the entangled resource assisting the teleportation process, where an imprecision in the teleported state can be introduced due to the difficulties for generate and maintain such entangled resource.

9.1 Conclusions

In this work, it has first been characterized arbitrary noisy channels for single qubits, which are modelled through Kraus operators in the form of Pauli channels for a better understanding of those channels. Then, an analysis on the application of two channels both sequentially and under an indefinite causal order scheme and supported by a post-measurement was made. The results obtained for the fidelity for the process showed advantages in the applying of indefinite causal order regarding the redundant case. It was also shown that a perfect fidelity in a scenario with a very noisy channel can be reached by applying two of them under indefinite causal order, nevertheless, due to the fact that the probability of measurement is not outstanding, it was found that additional treatment could be applied in order to improve it.

From the mentioned work, an analysis was also made in relation with channels used in the context of teleportation. Such teleportation channels were also implemented for both sequentially and under indefinite causal order. Firstly, the analysis for the redundant scenario where quantum teleportation channels are simply applied sequentially (those channels are assumed to be identical for simplicity), shows that as the number N of channels sequentially applied increases, rapidly decreases the fidelity. thus converging to the maximal depolarization channel of the teleported state and, therefore, obtaining $\mathcal{F}_{N \rightarrow \infty} = \frac{1}{2}$. In this sense, there is no advantage when the channels are applied sequentially, it only worsens the process. There is only a slight advantage when two very noisy channels are applied sequentially in comparison when just one noisy channel y used for the teleportation process, but this advantage is not outstanding, since the fidelity is still low.

Therefore, by modifying the process under indefinite causal order for two or more teleportation channels as it was proposed by [22] and later discussed in [42], it was then advised advantages on the quantum fidelity of the teleported state for a few number N of sequential teleportation channels. The results obtained from analyzing the features of those two teleportation channels in superposition, showed that for the specific case when the entangled state is in the form $p_1 = p_2 = p_3 = p = \frac{1}{3}$ (and therefore $P_0 = 0$ which denotes the worst case with a very noisy channel), it has been shown that $\mathcal{F} = 1$ can be obtained aided by measurement and, this measurement can be not only with the state $|+\rangle$ with a probability in the control $q_0 = \frac{1}{2}$, but as far as the measurement state given in (3.12) is chosen correctly in the range for $\phi = 0$ and $\theta \in [0, \pi]$, a perfect teleportation can be reached as function of arbitrary p_0 . Also for the case with two teleportation channels, an analysis for other values when $p \neq 1/3$ was made, and it was found that $\mathcal{F} = 1$ cannot be reached no matter the measurement state chosen. Nevertheless, the best strategy to follow in such case is to figure out the best choice for the measurement state, in order to reach the optimal fidelity. Something interesting found is that \mathcal{F} does not depend on the value for q_0 , so that it is fixed the maximum for \mathcal{F} once p is selected and, by choosing the correct values for θ and ϕ in the measurement basis, it is reached.

From the results obtained in Chapter 5 and in order to look for improvements on \mathcal{F} , in Chapter 6 are obtained similar outcomes for \mathcal{F} by managing independently the values for p_0, p_1, p_2, p_3, q_0 together with θ and ϕ in order to search the maximum \mathcal{F} for each case. A categorization was then performed in order to analyze the effects on the entangled state, thus obtaining an enhancement for the case when the most imperfect entangled resource is used, where $p_0 = 0$ and with the absence of the ideal entangled resource represented by $|\beta_0\rangle$, and even for near regions of it that ideal state when $p_0 \approx 0$ as N increases. Notably for the first case, it is shown the possibility of obtain a perfect teleportation process with $\mathcal{F}_N = 1$. However, issues are presented when N increases, since the principal downside in this case is the reduction of the probability of successful measurement \mathcal{P}_m , which decreases drastically as the number of channels applied in superposition of causal order N increases.

Now, in order to improve the global probability of success, it has then been proposed a combined strategy using weak measurement to first projecting the entangled resource to one of two cases: the case where $p_0 = 1$ with $p_1, p_2, p_3 = 0$ or the case where $p_1 + p_2 + p_3 = 1$ with $p_0 = 0$, where the most notable enhancement is generated with indefinite causal order aided by post-measurement. In such cases, a remarkable aspect is that for such notable cases the outcome becomes independent from the teleported state and, therefore, it can always be obtained a fidelity $\mathcal{F} = 1$ and, furthermore, the probability of successful measurement \mathcal{P}_m is improved. Interestingly, those notable process are possible not only for pure states but also for mixed states.

Also, a more detailed process for the weak measurement first barely discussed for the projection of the entangled state in Chapter 7 is after detailed and oriented to the description of a practical experimental implementation in accordance to the current experimental developments for light and matter in Chapter 8. The central part of the implementation is the development of Toffoli gate. Additionally, an introductory analysis for a proposal for an experimental implementation has been made for the application of teleportation process under indefinite causal order using two teleportation channels. Such approach is not yet optimal

despite it reproduces the main features found in the development. For the experimental proposal, recent experiments and technological developments in optics become the central part, particularly the implementation of the *SWAP* gate and the generation of $|GHZ\rangle$ states. An important aspect to be noticed for this part is the use of post-measurement in the teleportation process in order not to affect the state in the middle of the process. The scheme for the implementation has been planned with photons.

The superposition of causal order has been compared with superposition of paths in order to enhance quantum communications. Superposition of paths cannot give a maximal activation of the quantum capacity [17] due to the paths are independent. In fact, superposition of paths has been considered in the experimental implementation proposal presented to emulate the superposition of causal orders, giving only a limited approach.

The experimental implementation is still in development, because of the complication that theoretical analysis consider the input and output systems on a different system. All along the work, the entangled resource needed in the teleportation process has been taken as a superposition of lineal Bell states, nevertheless, it is important to mention that, instead of these Bell states, it can be used a mixed state as the entangled resource, nevertheless, the use of mixed states introduces more parameters. Despite, if $|\chi\rangle$ is instead introduced as a mixed state, its parameters should be reflected on a similar form for $\Lambda[\rho] = \sum_{i=0}^3 p_i \sigma_i \rho \sigma_i$ because teleportation algorithm is by itself a quantum channel. In addition, in [55] it has been shown that for that formula, the channels on the frontal face behave as transparent channels under indefinite causal order, which showed that the outcomes presented in this work are immediately fulfilled for a mixed states treatment in teleportation.

9.2 Future work

Future works are oriented to the extension of the algorithm to bigger systems, this means, to improve quantum teleportation under an indefinite causal order scheme with channels for d -dimensions (and not only qubits as the case for the work developed here) or with a composition of various systems. Also, regarding the probability of successful measurement, improvements are needed to be sought by exploring alternatives schemes with other strategies in addition to weak measurement in order to enhance that probability of success. For the case of $N > 2$, an analysis considering other control states and, therefore, other measurement states must be considered, since all along the work the control system has been considered with the values for the probabilities to be equal, then, it can be explored the possibility for other initial states on the control to maximize the fidelity. For the future work regarding the experimental approach, it is recommended to look for a way to improve the proposed scheme, as well as to launch the enhanced experimental proposal.

Appendix A

Formulas \mathcal{F}_N and \mathcal{P}_N for $N = 2, 3, 4$

Formulas indicated in Chapter 6 for probability and fidelity as the number of channels in indefinite causal order increases have been obtained.

For the case $N = 2$, when $|\psi_m\rangle = |\varphi_m^-\rangle$ the outcomes are:

$$\mathcal{F}_2 = \frac{1}{3} \quad (\text{A.1})$$

$$\mathcal{P}_2 = 6p^2 \quad (\text{A.2})$$

and for the case when $|\psi_m\rangle = |\varphi_m^+\rangle$, the outcomes become:

$$\mathcal{F}_2 = \frac{1}{\mathcal{P}_2}(6p^2 - 4p + 1) \quad (\text{A.3})$$

$$\mathcal{P}_2 = 1 - 6p^2 \quad (\text{A.4})$$

For the case $N = 3$, when $|\psi_m\rangle = |\varphi_m^-\rangle$ the outcomes are:

$$\mathcal{F}_3 = 2p + \frac{1}{3} \quad (\text{A.5})$$

$$\mathcal{P}_3 = 2p^2 \quad (\text{A.6})$$

and for the case when $|\psi_m\rangle = |\varphi_m^+\rangle$, the outcomes become:

$$\mathcal{F}_3 = \frac{1}{3\mathcal{P}_3}(-76p^3 + 54p^2 - 18p + 3) \quad (\text{A.7})$$

$$\mathcal{P}_3 = 32p^3 - 18p^2 + 1 \quad (\text{A.8})$$

For the case $N = 4$, when $|\psi_m\rangle = |\varphi_m^-\rangle$ we get $\mathcal{P}_m = 0$, thus \mathcal{F}_4 becomes undefined in such case, and for the case when $|\psi_m\rangle = |\varphi_m^+\rangle$, the outcomes become:

$$\mathcal{F}_4 = \frac{360p^4 - 304p^3 + 108p^2 - 24p + 3}{-408p^4 + 384p^3 - 108p^2 + 3} \quad (\text{A.9})$$

$$\mathcal{P}_4 = -136p^4 + 128p^3 - 36p^2 + 1 \quad (\text{A.10})$$

Appendix B

Channel characterization for mixed states

Formulas obtained in Chapter 6 can be applied for a Pauli channel. The development made here is exactly the same and the same properties for both teleportation and communication are accomplished, the only difference is that, in communication, there is no an entangled state along the process, but in this case, α take the place of p and they are parameter that characterise the channel as it is shown in the Figure 2.1.

Particularly, it will be shown some results for channels that are located in the face where $\alpha_0 = 0$ and there are only components from $\alpha_1, \alpha_2, \alpha_3$ in the context of communication. Notice that on that face with $\alpha_0 = 0$ it is fulfilled B.1, which is the same for the case of teleportation as it is shown in 6.11.

It will be interesting to analyse the situation for mixed states at least for the more notable cases. In such case, formula (6.8) should be replaced by (2.6). The analysis becomes more complex because the parameter \vec{n} with $n \equiv |\vec{n}| \neq 1$ appears together with the parameters $\alpha_1, \alpha_2, \alpha_3$. For that reason, we will restrict our analysis to the frontal face with $\alpha_0 = 0$ which has become a valuable outcome for pure states. In this case, we could obtain $\Lambda^{N,\pm}[\rho] \equiv \frac{1}{\mathcal{P}_m} \langle \psi_m^{N,\pm} | \Lambda^N[\rho \otimes \rho_c] | \psi_m^{N,\pm} \rangle$ through (6.2), with \mathcal{P}_m still given by (6.9). The outcomes were analytically addressed yet (Appendix C reports the corresponding expressions) from (6.7):

$$\Lambda^{N,\pm}[\rho] = \frac{1}{\mathcal{P}_m N!^2} \sum_{t_1=0}^N \sum_{t_2=0}^{N-t_1} \prod_{j=1}^3 \alpha_j^{t_j} \sum_k \sum_{k'} (\pm 1)^{\sigma(\pi_k) + \sigma(\pi_{k'})} \cdot \sum_{p=1}^{N'} \pi_k \left(\pi_{k_p}^{t_1, t_2, t_3} \left(\sigma_1^{t_1} \sigma_2^{t_2} \sigma_3^{t_3} \right) \right) \rho \left(\pi_{k'} \left(\pi_{k_p}^{t_1, t_2, t_3} \left(\sigma_1^{t_1} \sigma_2^{t_2} \sigma_3^{t_3} \right) \right) \right)^\dagger \quad (\text{B.1})$$

where $N' = \frac{N!}{t_1! t_2! t_3!}$ and $t_3 = N - t_1 - t_2$. In this formula we need to take care about the meaning, the permutation π_{k_p} does not distinguish among identical objects in $\sigma_1^{t_1} \sigma_2^{t_2} \sigma_3^{t_3}$, while $\pi_k, \pi_{k'}$ do because they permute positions, not objects. Finally, with $\Lambda^{N,\pm}[\rho]$, we can easily obtain $\mathcal{F}_N^\pm, \mathcal{P}_m$.

In the analysis, we get \mathcal{P}_m as it was respectively given in (D.1-D.5) for each point on the frontal face $\alpha_0 = 0$ colored in agreement with such quantity in the 0(red)-1(blue) scale. Due to the fidelity of communication depends on ρ in general, we are selected three illustrative points to compare the outcomes: a) $\text{P}_a : \alpha_1 = \alpha_2 = \alpha_3 = \frac{1}{3}$ (central ICO channel), b)

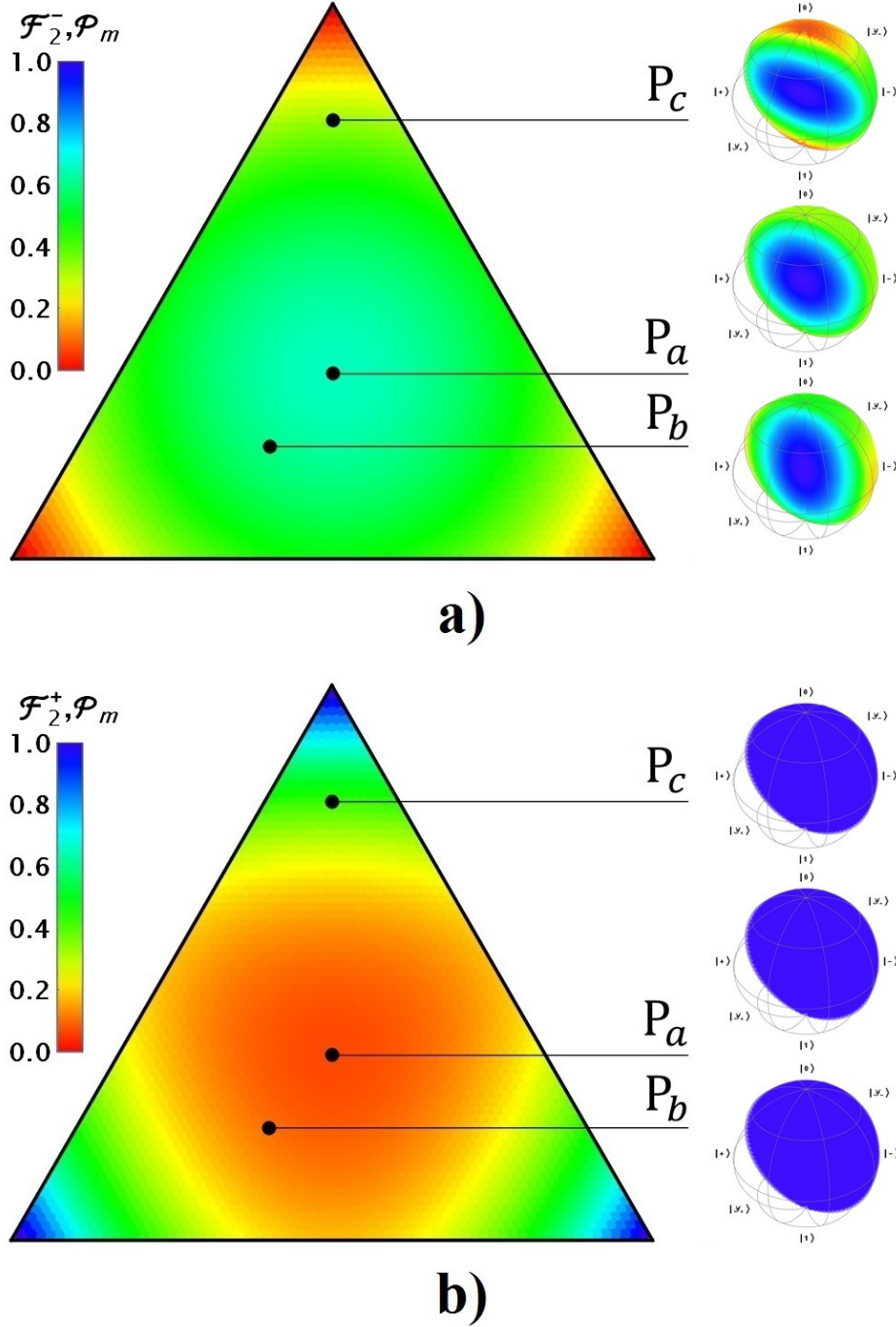


Figure B.1: \mathcal{P}_m on the $\alpha_0 = 0$ face together with the fidelity on the Bloch ball for the input ρ for three specific channels P_a, P_b, P_c with $N = 2$ using a) $|\psi_m^{N=2,-}\rangle$, and b) $|\psi_m^{N=2,+}\rangle$ for the control measurement. Both, \mathcal{P}_m and $\Lambda^{2,\pm}[\rho]$ are reported in color in the scale 0(red)-1(blue).

P_b : $\alpha_1 = 0.5, \alpha_2 = 0.3, \alpha_3 = 0.2$ (nearer from the bit-flipping noise channel), and c) P_c : $\alpha_1 = 0.1, \alpha_2 = 0.1, \alpha_3 = 0.8$ (extremely near from the dephasing noise channel). Then, for each example, we take the Bloch sphere $n \leq 1$ to get \mathcal{F}_N^\pm for each point inside, coloring it in agreement with such fidelity in the same scale 0(red)-1(blue). The color scale will be

shown together for \mathcal{P}_m and \mathcal{F}_N^\pm on the left and in only one half of the Bloch ball ($n_2 \geq 0$) in order to exhibit its inner structure. In each plot the eigenvectors of Pauli matrices $\sigma_1, \sigma_2, \sigma_3$ are shown on the poles and equator ball as reference: $|+\rangle, |-\rangle, |\mathcal{Y}_+\rangle, |\mathcal{Y}_-\rangle, |0\rangle, |1\rangle$.

Thus, Figure B.1 shows the case $N = 2$ for a) $|\psi_m^{N=2,-}\rangle$ and b) $|\psi_m^{N=2,+}\rangle$. For Figure B.1a, because the central ICO channel maps the Bloch ball into a deformed ball, then the corresponding plot of \mathcal{F}_2^- for P_a becomes radially symmetric in Figure B.1a (note the representation was made on the original ball for ρ , thus such plots do not exhibit the ball deformation being present in $\Lambda^{2,-}[\rho]$). Together, the cases P_b and P_c exhibit an ellipsoidal distribution of \mathcal{F}_N^\pm compressed on the x -direction for the bit-flipping noise case (P_b) and in the z -direction for the dephasing noise case (P_c). Note that it does not fit with the expected behavior of the single channel in agreement with (2.4) when $\alpha_0 = 0$, which reduces and flips the ball: $n'_i = -(1 - 2\alpha_i)n_i$, a consequence of the indefinite causal order and measurement. They clearly exhibit the deep worsen of fidelity in the same direction to the nearest syndrome among the states $\rho, \Lambda^{2,-}[\rho]$. For P_c and P_b closer than syndromes $\sigma_3\rho\sigma_3$ and $\sigma_1\rho\sigma_1$ respectively, the single channel holds that direction of the ball, $n'_3 = n_3$ and $n'_1 = n_1$, the opposite behavior observed under indefinite causal order. There, while more deformed is the Bloch ball by the the single channel, better the fidelity in the same direction and worse the fidelity in the transverse directions due to the sequential use of the channel under indefinite causal order and the post-measurement of the control state. Note in any case that the core is blue (\mathcal{F}_2^-) due to the proximity with the totally depolarized state $\rho = \frac{1}{2}\sigma_0$, which is always transmitted faithfully. Otherwise, Figure B.1b exhibits a surprisingly outcome with $\mathcal{F}_2^+ \equiv 1$ (it means $\Lambda^{2,+}[\rho] = \rho$) on the frontal face ($\alpha_0 = 0$), thus the fidelity P_a, P_b and P_c plots completely in blue. This is an effect generated directly from the indefinite causal order and the measurement, as an extension of our same result for pure states in the same frontal face: the behavior as transparent channel of such composed arrangement under indefinite causal order.

Appendix C

Formulas of output for mixed states under indefinite causal order

We report in this section the formulas for the output states for mixed states as input on the frontal face of the parametric space $(\alpha_1, \alpha_2, \alpha_3)$. In each case, \mathcal{P}_m corresponds to the respective formula given in (D.1-D.4). For $N = 2$ and $|\psi_m^{N=2,-}\rangle$:

$$\Lambda^{2,-}[\rho] = \frac{1}{2} \left(\sigma_0 + \frac{\vec{n} \cdot \vec{\Delta}}{\mathcal{P}_m} \right) \quad (\text{C.1})$$

with : $\Delta_\mu = \sigma_\mu(\alpha_\nu \alpha_o - \alpha_\mu(\alpha_\nu + \alpha_o))$

being μ, ν, o a cyclic permutation of 1, 2, 3. Similarly for $N = 3$ and $|\psi_m^{N=3,+}\rangle$:

$$\Lambda^{3,+}[\rho] = \frac{1}{2} \left(\sigma_0 + \frac{\vec{n} \cdot \vec{\Delta}}{\mathcal{P}_m} \right) \quad (\text{C.2})$$

with : $\Delta_\mu = \sigma_\mu(1 - 6(\alpha_\nu + \alpha_o) + 12(\alpha_\nu^2 + \alpha_o^2)) + 6(\alpha_\mu(\alpha_\nu + \alpha_o) + 3\alpha_\nu \alpha_o)$
 $-8(\alpha_\nu^3 + \alpha_o^3) - \frac{10}{3}\alpha_\mu^2(\alpha_\nu + \alpha_o) - \frac{26}{3}\alpha_\mu(\alpha_\nu^2 + \alpha_o^2)$
 $-\frac{46}{3}\alpha_\nu \alpha_o(\alpha_\nu + \alpha_o) - 12\alpha_\mu \alpha_\nu \alpha_o$

with μ, ν, o a cyclic permutation of 1, 2, 3. We should note that in the last formulas $\alpha_1 + \alpha_2 + \alpha_3 = 1$. Finally for the cases $N = 2$ with $|\psi_m^{N=2,+}\rangle$, $N = 3$ with $|\psi_m^{N=3,-}\rangle$, and $N = 4$ with $|\psi_m^{N=4,+}\rangle$:

$$\Lambda^{2,+}[\rho] = \rho \quad (\text{C.3})$$

$$\Lambda^{3,-}[\rho] = \rho \quad (\text{C.4})$$

$$\Lambda^{4,+}[\rho] = \rho \quad (\text{C.5})$$

Appendix D

Probabilities of successful measurement

\mathcal{P}_m

Probabilities of successful measurement on the bases $|\psi_m^{N,\pm}\rangle$ for the channels on the entire region could be analytically obtained. They are polynomials of order N on the coefficients channel $\{\alpha_i\}$. In all cases, $\alpha_0 = 1 - \sum_{i=1}^3 \alpha_i$ has been assumed. For $N = 2$, we get the complementary cases:

$$\mathcal{P}_m^{N=2,+} = 1 - \sum_{i,j=1}^3 \alpha_i \alpha_j \quad (\text{D.1})$$

$$\mathcal{P}_m^{N=2,-} = \sum_{i,j=1}^3 \alpha_i \alpha_j \quad (\text{D.2})$$

for $N = 3$, the two cases being considered have the probabilities:

$$\mathcal{P}_m^{N=3,+} = 1 - 3 \sum_{i \neq j=1}^3 \alpha_i \alpha_j + \frac{10}{3} \sum_{i \neq j=1}^3 \alpha_i \alpha_j^2 + 12 \alpha_1 \alpha_2 \alpha_3 \quad (\text{D.3})$$

$$\mathcal{P}_m^{N=3,-} = \frac{1}{3} \sum_{i \neq j=1}^3 \alpha_i \alpha_j - \frac{2}{3} \sum_{i \neq j=1}^3 \alpha_i \alpha_j^2 + 4 \alpha_1 \alpha_2 \alpha_3 \quad (\text{D.4})$$

and finally for $N = 4$ both cases are (with one of them identically equal to zero):

$$\mathcal{P}_m^{N=4,+} = 1 - 6 \sum_{i \neq j=1}^3 \alpha_i \alpha_j + \frac{40}{3} \sum_{i \neq j=1}^3 \alpha_i \alpha_j^2 + 48 \alpha_1 \alpha_2 \alpha_3 \quad (\text{D.5})$$

$$- \frac{16}{3} \sum_{i \neq j=1}^3 \alpha_i \alpha_j^3 - 4 \sum_{i \neq j=1}^3 \alpha_i^2 \alpha_j^2 - \frac{40}{3} \sum_{i \neq j \neq k=1}^3 \alpha_i \alpha_j \alpha_k^2 \quad (\text{D.6})$$

$$\mathcal{P}_m^{N=4,-} = 0$$

Appendix E

Formulas for $\mathcal{P}_{m,N}^{\text{ff},\{p_i\}}$ and \mathcal{F}

In this section, formulas for $\mathcal{P}_{m,N}^{\text{ff},\{p_i\}}$ and \mathcal{F} when the entangled state has different values for p_1, p_2 and p_3 (note they are restricted to the frontal face of) and the measurement state is either $|\varphi_m^+\rangle$ or $|\varphi_m^-\rangle$. In those results, the angles θ and ϕ corresponds to the state being teleported ($|\psi\rangle = \cos\frac{\theta}{2}|0\rangle + \sin\frac{\theta}{2}e^{i\phi}|1\rangle$), thus meaning a dependence of those values on this state. For the case $N = 2$, when the measurement state is $|\varphi_m^+\rangle$ the outcomes are:

$$\mathcal{F}_2 = 1 \quad (\text{E.1})$$

$$\mathcal{P}_{m,N=2}^{\text{ff},\{p_i\}} = p_1^2 + p_2^2 + p_3^2 \quad (\text{E.2})$$

and with the privileged state as $|\varphi_m^-\rangle$, the corresponding expressions are:

$$\begin{aligned} \mathcal{F}_2 = \frac{1}{2\mathcal{P}_{m,N=2}^{\text{ff},\{p_i\}}} & \left(2p_1p_2(1 + \cos 2\theta) + p_3(p_1 + p_2)(1 - \cos 2\theta) \right. \\ & \left. + 2p_3(p_2 - p_1) \sin^2 \theta \cos 2\phi \right) \end{aligned} \quad (\text{E.3})$$

$$\mathcal{P}_{m,N=2}^{\text{ff},\{p_i\}} = 2(p_1p_2 + p_2p_3 + p_3p_1) \quad (\text{E.4})$$

For the case $N = 3$, with the privileged measurement state as $|\varphi_m^+\rangle$, the outcomes are:

$$\begin{aligned} \mathcal{F}_3 = \frac{1}{12\mathcal{P}_{m,N=3}^{\text{ff},\{p_i\}}} & \left((3(p_1^3 + p_2^3 + 2p_3^3) + p_1(p_2^2 + p_3^2) + p_2(p_1^2 + p_3^2))(1 - \cos 2\theta) \right. \\ & + 2p_3(p_1^2 + p_2^2)(1 + \cos 2\theta) + 2(3(p_1^3 - p_2^3) + p_1(p_2^2 + p_3^2) \\ & \left. - p_2(p_1^2 + p_3^2)) \sin^2 \theta \cos 2\phi \right) \end{aligned} \quad (\text{E.5})$$

$$\mathcal{P}_{m,N=3}^{\text{ff},\{p_i\}} = p_1^3 + p_2^3 + p_3^3 + \frac{1}{3}(p_1^2(p_2 + p_3) + p_2^2(p_1 + p_3) + p_3^2(p_1 + p_2)) \quad (\text{E.6})$$

while with the privileged state as $|\varphi_m^-\rangle$, they become:

$$\mathcal{F}_3 = 1 \quad (\text{E.7})$$

$$\mathcal{P}_{m,N=3}^{\text{ff},\{p'_i\}} = 6p_1p_2p_3 \quad (\text{E.8})$$

Finally, for the case $N = 4$, with the privileged measurement state as $|\varphi_m^+\rangle$, then:

$$\mathcal{F}_4 = 1 \quad (\text{E.9})$$

$$\mathcal{P}_{m,N=4}^{\text{ff},\{p_i\}} = p_1^4 + p_2^4 + p_3^4 + \frac{2}{3}(p_1^2p_2^2 + p_1^2p_3^2 + p_2^2p_3^2) \quad (\text{E.10})$$

and if the privileged state is $|\varphi_m^-\rangle$ then we get $\mathcal{P}_{m,N=4}^{\text{ff},\{p_i\}} = 0$, thus \mathcal{F} gets undetermined.

Bibliography

- [1] C. H. Bennet, G. Brassard, C. Crépeau, R. Jozsa, A. Peres, and W. K. Wootters, “Teleporting an Unknown Quantum State via Dual Classical and Einstein-Podolsky-Rosen Channels,” *Physical Review Letters*, vol. 70, no. 13, pp. 1895–1899, 1993.
- [2] D. Bouwmeester, J. Pan, K. Mattle, M. Eibl, H. Weinfurter, and A. Zeilinger, “Experimental quantum teleportation,” *Nature*, vol. 390, p. 575, 1997.
- [3] D. Boschi, S. Branca, F. De-Martini, L. Hardy, and S. Popescu, “Experimental Realization of Teleporting an Unknown Pure Quantum State via Dual Classical and Einstein-Podolsky-Rosen Channels,” *Physical review letters*, vol. 80, no. 6, pp. 1121–1125, 1998.
- [4] D. Bouwmeester, K. Mattle, J.-W. Pan, H. Weinfurter, A. Zeilinger, and M. Zukowski, “Experimental quantum teleportation of arbitrary quantum states,” *Applied Physics B*, vol. 67, pp. 749–752, 1998.
- [5] D. Bouwmeester, J.-W. Pan, K. Mattle, M. Eibl, H. Weinfurter, and Z. A., “Experimental quantum teleportation,” *Philosophical Transactions of the Royal Society A*, vol. 356, pp. 1733–1737, 1998.
- [6] D. Fattal, E. Diamanti, K. Inoue, and Y. Yamamoto, “Quantum Teleportation with a Quantum Dot Single Photon Source,” *Physical review letters*, vol. 92, no. 3, pp. 1–4, 1998.
- [7] C. Santori, D. Fattal, J. Vučković, G. Solomon, and Y. Y., “Indistinguishable photons from a single-photon device,” *Nature*, vol. 419, pp. 594–597, 2002.
- [8] H. de Riedmatten, I. Marcikic, W. Tittel, H. Zbinden, D. Collins, and N. Gisin, “Long distance quantum teleportation in a quantum relay configuration,” *Phys. Rev. Let.*, vol. 92, no. 4, p. 047904, 2004.
- [9] R. Ursin, T. Jennewein, M. Aspelmeyer, R. Kaltenbaek, M. Lindenthal, P. Walther, and A. Zeilinger, “Quantum teleportation across the danube,” *Nature*, vol. 430, p. 849, 2004.
- [10] H. Takesue, S. D. Dyer, M. J. Stevens, V. Verma, R. P. Mirin, and S. W. Nam, “Quantum teleportation over 100km of fiber using highly efficient superconducting nanowire single-photon detectors,” *Optica*, vol. 2, pp. 832–835, Oct 2015.
- [11] F. Delgado, “Quantum control on entangled bipartite qubits,” *Physical Review A*, vol. 81, pp. 1–10, 2010.

- [12] M. Caleffi and A. S. Cacciapuoti, “Quantum switch for the quantum internet: Noiseless communications through noisy channels,” *IEEE Journal on Selected Areas in Communications*, vol. 38, no. 3, pp. 575–588, 2020.
- [13] D. Ebler, S. Salek, and G. Chiribella, “Enhanced Communication With the Assistance of Indefinite Causal Order,” *Physical review letters*, vol. 120, no. 120502, pp. 1–4, 2018.
- [14] L. M. Procopio, A. Moqanaki, M. Araújo, F. Costa, I. A. Calafell, E. G. Dowd, D. R. Hamel, L. A. Rozema, C. Brukner, and P. Walther, “Experimental superposition of orders of quantum gates,” *Nature Communications*, vol. 6, p. 7913, 2015.
- [15] Y. Guo, X.-M. Hu, Z.-B. Hou, H. Cao, J.-M. Cui, B. Liu, Y. Huang, C.-F. Li, and G.-C. Guo, “Experimental investigating communication in a superposition of causal orders,” *arXiv:1811.07526v1*, 11 2018.
- [16] Y. Guo, X.-M. Hu, Z.-B. Hou, H. Cao, J.-M. Cui, B.-H. Liu, Y.-F. Huang, C.-F. Li, G.-C. Guo, and G. Chiribella, “Experimental transmission of quantum information using a superposition of causal orders,” *Phys. Rev. Lett.*, vol. 124, p. 030502, Jan 2020.
- [17] G. Chiribella, M. Banik, S. S. Bhattacharya, T. Guha, M. Alimuddin, A. Roy, S. Saha, S. Agrawal, and G. Kar, “Indefinite causal order enables perfect quantum communication with zero capacity channel,” *arXiv:1810.10457*, pp. 1–14, 2018.
- [18] G. Chiribella, “Perfect discrimination of no-signalling channels via quantum superposition of causal structures,” *Phys. Rev. A*, vol. 86, p. 040301, Oct 2012.
- [19] S. Lloyd, *The Physics of Communication*, ch. Quantum enhancements to channel capacity, pp. 561–567. Department of Mechanical Engineering, Massachusetts Institute of Technology (Cambridge, Massachusetts), 2003.
- [20] G. Rubino, L. A. Rozema, D. Ebler, H. Kristjánsson, S. Salek, P. A. Guérin, A. A. Abbott, C. Branciard, Časlav Brukner, G. Chiribella, and P. Walther, “Experimental quantum communication enhancement by superposing trajectories,” *arXiv:2007.05005*, pp. 1–16, 2020.
- [21] K. Goswami, Y. Cao, G. A. Paz-Silva, J. Romero, and A. G. White, “Increasing communication capacity via superposition of order,” *Phys. Rev. Research*, vol. 2, p. 033292, Aug 2020.
- [22] C. Mukhopadhyay and A. K. Pati, “Superposition of causal order enables quantum advantage in teleportation under very noisy channels,” *Journal of Physics Communications*, vol. 4, p. 105003, oct 2020.
- [23] L. M. Procopio, F. Delgado, M. Enríquez, N. Belabas, and J. A. Levenson, “Communication enhancement through quantum coherent control of N channels in an indefinite causal-order scenario,” *Entropy*, vol. 21, p. 1012, 2019.
- [24] L. M. Procopio, F. Delgado, M. Enríquez, N. Belabas, and J. A. Levenson, “Sending classical information via three noisy channels in superposition of causal orders,” *Phys. Rev. A*, vol. 101, p. 012346, Jan 2020.

- [25] O. Oreshkov, F. Costa, and C. Brukner, “Quantum correlations with no causal order,” *Nature Communications*, vol. 3, p. 1092, 2012.
- [26] X. Zhao, Y. Yang, and G. Chiribella, “Quantum metrology with indefinite causal order,” *Phys. Rev. Lett.*, vol. 124, p. 190503, May 2020.
- [27] K. Goswami and F. Costa, “Classical communication through quantum causal structures,” *arXiv:2007.05051v1*, 2020.
- [28] C. E. Shannon, “A mathematical theory of communication,” *The Bell System Technical Journal*, vol. 27, no. 3, pp. 379–423, 1948.
- [29] G. Chiribella, G. M. D’Ariano, P. Perinotti, and B. Valiron, “Quantum computations without definite causal structure,” *Phys. Rev. A*, vol. 88, p. 022318, Aug 2013.
- [30] O. Oreshkov and C. Giarmatzi, “Causal and causally separable processes,” *New Journal of Physics*, vol. 18, p. 093020, sep 2016.
- [31] J. Wechs, A. A. Abbott, and C. Branciard, “On the definition and characterisation of multipartite causal (non)separability,” *New Journal of Physics*, vol. 21, p. 013027, jan 2019.
- [32] G. Rubino, L. A. Rozema, A. Feix, M. Araújo, J. M. Zeuner, L. M. Procopio, Č. Brukner, and P. Walther, “Experimental verification of an indefinite causal order,” *Science Advances*, vol. 3, no. 3, 2017.
- [33] K. Goswami, C. Giarmatzi, M. Kewming, F. Costa, C. Branciard, J. Romero, and A. G. White, “Indefinite causal order in a quantum switch,” *Phys. Rev. Lett.*, vol. 121, p. 090503, Aug 2018.
- [34] C. H. Bennett and S. J. Wiesner, “Communication via One- and Two-Particle Operators on Einstein-Podolsky-Rosen States,” *Physical review letters*, vol. 69, pp. 2881–2884, 1992.
- [35] F. Delgado, “Teleportation based on control of anisotropic Ising interaction in three dimensions,” *Journal of Physics: Conference Series*, vol. 624, p. 012006, 2015.
- [36] F. Yan and L. Yang, “Teleportation of multiparticle quantum state,” *Nuovo Cimento B*, vol. 118, no. 1, p. 79, 2003.
- [37] B. J. Metcalf, J. B. Spring, P. C. Humphreys, N. Thomas-Peter, M. Barbieri, W. S. Kolthammer, X.-M. Jin, N. K. Langford, D. Kundys, J. C. Gates, B. J. Smith, P. G. R. Smith, and I. A. Walmsley, “Quantum teleportation on a photonic chip,” *Nature Photonics*, vol. 8, pp. 770–774, 2014.
- [38] M. A. Nielsen, E. Knill, and R. Laflamme, “Complete quantum teleportation using nuclear magnetic resonance,” *Nature*, vol. 396, p. 52, 1998.

- [39] F. Delgado, “Teleportation algorithm settled in a resonant cavity using non-local gates,” in *Quantum Information and Measurement (QIM) V: Quantum Technologies*, p. F5A.17, Optical Society of America, 2019.
- [40] X.-S. Ma, T. Herbst, T. Scheidl, D. Wang, S. Kropatschek, W. Naylor, B. Wittmann, A. Mech, J. Kofler, E. Anisimova, V. Makarov, T. Jennewein, R. Ursin, and A. Zeilinger, “Quantum teleportation over 143 kilometres using active feed-forward,” *Nature*, vol. 489, p. 269, 2012.
- [41] Y.-H. Luo, H.-S. Zhong, M. Erhard, X.-L. Wang, L.-C. Peng, M. Krenn, X. Jiang, L. Li, N.-L. Liu, C.-Y. Lu, A. Zeilinger, and J.-W. Pan, “Quantum Teleportation in High Dimensions,” *Phys. Rev. Lett.*, vol. 123, p. 070505, 2019.
- [42] C. Cardoso-Isidoro and F. Delgado, “Featuring causal order in teleportation of two quantum teleportation channels,” *J. Phys.: Conf. Ser.*, vol. 1540, p. 012024, 2020.
- [43] S. Salek, D. Ebler, and G. Chiribella, “Quantum communication in a superposition of causal orders,” *arXiv:1809.06655*, pp. 1–6, 2018.
- [44] E. B. Davies, *Quantum Theory of Open Systems*. Academic Press (London), 1976.
- [45] M. A. Nielsen and I. L. Chuang, *Quantum Computation and Quantum Information (10th Anniversary Edition)*. Cambridge University Press (Cambridge, UK, 2000).
- [46] L. Gyongyosi and S. Imre, “Properties of the quantum channel,” *arXiv:1901.07626v1*, 2012.
- [47] K. Kraus, *States, Effects and Operations: Fundamental Notions of Quantum Theory*, Springer. Springer-Verlag Berlin Heidelberg, 1983.
- [48] W. G. Ritter, “Quantum channels and representation theory,” *Journal of Mathematical Physics*, vol. 46, no. 8, p. 082103, 2005.
- [49] D. Petz, *Quantum Information Theory and Quantum Statistics*. Springer-Verlag Berlin Heidelberg, 2008.
- [50] S. T. Flammia and J. J. Wallman, “Efficient estimation of pauli channels,” *arXiv:1907.12976*, 2019.
- [51] S. Katarzyna, “Geometry of pauli maps and pauli channels,” *Phys. Rev. A*, vol. 100, p. 062331, 2019.
- [52] R. Jozsa, “Fidelity for mixed quantum states,” *Journal of Modern Optics*, vol. 41, no. 12, pp. 2315–2323, 1994.
- [53] C. Cardoso-Isidoro and F. Delgado, “Performance of two redundant quantum channels for single qubits under indefinite causal order,” *J. Phys.: Conf. Ser.*, 2020.
- [54] G. Bowen and S. Nose, “Teleportation as a Depolarizing Quantum Channel, Relative Entropy, and Classical Capacity,” *Physical review letters*, vol. 87, p. 267901, 2001.

- [55] F. Delgado and C. Cardoso-Isidoro, “Performance characterization of N quantum channels for single qubits assisted by indefinite causal order and measurement,” *submitted to QIC*, 2020.
- [56] F. Schmidt-Kaler, H. Häffner, M. Riebe, S. Gulde, G. P. T. Lancaster, T. Deuschle, C. Becher, C. F. Roos, J. Eschner, and R. Blatt, “Realization of the cirac–zoller controlled-not quantum gate.,” *Nature*, vol. 422, pp. 408–422, 2003.
- [57] D. Maslov, “Basic circuit compilation techniques for an ion-trap quantum machine,” *New Journal of Physics*, vol. 19, p. 023035, feb 2017.
- [58] J.-H. Lopes, W.-C. Soares, B. de Lima Bernardo, D. P. Caetano, and A. Canabarro, “Linear optical cnot gate with orbital angular momentum and polarization.,” *Quantum Inf Processing*, vol. 18, p. 256, 2019.
- [59] T. Sleator and H. Weinfurter, “Realizable universal quantum logic gates,” *Phys. Rev. Lett.*, vol. 74, pp. 4087–4090, May 1995.
- [60] T. Monz, K. Kim, W. Hänsel, M. Riebe, A. S. Villar, P. Schindler, M. Chwalla, M. Hennrich, and R. Blatt, “Realization of the quantum toffoli gate with trapped ions,” *Phys. Rev. Lett.*, vol. 102, p. 040501, Jan 2009.
- [61] H.-L. Huang, W.-S. Bao, T. Li, F.-G. Li, X.-Q. Fu, S. Zhang, H.-L. Zhang, and X. Wang, “Deterministic linear optical quantum toffoli gate.,” *Physics Letters A*, vol. 381, no. 33, pp. 2673–2676, 2017.
- [62] D. Boschi, S. Branca, F. D. Martini, L. Hardy, and S. Popescu, “Teleporting an unknown pure quantum state via dual classical and einstein-podolsky-rosen channels.,” *Phys. Rev. Lett.*, vol. 80, p. 1121, 1998.
- [63] R. Boyd, *Nonlinear Optics*. Academic Press: Rochester, New York, 2018.
- [64] M. Bass, C. DeCusatis, J. Enoch, V. Lakshminarayanan, G. Li, C. MacDonald, V. Mahajan, and E. V. Stryland, *Handbook of Optics*, vol. I. McGraw-Hill Professional: New York, third edition ed., 2009.
- [65] M. Erhard, M. Malik, M. Krenn, and A. Zeilinger, “Experimental greenberger–horne–zeilinger entanglement beyond qubits.,” *Nature Photonics*, vol. 12, p. 759–764, 2018.
- [66] M. Zhu and L. Ye, “Implementation of swap gate and fredkin gate using linear optical elements.,” *International Journal of Quantum Information*, vol. 11 (3), p. 1350031, 2013.
- [67] T. Ono, R. Okamoto, M. Tanida¹, H. Hofmann, and S. Takeuchi, “Implementation of a quantum controlled-swap gate with photonic circuits.,” *Scientific Reports*, vol. 7, p. 45353, 2017.

Curriculum Vitae

Carlos Cardoso Isidoro Master student was born in Puebla, México, on October 28, 1992. He earned the Electronics Engineering degree from the Tecnológico Nacional de México, Morelia Campus in Feb 2019. He was accepted in the graduate programs in Nanotechnology in Jan 2019. He has participated in the following conferences:

- International Conference on Quantum Phenomena, Quantum Control and Quantum Optics, *Featuring causal order in teleportation of two quantum teleportation channels, October 28-November 1, 2019, Mexico.*
- *50 Congreso de Investigación y Desarrollo, Teleportation with two quantum channels in superposition of causal order, February 25-28, 2020, Mexico.*
- *9th International Conference on Mathematical Modeling in Physical Sciences, Performance of two redundant quantum channels for single qubits under indefinite causal order, September 7-10, 2020, Greece.*
- *NQN Quantum Programming in Theory, Experiment and In the Classroom (QPTEC), Indefinite causal order enhances quantum teleportation, September 16-18, 2020, United States of America.*
- *Quantum 2020, Improving imperfect quantum teleportation with indefinite causal order assisted by post-measurement and weak measurement, October 19-22, 2020, United States of America.*

Carlos Cardoso Isidoro has participated in the publication of the following works:

- "Featuring Causal Order in Teleportation With Two Quantum Teleportation Channels", *Journal of Physics: Conference Series*, vol. 1540, p. 012024, 2020.
- "Performance of two redundant quantum channels for single qubits under indefinite causal order", *Journal of Physics*, 2020.
- "Characterization of N quantum channels assisted by indefinite causal order and measurement", *Quantum Information & Computation*, vol. 20, No. 15&16, p. 1261-1280, 2020.
- "Teleportation assisted by N –channels in an indefinite causal order and measurement", *Symmetry*, vol. 12, p. 1904, 2020.

This document was typed in using L^AT_EX 2_ε^a by Carlos Cardoso Isidoro.

^aThe style file `phdThesisFormat.sty` used to set up this thesis was prepared by the Center of Intelligent Systems of the Instituto Tecnológico y de Estudios Superiores de Monterrey, Monterrey Campus